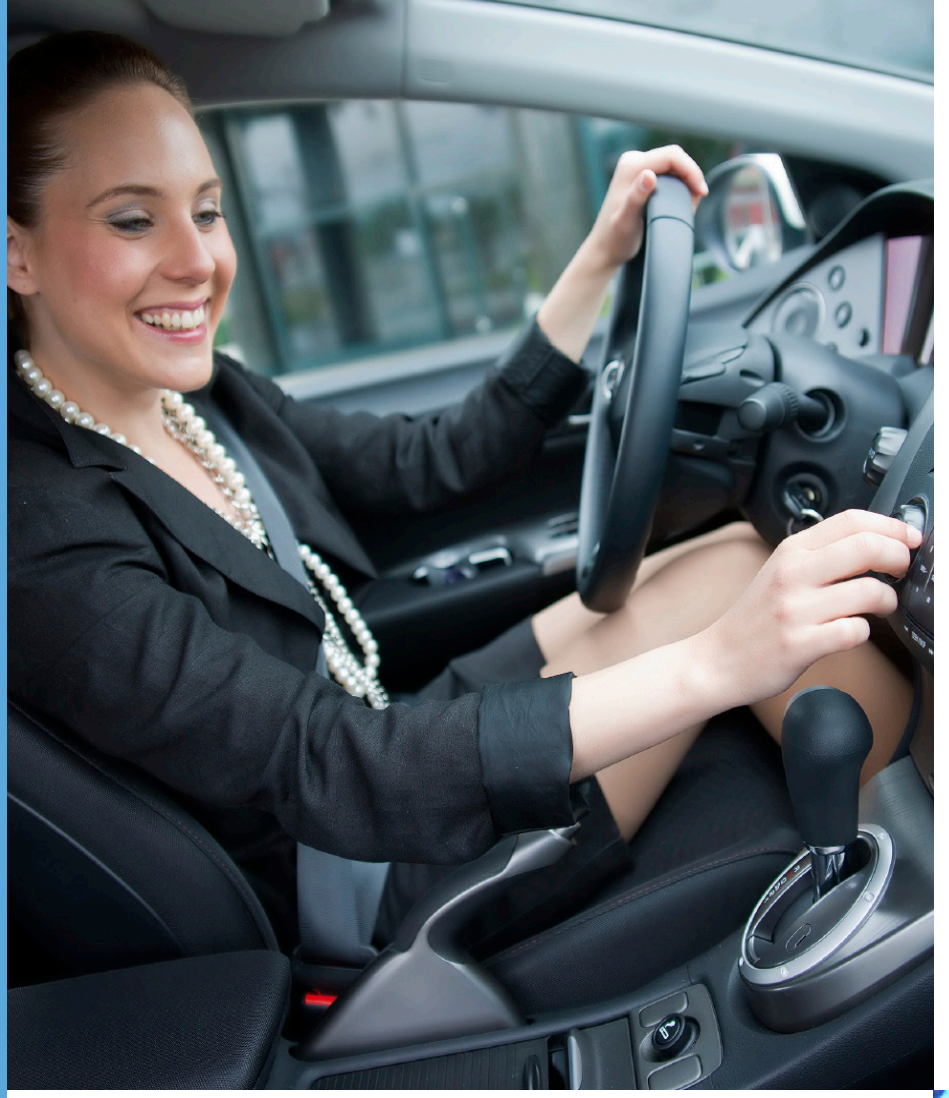

SCIENCE • TECHNOLOGY • RESEARCH HIGHLIGHTS • VISIONS

5

Development of a robust and computationally-efficient active sound profiling algorithm in a passenger car

Jari Kataja

VTT SCIENCE 5

Development of a robust and computationally-efficient active sound profiling algorithm in a passenger car

Jari Kataja

ISBN 978-951-38-7457-5 (soft back ed.)
ISSN 2242-119X (soft back ed.)

ISBN 978-951-38-7458-2 (URL: http://www.vtt.fi/publications/index.jsp)
ISSN 2242-1203 (URL: http://www.vtt.fi/publications/index.jsp)

JULKAISIJA – UTGIVARE – PUBLISHER

VTT
PL 1000 (Vuorimiehentie 5, Espoo)
02044 VTT
Puh. 020 722 111, faksi 020 722 4374

VTT
PB 1000 (Bergsmansvägen 5, Esbo)
FI-2044 VTT
Tfn. +358 20 722 111, telefax +358 20 722 4374

VTT Technical Research Centre of Finland
P.O. Box 1000 (Vuorimiehentie 5, Espoo)
FI-02044 VTT, Finland
Tel. +358 20 722 111, fax + 358 20 722 4374

Kopijyvä Oy, Kuopio 2012

Development of a robust and computationally-efficient active sound profiling algorithm in a passenger car

[Robustin ja laskennallisesti tehokkaan aktiivisen äänenprofilointialgoritmin kehittäminen henkilöautoon]. **Jari Kataja.** Espoo 2012. VTT Science 5. 77 p. + app. 15 p.

Abstract

Active noise control is a technique to cancel unwanted sound using adjustable secondary sound. In active sound profiling, the target is to obtain a certain sound field or profile and the power over specific frequencies can be altered in a desired way, even by amplifying it. Active sound profiling can be used for increasing the sound quality in a passenger car, for example, by modifying the engine noise inside the car cabin.

A fundamental algorithm in active sound profiling is the command-FXLMS (C-FXLMS) algorithm, which is an extension of the famous FXLMS algorithm widely used in active noise control. The computational demand of the C-FXLMS algorithm becomes excessive in multiple-channel systems with engine noise components to be controlled using several loudspeakers and microphones. The most time-consuming part of the C-FXLMS algorithm is the filtering of the reference signals. In order to reduce the computational burden, a new way to modify the reference signals in narrowband systems has been developed in this work. Instead of conventional filtering operations, the new method is based on delaying the sinusoidal reference signals and modifying their amplitude.

The algorithm should work reliably and maintain stability in all operating points. In this work, an adaptive leakage has been developed for the C-FXLMS algorithm to increase its robustness. The objective is to limit the adaptive filter coefficients at frequencies where the phase shift of the plant is large. Such phase shifts occur at resonances, for example, and the performance of the algorithm is drastically degraded. In this work, the C-FXLMS algorithm has also been combined with the EE-FXLMS algorithm so that frequency-independent step sizes can be used. This increases robustness and enables faster tuning of the algorithm.

The developed algorithm has been tested in a simulation model and in an experimental active sound profiling system installed in a car. The results prove that the algorithm works with sufficient accuracy. The convergence is fast and stability is maintained in all operating points.

Keywords active noise control, active sound profiling, command-FXLMS algorithm, sinusoidal signal filtering, adaptive leakage factor

Robustin ja laskennallisesti tehokkaan aktiivisen äänenprofilointialgoritmin kehittäminen henkilöautoon

[Development of a robust and computationally-efficient active sound profiling algorithm in a passenger car]. **Jari Kataja.** Espoo 2012. VTT Science 5. 77 s. + liitt. 15 s.

Tiivistelmä

Aktiivinen melunvaimennus on menetelmä, jossa melua vaimennetaan säädettävällä vastaäänellä. Aktiivisessa äänenprofiloinnissa puolestaan on tavoitteena halutun ääniprofiilin saavuttaminen, jolloin tiettyjä taajuuksia voidaan jopa korostaa vaimentamisen sijaan. Aktiivista äänenprofilointia voidaan käyttää esimerkiksi äänenlaadun parantamiseen henkilöauton sisällä moottoriääntä muokkaamalla.

Aktiivisen äänenprofiloinnin perusalgoritmi on command-FXLMS (C-FXLMS) -algoritmi, joka on kehitetty aktiivisessa melunvaimennuksessa paljon käytetystä FXLMS-algoritmista. C-FXLMS -algoritmi tarvitsee huomattavasti laskentatehoa monikanavaisessa muodossaan, jolloin useita moottoriäänen kerrannaisia muokataan usealla vastaäänilähteellä ja virhesensorilla. Suurimman osan laskentatehosta vie referenssisignaalien suodatus ja tehontarpeen vähentämiseksi on kehitetty uusi menetelmä sinimuotoisten referenssisignaalien suodatukseen. Uusi menetelmä perustuu signaalien viivästämiseen ja amplitudin muokkaamiseen.

Algoritmin luotettavuus on myös tärkeä tekijä. Algoritmin pitää säilyttää suorituskykynsä kaikissa toimintapisteissä ja toimia stabiilisti. Robustisuuden parantamiseksi on C-FXLMS -algoritmiin kehitetty adaptiivinen vuotokerroin. Sen tarkoituksena on rajoittaa adaptiivisia suodinkertoimia toimintapisteissä, joissa järjestelmän vaihevaste muuttuu äkisti. Sellaisia muutoksia tapahtuu esimerkiksi resonanssitaajuuksilla, jotka aiheuttavat algoritmin suorituskyvyn heikkenemistä. Vuotokertoimen lisäksi C-FXLMS -algoritmi on yhdistetty EE-FXLMS -algoritmin kanssa, jolloin samaa askelpituutta voidaan käyttää kaikilla taajuuksilla. Se lisää robustisuutta ja nopeuttaa algoritmin virittämistä.

Kehitettyä algoritmia on testattu simulointimallissa ja henkilöautoon asennetussa aktiivisessa äänenprofilointijärjestelmässä. Tulokset osoittavat, että algoritmi pystyy seuraamaan haluttua ääniprofiilia riittävällä tarkkuudella. Algoritmi myös suppenee nopeasti ja toimii stabiilisti kaikissa toimintatiloissaan.

Avainsanat active noise control, active sound profiling, command-FXLMS algorithm, sinusoidal signal filtering, adaptive leakage factor

Preface

Work related to this licentiate thesis has been carried out in an EU-funded InMAR project (Intelligent Materials for Active Noise Reduction) during 2004–2008 and in a VTT-funded ANRAC project (Advanced Noise Reduction and Alteration Concepts) during 2009. One of the main objectives in InMAR was to develop and construct an active sound profiling system in a passenger car. This objective was achieved in the project. In ANRAC, the system was further enhanced and the new algorithm was developed and tested.

In InMAR, my work included studying active sound profiling algorithms and their implementation in Matlab/Simulink programming and simulation environment. The main work described in this licentiate thesis was done in ANRAC, in which the existing active sound profiling algorithm was enhanced to be more robust and computationally-efficient. My tasks included the development of the alternative method for reference signal filtering and the adaptive leakage factor. Together with my team members, the algorithm was programmed and its operation was evaluated in a simulation model. Finally, the algorithm was transferred to an experimental active sound profiling system installed in the passenger car. Implementation of the system and the experiments were mostly carried out by my team members. They also successfully tested the performance of the developed active sound profiling system.

Jari Kataja
Tampere, 22nd March 2012

Contents

List of abbreviations

ANC	Active Noise Control
ANE	Adaptive Noise Equaliser
ANF	Adaptive Notch Filter
ASP	Active Sound Profiling
CAN	Controller Area Network
C-FXLMS	Command-FXLMS
DSP	Digital Signal Processing or Processor
EE-FXLMS	Eigenvalue-Equalised FXLMS
ECU	Electronic Control Unit
FFT	Fast Fourier Transform
FIR	Finite Impulse Response
FXLMS	Filtered-Reference LMS
IIR	Infinite Impulse Response
LMS	Least-Mean-Squares
LTI	Linear and Time-Invariant
LUT	Lookup Table
RPM	Revolutions Per Minute

List of symbols

β	smoothing factor (in adaptive leakage factor) or gain parameter (in adaptive noise equaliser)
$\delta\varphi$	difference in phase response (in adaptive leakage factor)
λ	leakage factor
μ	step size
$\xi(n)$	mean-square error
τ	delay [s]
φ	phase response
ω	angular frequency
Δ	delay [samples]
$\boldsymbol{\Lambda}$	leakage factor matrix
a	scaling constant (in adaptive leakage factor)
$c(n)$	command signal
$d(n)$	disturbance
$e(n)$	error signal
$e'(n)$	modified error or pseudo-error signal
f_0	fundamental engine rotation frequency [Hz]
f_s	sampling frequency [Hz]
$\mathbf{s}(n)$	impulse response of the secondary path
$w(n)$	adaptive filter weight
$x(n)$	reference signal
$x_1(n)$	reference sine

$x_2(n)$	reference cosine
$x'(n)$	filtered reference signal
$y(n)$	output signal
$y'(n)$	filtered output signal
A	magnitude
J	number of reference signals or sinusoids to be cancelled
K	number of output signals or secondary sources
L_w	adaptive filter length
L_s	length of the secondary-path model
M	number of error signals or error sensors
$P(z)$	primary path
$S(z)$	secondary path
$\hat{S}(z)$	secondary-path model
$\hat{S}(j\omega)$	FFT of the secondary-path model
T	sampling period [s]
$\boldsymbol{W}(n)$	matrix of adaptive filter weights
$W(z)$	adaptive filter
$\boldsymbol{W}_1(n)$	adaptive notch filter weights for reference sines
$\boldsymbol{W}_2(n)$	adaptive notch filter weights for reference cosines

1. Introduction

1.1 Fundamentals of active noise control

Active noise control is a technique for attenuating unwanted acoustic disturbances by controllable secondary sources. The outputs of the secondary sources are arranged to interfere destructively with the disturbance from the original primary source. Successful application of active noise control requires that there is both a good spatial and a good temporal matching between the field due to the secondary sources, and that due to the primary source. The requirement for spatial matching gives rise to clear limits on the upper frequency of active noise control, due to the physical requirement that the acoustic wavelength must be small compared with the zone of control. The requirement for temporal matching requires a signal processing system that can adapt to changes in the primary noise. Active noise control works at low frequencies, up to 500–1000 Hz. where the acoustic wavelengths are long and passive noise control methods are inefficient. Active noise control is thus an excellent candidate for attenuating low frequency noise if the requirements mentioned above are closely studied [1], [2].

The components of an active noise control system include the secondary source, at least one sensor and the control system which is typically an analogue filter or a digital signal processor. The secondary source can be a loudspeaker or a structural actuator producing vibration. The sensors are microphones, accelerometers, tachometers or optical sensors. The primary noise can be broadband or narrowband. Broadband noise is caused, for example, by turbulence which is totally random. The energy of broadband noise is distributed over a large frequency band. Examples of broadband turbulence noise are low-frequency noise from jet planes and road noise inside a moving vehicle. By contrast, narrowband noise concentrates most of its energy at specific frequencies. Narrowband noise is related to rotating or repetitive machines and is periodic or nearly periodic. Examples of narrowband noise sources include internal combustion engines, turbines, compressors, pumps and fans [3].

The concept for active noise control was first introduced in 1936 by Paul Lueg, who patented his idea that unwanted sound in a duct could be cancelled with a loudspeaker [4]. In the 1950's, the first active noise control systems were constructed. After that, the development of active noise control was halted for twenty

years because of the lack of required technology. With the existing manual analogue techniques, it was extremely difficult to produce secondary sound that had the amplitude and phase required to attenuate the primary noise. The advent of the microprocessor in 1970's made it possible to apply digital signal processing techniques and devices for active noise control and construct practical active noise control systems. Since 1970's digital systems have developed enormously and become more affordable. Nowadays, active noise control has various applications, from active hearing protectors to active control of cabin noise inside aircrafts. Depending on the application, active noise control can be implemented using different control strategies, feedforward or feedback [5].

1.1.1 Feedforward control

Feedforward control is typically used when time-advanced information about the primary noise can be obtained. This information is called as the reference signal and is obtained by a reference sensor located near or inside the primary noise source. A feedforward active noise control system is shown in Figure 1. The reference signal is fed to the controller and processed to form an output signal that cancels the primary noise. A feedforward active noise control system is typically adaptive so that the controller is automatically tuned if the primary noise varies. In an adaptive system, an error sensor is used for detecting the residual noise. The signal from the error sensor, called as the error signal, is used to adapt the controller [3].

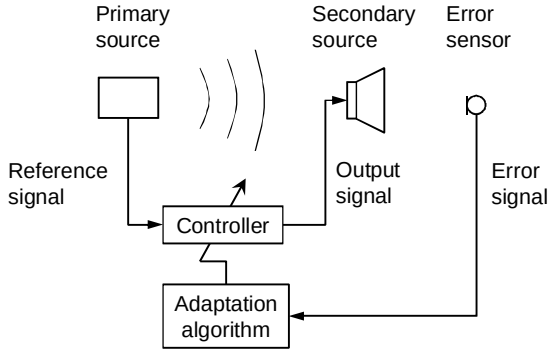

Figure 1. Feedforward active noise control system.

As an open-loop system, feedforward control is inherently stable. The algorithm can become unstable, however. Reference signal has to be coherent with the disturbance. Drawbacks are the acoustic feedback from the secondary source to the reference sensor if an acoustic reference sensor is used. The reference sensor has to be located far enough from the secondary source to ensure causality. This means that the processing time of the controller has to be less than the propagation time of the primary sound to the secondary source [3].

The feedforward active noise control was first proposed in 1956 by Conover, who worked with active reduction of acoustic noise from large mains transformers [6]. The most famous application of active noise control is probably the feedforward active control of noise propagating in a ventilation duct. This application has been studied in various books and articles (e.g. in [1], [2], [3]) and also by the author [7], [8]. Even one of the fundamental papers about the famous and widely-used filtered-reference least-mean-squares (FXLMS) algorithm deals with the active noise control in a duct [9]. Active noise control in a ventilation duct is illustrated in Figure 2. With a simple single-channel system containing only one reference, one error sensor and one secondary source, noise propagating downstream from the error sensor location can be attenuated if the diameter of the duct is small compared to the acoustic wavelength of the noise. Controlling higher order modes require a more complicated multichannel system [10].

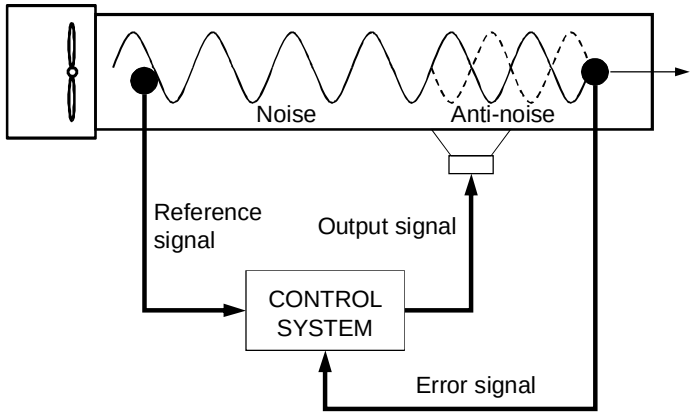

Figure 2. Active noise control in a ventilation duct.

Feedforward active noise control has also been applied for attenuating engine noise inside car and aircraft cabins. Since a well correlated reference signal can be obtained by monitoring the engine, active noise control has typically been addressed with feedforward control. An active system in a cabin is a multichannel system containing several secondary sources and error sensors. In car industry, feedforward active control of engine noise has been applied to production cars by Lotus, Nissan Bluebird, Honda in variable cylinder management systems and hybrid vehicles and Toyota in hybrid vehicles [11], [12]. In propeller aircraft such as B.Ae. 748, Saab 340/2000, C130 Hercules and King Air series, active systems have been installed to attenuate propeller-induced cabin noise [13], [14]. Propeller-driven aircraft are prone to high noise levels which are related to the blade passage frequency of the engine. Active control of broadband noise inside jet aircraft has also been recently studied [15], [16]. Tractor and moving machinery cabin noise has been addressed in [17] and [18].

1.1.2 Feedback control

In feedback control, the error signal is fed back to the controller and used to process the output signal. A feedback active noise control system is shown in Figure 3.

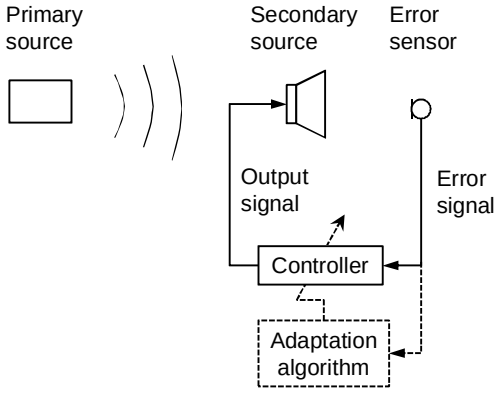

Figure 3. Feedback active noise control system.

Feedback systems are typically fixed analogue systems or adaptive digital systems. A fixed analogue system can be efficiently built using analogue electronics. Another advantage is that no reference signal is required. Feedback systems have, however, several serious disadvantages. One disadvantage is that the control is not selective, i.e. any signal will be attenuated, not just those correlated with the reference signal. Another disadvantage is that the error sensor must be placed close to the secondary loudspeaker since the delay from the secondary source to the error sensor has to be kept minimal. The performance of feedback systems is limited by the stability of the feedback loop. Feedback systems may also suffer from spillover, also called waterbed effect, which causes amplification of noise outside the attenuated frequency band [1], [19].

The theory of feedback was first applied to active noise control by Olsen and May in 1953 [20]. They developed a device known as “electronic sound absorber” which improved sound absorption at low frequencies. Due to the limited distance between the secondary source and the error sensor, feedback active control is used in applications in which the zone of silence, i.e. the controlled space around the error sensor, can be relatively small. Applications in which feedback active control has proven to be useful are active headsets, active headphones and active hearing protectors. The principle of an active headset is illustrated in Figure 4. Such devices can be based on analogue or digital feedback control [21], [22]. Another area in which feedback active control has been studied is improvement of structural sound insulation by active means. For example, the sound insulation of aircraft cabin walls can be improved by using active panels [15].

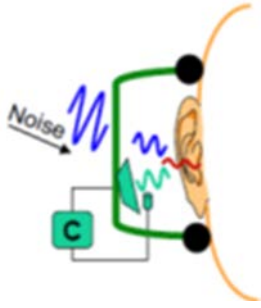

Figure 4. Active headset [22].

1.2 Active noise control in cars

The acoustics of cars have always been an important marketing issue to car manufacturers, especially in luxury vehicles. Since 1980's, active noise control has been applied to cars and some systems have even reached the mass-production level. There were several problems with the early ANC systems in cars, however, that prevented a broader use of such systems. The reasons were technical (absence of long-term experience, lack of understanding in robustness and reliability), commercial (cost of components) and legal (patent right issues). At the same time, passive noise control methods were successfully applied, although they usually added weight and fuel consumption [11], [12], [23].

During the last two decades, the situation has changed to favour the active methods. The concept of mechatronics (coupling electronics and signal processing with mechanical systems) has become more accepted in general. The cost for ANC systems has dropped dramatically, due to cheaper DSP hardware and the possibility to integrate the active system with the other systems already existing in cars (audio system, CAN bus). The loudspeakers may need to be upgraded for low frequency active control use. The microphones and associated wiring remain an additional cost for active control systems on some vehicles, although others already have microphones fitted as standard, for hands-free telephone operation, for example. The general experience with the ANC technology has grown and many long-standing issues with respect to robustness have been solved. The patents of the late 1980's and early 1990's have also expired. An important overall trend in the automotive industry is to improve the fuel efficiency of the vehicles by reducing weight. Reducing the weight of the body panels inevitably degrades their ability to attenuate low frequency noise and thus provides a real opportunity for active systems to be used for controlling the low frequency noise and vibration without significantly increasing weight [11], [12], [23].

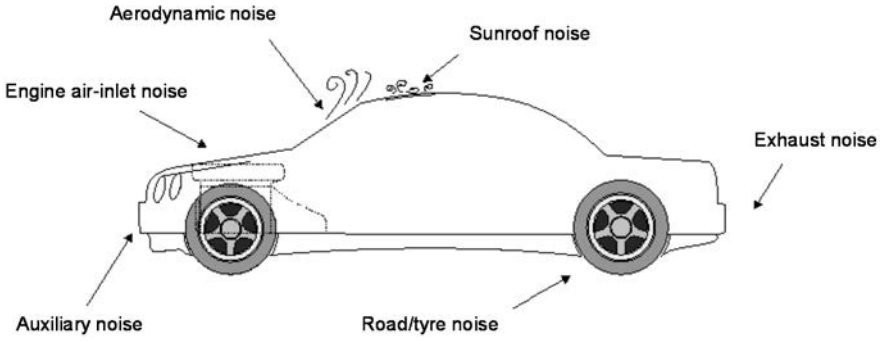

Figure 5. The sources of noise associated with a car [24].

There are many sources of noise associated with a car as can be seen in Figure 5. They can be divided into narrowband harmonic and broadband random noise. Narrowband noise sources include the engine, drive train, air intake, exhaust and auxiliary systems such as the radiator fan. Broadband noise is caused by road-tyre interaction and aerodynamic wind noise [24].

1.2.1 Control of narrowband noise

The fundamental source of narrowband noise in a car is the engine. Engine noise is radiated into the passenger cabin mainly via the air intake manifold. Other transfer paths include the bonnet panel through the wind screen, the bulkhead between the engine and the cabin and from the exhaust. The spectrum of the engine-generated noise is composed of the harmonics of the engine firing frequency and engine rotation. In a four-cylinder car, the engine firing frequency is at twice the engine rotation rate. This second harmonic of the engine rotation frequency is called as the second engine order. The engine noise excites acoustic modes inside the passenger cabin, and in most mid-sized four-cylinder cars the dominant problem is the boom excited by the second engine order. A spectrum of the engine noise inside a car is given in Figure 6, in which the first order, the second order and other dominant orders are marked. The engine rotation rate is about 2000 RPM so the second engine order is at 2000/60*2 ≈ 67 Hz.

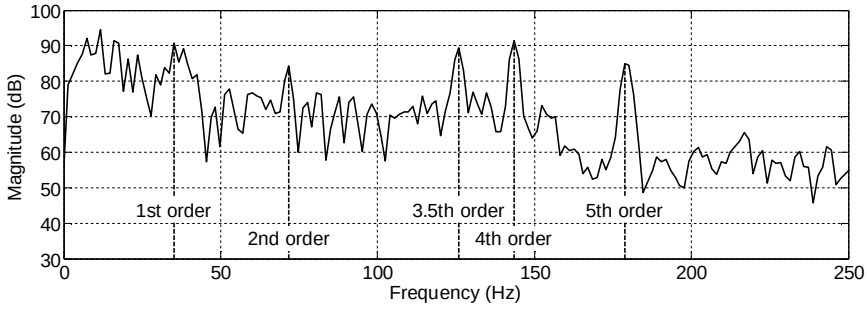

Figure 6. Spectrum of the engine noise inside a car.

For active control of the narrowband noise, the secondary sources can be located either in the cabin or at the air intake or exhaust outlet. With the latter approach, engine noise can be controlled for observers outside the car, not just those inside the cabin. Such system usually requires only one secondary source and a few error sensors, while a system inside the cabin requires several sources and sensors [24].

During the last decades, several systems for active engine noise cancellation inside the passenger cabin have been developed for production vehicles. The systems include:

- A system developed for a 1.1 litre 4-cylinder car by Lotus Engineering and ISVR in 1988. The system used 4 loudspeakers located in the dashboard and front doors (integrated into the car audio system) and 8 microphones mounted in the head lining. It controlled the engine firing frequency and its harmonics, and reductions of about 10 dB were measured in the front seats above about 3000 RPM. The improvement in the overall A-weighted sound pressure level was 4–5 dB. Reductions at lower speeds were measured in the rear due to the suppression of the first longitudinal acoustic mode, having a nodal line near the front passengers' heads [12].
- An almost identical system with the previous one implemented and mass-produced by Nissan for Bluebird model in 1992 to cancel the second order engine boom. The system was separated from the car audio system and was relatively expensive. The car was available for a short time in the Japanese market only and did not find any direct successors [12], [23], [24].
- An active system introduced by Honda in 2003 for a 3l iVTEC V6 engine with Variable Cylinder Management. In this engine, 3 of the 6 cylinders are temporarily deactivated. In the active system, active engine mounts are combined with an interior ANC system, which is integrated with the audio system. It uses 2 interior microphones but only 1 output signal which is distributed to both front and rear speakers with a fixed filtering. The ANC system focuses on the 1.5^{th} engine order below 60 Hz. This system has been later utilised in many other Honda luxury models [23].

- A 3-microphone 3-speaker system by Toyota in its 2008 Crown Hybrid made for Japanese market only. The feedforward system is illustrated in Figure 7 where the controller, ECU, is connected to the audio system of the car. During slow city drives of between 20 to 40 km/h where the engine RPM is between 1000 to 3000 RPM, muffled noise at 50–150Hz can typically be transmitted to the car, impairing the car's interior comfort. The active system is able to reduce noise levels by 5–8 dB [25].
- An ANC system by GM in its 2010 GMC Terrain and the Chevrolet Equinox SUV, having 2 microphones and 1 loudspeaker [23].

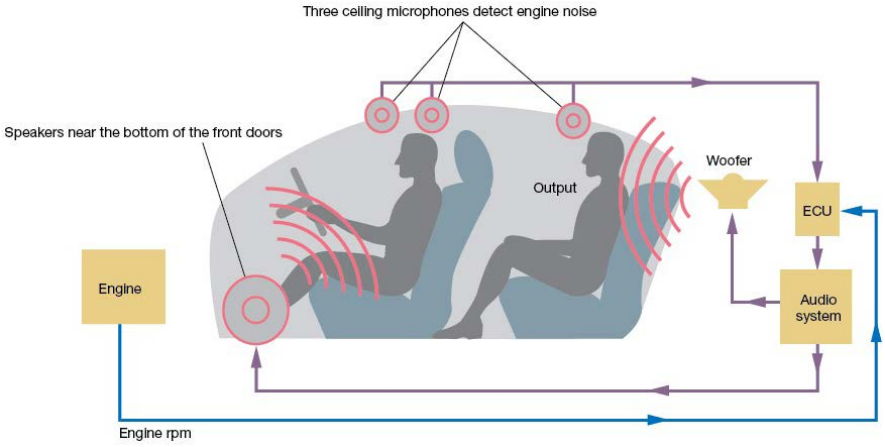

Figure 7. Active noise control system for attenuating engine noise by Toyota [26].

Several experimental systems for engine noise cancellation inside vehicles have also been constructed. They include a system with 4 loudspeakers and 4 error sensors in a passenger car [27], a system using 6 secondary sources and 8 error sensors for a van [28], and a system in a truck cabin mock-up with 3 secondary sources and 3 error sensors [29].

Active systems for controlling the noise radiating from the engine air intake orifice has been developed and tested by Siemens Automotive [30]. The secondary source was placed inside the air intake and the error sensor was located near the loudspeaker. The feedforward system was tested in several 6- and 8-cylinder cars, with the reference signal taken from a tachometer in the engine. The radiated engine noise from the induction system was effectively eliminated over the control bandwidth, the power draw of the loudspeaker was minimal and the flow restriction of the actively controlled inlet was significantly reduced compared to the production air induction system. A similar system was developed by Hyundai Motors and Seoul National University [31]. An active intake control system for a 4-cylinder engine was constructed, with two loudspeakers placed on the side of the intake duct. As a result, maximum reduction of 30 dB was measured at the dominant 2nd

order and 10 dB at the 3rd and 4th orders under stationary conditions and 20 dB at the 2nd order under sweeping conditions. Efforts have also been conducted to enhance robustness of the control algorithm of the active intake system under rapid acceleration [32].

The third way to control the engine noise is the active control of exhaust noise. With this approach, the active system can reduce the sound power output from the exhaust and may also improve the performance of the car by removing the need for current passive silencers [24], [33], [34]. Conventional silencers involve the use of a muffler system, which contains sound absorbing materials. It induces flow restriction and increased back pressure, which has a direct effect on the performance of the engine. Active exhaust noise control systems can be hybrid, including a simplified passive muffler and an active muffler, or totally active. Typically the systems include loudspeakers as the secondary source but also an electrically controlled valve has been used as the source [35].

Active vibration control has also been applied to vehicles for narrowband noise reduction. In vehicles with large engines and heavy duty trucks, the vibration from the engine can cause low-frequency booming inside the passenger cabin. In order to tackle this problem, active engine mounts adjusting the stiffness of the damping properties of the mount has been developed. Active engine mounts has been mass-produced by Toyota and Nissan. In 1997, Toyota developed an active mount based on feedforward control for reducing low-frequency idling boom in a V6 recreational vehicle. Nissan developed a similar system for diesel engines in 1998 [11], [24].

1.2.2 Control of broadband noise

Road noise is caused by interactions between the tyres of the car and irregularities in the road surface. Road noise is a strong contributor of unwanted sound power in many cars. The main processes of noise generation occurring within a rotating tyre are vibration of the tyre structure and acoustic phenomena caused by the tyre-road interaction. These noise sources combine to produce a broadband spectrum, which contains large amounts of energy in the sub-audio range [36]. The vibration of the tyres, as with most noise sources in a car, take more than one route into the passenger cabin. One such route is acoustic noise radiating from the tyres, which is amplified by the horn effect caused by the geometry of the tyre and the road, being channelled up through body panels on the car. Another route is structure-borne, in which vibration from the tyres is transmitted through the suspension and into the body structure. The primary path for the structural transmission is through the suspension mounts. Both transmission paths into the cabin result in the vibration of the car body, which leads to excitation of specific modes of different parts of the car. These include bending and torsional vibration of the whole body, “ring mode” vibration of the passenger compartment and bending modes of the engine and transmission, cabin acoustic resonances and body panel plate modes [24].

Over the years many active control systems have been developed to deal with the problem of road noise [11], [12], [37], [38], [39], [40]. Many of the systems used feedforward techniques, with reference signals derived from accelerometers on the vehicle suspension and body [12]. In order to obtain reasonable levels of active control, it was found that about six reference signals were required. This is because the tyre vibration is relatively uncorrelated in its various degrees of freedom, and reference signals have to be used for all the significantly contributing sources. Although many of these systems were experimentally successful, there is often a long way to go from initial development to the production line. One system that has made it to production was developed at Honda in 2000 [40]. The system is based on combined feedforward-feedback control so that a feedback loop is used to control noise in the front seats of the passenger cabin, while the error microphone of the feedback system provides a reference signal for a fixed feedforward system to control the noise in the rear seats. The whole system is incorporated into the music system in a Honda Accord station wagon. This system is designed to control a 40–50 Hz boom caused by the excitation of the first longitudinal acoustic mode by road vibration. Estate cars are particularly prone to this phenomenon due to the increased length of the passenger compartment. The control system configuration is able to achieve a 10 dB reduction at low-frequency road noise in the region of the front passenger seat. The commercial success of this system is due to the reduction in cost that has been made over previous ANC car systems. This has been achieved by the elimination of expensive DSP hardware, by using feedback and fixed forward control strategies, rather than the more expensive adaptive feedforward control.

Wind noise is a less significant source of random noise at low speeds than road noise, but becomes noticeable at high road speeds, approximately above 90 km/h. Wind noise is created by many different aerodynamic structures over the surface of a car, which excite a wide range of frequencies. These vary from low frequency noise produced by turbulence due to large-scale flow separation (6–100 Hz), to vortex shedding (at 100–500 Hz and 1000 Hz), leaking window seals (at 1000–8000 Hz) and turbulent flow over door and bodywork gaps (2000–4000 Hz). Preliminary work was conducted by Lotus engineering and the ISVR (Institute of Sound and Vibration Research at University of Southampton) in the early 1990's to create an adaptive feedback control system to reduce sound levels inside the cabin due to a low frequency tonal boom at a specific resonant road speed brought about by open sunroofs. The frequency of this resonance is dependent on both the volume of the cabin cavity and the size of aperture created by the open sunroof. At a frequency of 25 Hz, a reduction of 30 dB was achieved, although a slight increase in broadband noise was experienced [24].

1.3 Active sound profiling in cars

A recent trend with the active systems in cars is the active control of the overall sound quality, instead of the pure sound level. Many cases arise in the control of

sound quality when it is not necessary to completely cancel the sound field, but it is desirable to retain or even enhance specific frequencies of a given spectrum. This is often the case in the car industry, where the acoustic impression of a car can be altered by enhancing some engine orders and reducing others. The active control of sound quality generally involves a control system that drives the microphone signals inside the car towards a target, or command signal, instead of minimising it. Depending on the source, this has been termed *noise equalisation*, *sound design*/*synthesis*, *sound*/*noise profiling* and *sound quality control*. Recent trends also include the use of active control systems to provide a smoothly changing sound profile with engine speed, but with an emphasis on sporty sound during acceleration. Characteristics of different engine types could be an excellent starting point for designing the sound profile of a car. Depending on the number of cylinders and the engine configuration (straight or V-shaped), the engine noise may sound growly or smooth [41]. With sound profiling, it could also be possible to provide an acoustic environment inside the vehicle that encourages the owner to drive in a more fuel-efficient way, for example [12], [24].

Traditionally, enhancing the subjective engine sound quality has been tackled with passive, mechanical solutions while active approaches have not been taken into considerations even if they were viable and easier to implement [23]. Active sound profiling requires a substantial amount of digital signal processing and the hardware is often too expensive to be accepted by car manufacturers. During the last years, however, car manufacturers including Volkswagen, Mini, BMW and Audi have started to utilise active solutions for improving sound quality [23]. A prototype system has also been constructed in a Ford C-Max [42].

Active control of sound quality may become more important with the use of hybrid vehicles and in vehicles with variable cylinder management [43]. The quality of the sound inside these vehicles changes with the power source, which can be disconcerting to the driver. In conventional vehicles, certain noise phenomena are masked by the engine noise. In situations where the combustion engine is turned off in a hybrid vehicle, these noise components can become dominant and annoying [44]. This is a particular problem in electrical vehicles [45]. It is not yet clear how the interior noise of an electrical vehicle should sound like, but active sound profiling is an option for artificially generating the engine noise both inside and outside the vehicle. In hybrid concepts, the driving condition is often decoupled from the operation state of the combustion engine, which leads to unusual and unexpected acoustical behaviour. Pedestrian safety is also an issue with hybrid and electrical vehicles, since the electric motor operates nearly silently and the vehicle may not be heard by pedestrians. Lotus Engineering has addressed this problem in hybrid vehicles by projecting engine sounds externally to improve pedestrian safety [46]. The system also employs active noise cancellation to reduce noise inside the cabin.

2. Feedforward active noise control

Feedforward control has already been introduced in Chapter 1.1.1. The objective of this chapter is to describe the algorithms used for adapting the feedforward controller in single-channel and multi-channel systems. The stability of the algorithms is also analysed.

2.1 Adaptation algorithms

Algorithms for adapting the feedforward controller are considered. The algorithms are based on the famous LMS algorithm which minimises the mean-square value of the error signal. In active noise control systems, the influence of the secondary path from the secondary source to the error sensor has to be taken into account. The secondary path influences both the algorithm itself and the stability of the system.

2.1.1 LMS algorithm

When discussing about adaptive filtering, the LMS algorithm is typically referred to as a standard algorithm. The LMS algorithm is based on the method of steepest descent in which the adaptation is done recursively using the gradient vector of the squared error. The LMS algorithm for adaptive noise cancellation is illustrated in Figure 8. The objective is to cancel the disturbance signal $d(n)$ with the output of the adaptive filter, $y(n)$. The error signal $e(n)$, which is the sum of the disturbance and the adaptive filter output, is used for adapting the adaptive filter $W(z)$ so that the error is minimised. In the adaptation, also the reference signal $x(n)$ is needed. The reference signal contains information about the disturbance and thus correlates with it. If the reference signal is equal to the disturbance, the disturbance can be totally minimised. Otherwise, the disturbance is cancelled only at the frequencies where the signals correlate.

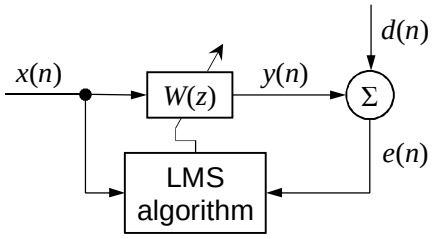

Figure 8. LMS algorithm.

The error signal is expressed as

$$e(n) = d(n) + y(n) = d(n) + \boldsymbol{w}^T(n)\boldsymbol{x}(n), \tag{1}$$

where $w(n)$ is the filter coefficient vector and $x(n)$ is the reference signal vector. In signal processing applications, the error signal is typically expressed as the difference of the disturbance and the output signal. In acoustic applications, however, the signals can be considered as interfering sound fields and summation of the signals is thus preferred.

The mean-square error can be written as

$$\xi(n) = E[e^2(n)] = E[d^2(n)] + 2\boldsymbol{p}^T\boldsymbol{w}(n) + \boldsymbol{w}^T(n)\boldsymbol{R}\boldsymbol{w}(n), \tag{2}$$

where $\boldsymbol{p}$ is the cross-correlation vector between the disturbance and the reference signal and $\boldsymbol{R}$ is the autocorrelation matrix of the reference signal.

Equation 2 requires the computation of the cross-correlation vector and autocorrelation matrix, which becomes too time-consuming in a practical system with nonstationary signals. To overcome this problem, the method of steepest descent is employed. The filter coefficients are updated towards the negative gradient at each time step as

$$\boldsymbol{w}(n+1) = \boldsymbol{w}(n) - \frac{\mu}{2}\nabla\xi(n), \tag{3}$$

where μ is the step size used for controlling the stability and the rate of convergence.

An instantaneous version of the squared error, $e^2(n)$, is used to estimate the mean-square error $\xi(n)$. The gradient estimate then becomes

$$\nabla\hat{\xi}(n) = 2[\nabla e(n)]e(n) = 2\boldsymbol{x}(n)e(n). \tag{4}$$

Substituting Equation 4 into Equation 3 as the gradient gives

$$\boldsymbol{w}(n+1) = \boldsymbol{w}(n) - \mu\boldsymbol{x}(n)e(n), \tag{5}$$

which is called the LMS algorithm [47].

The step size of the LMS algorithm has to be chosen so that

$$0 < \mu < \frac{2}{L_w P_x}, \tag{6}$$

where $P_x = E[x^2(n)]$ is the power of the reference signal and L_w is the length of the filter coefficient vector [3]. There are also other rules for choosing the step size, giving a smaller upper bound, but generally the factors restricting the step size are the filter length and the reference signal power.

2.1.2 FXLMS algorithm

The LMS algorithm cannot be used in active noise control as such, however. The adaptive filter is followed by the secondary path from the secondary source to the error sensor. The output signal is thus modified by the secondary-path transfer function before it reaches the cancellation point at the error sensor. In active noise control, the error signal becomes

$$\begin{aligned} e(n) &= d(n) + y'(n) = d(n) + \boldsymbol{s}(n) * y(n) \\ &= d(n) + \boldsymbol{s}(n) * [\boldsymbol{w}^T(n)\boldsymbol{x}(n)], \end{aligned} \tag{7}$$

where $\boldsymbol{s}(n)$ is the impulse response of the secondary path.

The gradient term in the LMS algorithm is then expressed as

$$\nabla\hat{\xi}(n) = 2[\nabla e(n)]e(n) = 2[\boldsymbol{s}(n) * \boldsymbol{x}(n)]e(n) = 2\boldsymbol{x}'(n)e(n), \tag{8}$$

where $\boldsymbol{x}'(n)$ is called the filtered reference signal vector. Substituting the gradient term into the equation of the steepest descent algorithm gives

$$\boldsymbol{w}(n+1) = \boldsymbol{w}(n) - \mu\boldsymbol{x}'(n)e(n), \tag{9}$$

which is the filtered-reference (or filtered-*x*) LMS (FXLMS) algorithm [3], [9].

The block diagram of the FXLMS algorithm is given in Figure 9. The secondary path is denoted as $S(z)$ and the secondary-path estimate as $\hat{S}(z)$.

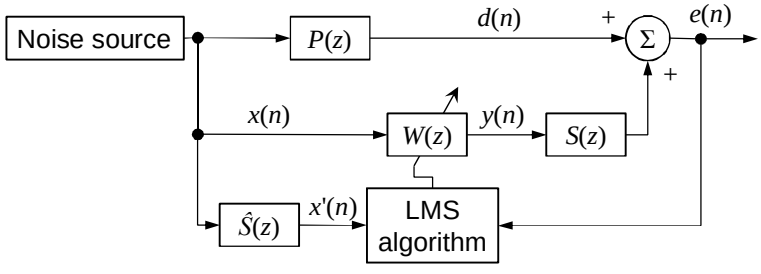

Figure 9. Block diagram of the filtered-x LMS algorithm.

It has been empirically found that the maximum step size for the FXLMS algorithm is approximately

$$\mu_{\max} = \frac{1}{P_{x'}(L_w+\Delta)}, \tag{10}$$

where $P_{x'} = \mathrm{E}[x'^2(n)]$ is the power of the filtered reference signal, L_w is the length of the adaptive filter and Δ is the overall delay in the secondary path in samples [5]. The delay in the secondary path is the most significant factor influencing the dynamic response of the feedforward active noise control system. Therefore, the delay should be kept small by decreasing the distance between the secondary source and the error sensor and reducing the delay of the control system components. In practice, the FXLMS algorithm is stable even if the adaptive filter coefficients change significantly on a timescale associated with the dynamic response of the secondary path [3].

2.1.3 Eigenvalue-equalised FXLMS algorithm

One of the limitations of the FXLMS algorithm is that it exhibits frequency-dependent convergence behaviour. This can lead to a significant degradation in the overall performance of the system if the noise is time-varying. In an engine, for example, the frequency changes as the speed of the engine varies during operation. If the frequency associated with the engine speed changes faster than the algorithm can converge and attenuate that particular frequency, the performance of the ANC system will be degraded. Poor performance is expected at frequencies where the convergence of the algorithm is slow.

The frequency-dependent convergence is related to the eigenvalues of the autocorrelation matrix of the filtered reference signal. The step size of the FXLMS algorithm has to be chosen so that

$$0 < \mu < \frac{2}{\lambda_{\max}}, \tag{11}$$

where $\lambda_{\max}$ is the largest eigenvalue of the reference signal autocorrelation matrix [3]. The selection of the step size is thus based on the maximum eigenvalue in the frequency range of interest, and performance is degraded at frequencies where the eigenvalues are small. The filtered reference signal is obtained by filtering the reference signal with the secondary-path model. If all frequencies in the reference signal were equally weighted, the maximum step size could be determined by the magnitude of the secondary-path model $\hat{S}(z)$. In order to ensure stability, the step size has to be chosen based on the frequency where the magnitude of $\hat{S}(z)$ is the largest [48]. This slows down the convergence at frequencies where the magnitude of $\hat{S}(z)$ is small. The eigenvalues of the autocorrelation matrix and the magnitude of $\hat{S}(z)$ are related so that the maximum eigenvalue occurs where the response of $\hat{S}(z)$ is large. Manipulating the magnitude coefficients of $\hat{S}(z)$ thus modifies the eigenvalue spread. If the magnitude coefficients were flat over frequency, the eigenvalue spread should also be more flat over frequency. In [17], a method for flattening the magnitude coefficients has been described. It can be summarised as

1. Obtain the time domain impulse response $\hat{\boldsymbol{s}}(n)$ for each secondary path through an offline system identification process.
2. Take the fast Fourier transform (FFT) to obtain $\hat{S}(j\omega)$.
3. Divide each value in the FFT by its magnitude and then multiply by the mean value of the FFT:

$$\hat{S}_{new}(j\omega) = \frac{\hat{S}(j\omega)}{|\hat{S}(j\omega)|}\text{mean}\left(\hat{S}(j\omega)\right) \tag{12}$$

4. Compute the inverse FFT to obtain a new $\hat{\boldsymbol{s}}(n)$.

The new $\hat{S}(z)$ can then be used in the FXLMS algorithm for filtering the reference signal. The algorithm is called as the eigenvalue-equalised FXLMS (EE-FXLMS) algorithm [17], [49].

In the previous process, the resulting $\hat{S}(z)$ has an inverted phase response if the mean value of the FFT is negative. This leads to unstable operation of the FXLMS algorithm. It is thus proposed that the modified $\hat{S}(z)$ is calculated as

$$\hat{S}_{new}(j\omega) = \frac{\hat{S}(j\omega)}{|\hat{S}(j\omega)|}\text{mean}\left(|\hat{S}(j\omega)|\right) \tag{13}$$

so that, instead of taking the mean of the FFT, the mean value of the magnitude of the FFT is used.

Further development of the EE-FXLMS algorithm has been carried out in [50]. A genetic algorithm has been used for optimizing the magnitude coefficients of $\hat{S}(z)$ in order to obtain a more uniform eigenvalue span. The reference signal was assumed to consist of several tones that have a constant frequency and amplitude. Therefore, if the frequency or amplitude changes, the optimal performance of the algorithm is lost.

2.1.4 Leaky FXLMS algorithm

In order to increase the robustness of the FXLMS algorithm, a leakage factor can be introduced to limit the output of the adaptive filter. The update equation of the leaky FXLMS algorithm is

$$\boldsymbol{w}(n+1) = \lambda\boldsymbol{w}(n) - \mu\boldsymbol{x}'(n)e(n), \tag{14}$$

where λ is the leakage factor with $0 < \lambda \leq 1$.

Using the leakage factor, divergence of the filter coefficients can be avoided and the stability of the FXLMS algorithm can be improved. The leakage factor should be kept larger than $1\text{-}\mu$ in order to maintain an acceptable level of performance [3].

2.2 Multichannel control

In multiple-channel active noise control systems, several secondary sources and error sensors are used. Multichannel systems are used for controlling three-dimensional enclosure like a car or aircraft cabin. Selecting the number of secondary sources and error sensors as well as the optimisation of their locations has been widely studied [1], [2], [3]. In principle, the number of secondary sources is related to the acoustic modes that have been excited. In an enclosure with a reverberant noise field, it is difficult or even impossible to obtain a reasonable estimate of the reference signal. In a cabin where noise is engine-related, the reference signal can be measured from the engine using a tachometer, for example. Control of noise field in an enclosure or free space may be global or local. With the local approach, noise is controlled locally around the error sensors and noise level may even be increased in some other areas. In a car cabin, local control is typically used with error sensors positioned near the passengers' heads. Several reference signals are needed if the harmonics of the engine noise are controlled separately. This is typically the case in active sound profiling where the level of each harmonic is driven to a pre-determined value, not zero.

A simplified block diagram of the multichannel ANC system is illustrated in Figure 10. The reference signals form a reference signal vector $\boldsymbol{x}(n)$ which drives the $K \times J$ adaptive filters $\boldsymbol{W}(n)$ from the J reference inputs to the K secondary sources. The primary noise field $\boldsymbol{d}(n)$ is cancelled by minimizing the sum of squares of residual noise measured by M error sensors. The components of the error signal vector $\boldsymbol{e}(n)$ are formed by the M error sensor outputs. The matrix $\hat{\boldsymbol{S}}$ represents estimates of the $M \times K$ secondary paths from the K secondary sources to the M error sensors.

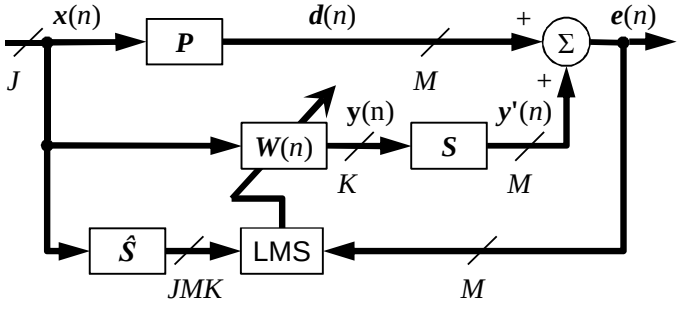

Figure 10. Multiple-channel ANC system using the FXLMS algorithm.

The multichannel FXLMS algorithm for updating the adaptive filters can be written as

$$\boldsymbol{w}_{kj}(n+1) = \boldsymbol{w}_{kj}(n) - \mu \sum_{m=1}^{M} \boldsymbol{x}'_{jkm}(n) e_m(n) \tag{15}$$

for k = 1,2,…,K and j = 1,2,…,J. There are JKM filtered reference signals that are calculated as

$$\boldsymbol{x}'_{jkm}(n) = \hat{\boldsymbol{s}}_{mk}(n) * \boldsymbol{x}_j(n), \tag{16}$$

where $\hat{\boldsymbol{s}}_{mk}(n)$ is the impulse response of the secondary path model from kth output to mth error sensor.

The output to the kth secondary source is

$$y_k(n) = \sum_{j=1}^{J} y_{kj}(n), \tag{17}$$

where

$$y_{kj}(n) = \boldsymbol{w}_{kj}^T(n)\boldsymbol{x}_j(n) \tag{18}$$

is the output of the adaptive filter from jth reference to kth output [51].

The multichannel FXLMS algorithm requires a significant amount of computation, especially if long adaptive filters and secondary-path models are used. At each time step, there are JKM reference signals to be filtered, JK adaptive filters to be updated and K output signals to be computed. The computational demand of the algorithm is summarised in Table 1.

Table 1. Computational demand of the multichannel FXLMS algorithm.

	Multiplications	**Additions**
Filter adaptation	$JK(L_wM + L_w)$	$2JKML_w$
Output computation	JKL_w	$JK(L_w - 1)$
Reference signal filtering	$JKML_s$	$JKM(L_s - 1)$

2.3 Secondary-path modelling

The FXLMS algorithm and its variants require the model of the secondary path. Assuming that the characteristics of the secondary path are time-invariant, the model can be obtained from an offline system identification process illustrated in Figure 11. During the identification, white noise is fed to the secondary source and the impulse response of the secondary path is estimated using LMS algorithm. The model of the secondary path, $\hat{S}(z)$, is typically an FIR filter. The identification process should be long enough so that the error signal $e(n)$ is minimised and the model has converged.

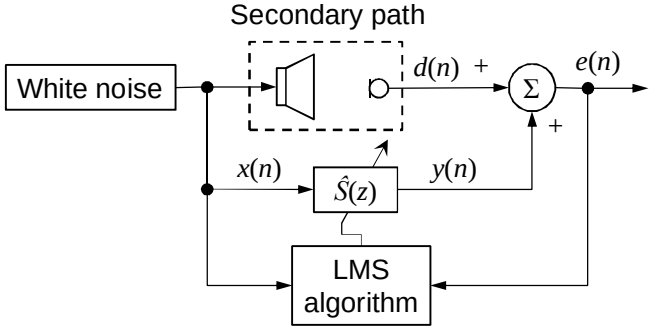

Figure 11. Identification of the secondary path.

The accuracy of the secondary-path model has a clear effect on the stability of FXLMS algorithm. The response of the model does not have to exactly match that of the secondary path and it is often sufficient to use a relatively low-order filter. For convergence, the phase error of the model should be within ±90˚. Phase errors of 40° hardly affect the convergence speed of the algorithm [3].

3. Active sound profiling algorithms

In this chapter, algorithms targeted for active sound profiling are described. Active sound profiling is typically used for obtaining a desired engine noise spectrum inside a car cabin. In this case, the active system works at single frequencies and narrowband algorithms can be utilised.

3.1 Narrowband noise cancellation/equalisation

A simple way to control narrowband noise is an adaptive notch filter (ANF). An adaptive notch filter uses a sinusoidal reference signal and two adaptive weights to cancel narrowband noise. The advantages of the adaptive notch filter are easy control of bandwidth and the capability to adaptively track the exact frequency of the disturbance.

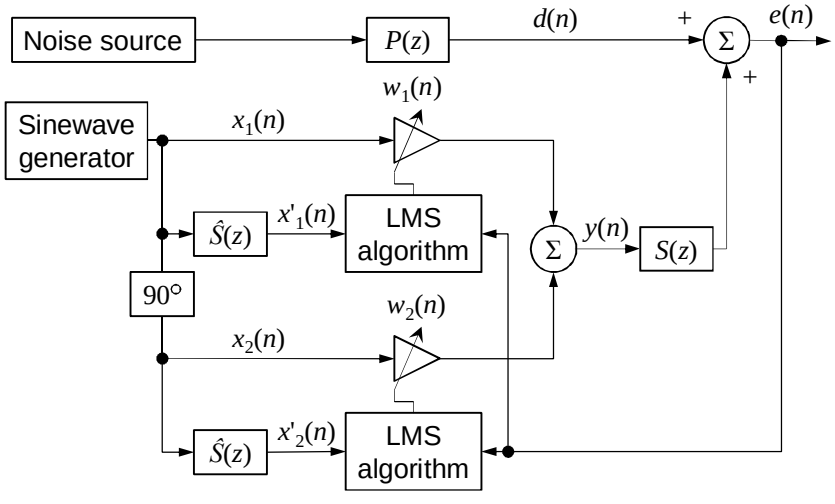

Figure 12. Adaptive notch filter used for noise cancellation.

The block diagram of a single-frequency adaptive notch filter used for cancelling narrowband noise is shown in Figure 12. The noise source produces narrowband noise which propagates through the primary path $P(z)$ to the cancellation point. The output of the adaptive notch filter, $y(n)$, is fed through the secondary path $S(z)$ and interferes with the primary noise so that the error signal $e(n)$ is driven towards zero. The sinewave generator produces a sinusoidal reference signal having the same frequency as the primary noise. The sine wave is used as the input signal for the adaptive weight w_1 while the input signal for the other adaptive weight, w_2, is a cosine wave obtained by shifting the phase of the sine wave by 90°. The output of the adaptive notch filter is the sum of the weighted sine and cosine waves. The secondary-path model $\hat{S}(z)$ is used for filtering the input signals. The filtered signals are then used for adapting the weights.

The adaptive notch filter can be extended to an adaptive noise equaliser (ANE), which can either amplify or attenuate narrowband noise. The block diagram of the adaptive noise equaliser is given in Figure 13.

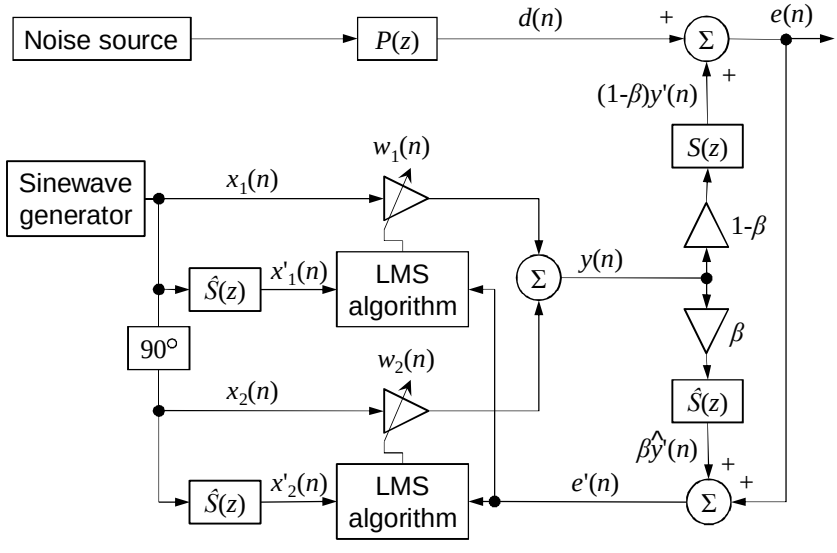

Figure 13. Adaptive noise equaliser.

In the adaptive noise equaliser, the amplitude of the residual harmonic is determined by a gain parameter β. In convergence, the modified error, $e'(n)$, becomes

$$e'(n) = e(n) + \beta\hat{y}'(n) = d(n) + (1-\beta)y'(n) + \beta\hat{y}'(n) = 0, \quad (19)$$

where $y'(n) = \mathbf{s}(n)*y(n)$ and $\hat{y}'(n) = \hat{\mathbf{s}}(n)*y(n)$ are the output signals filtered by the secondary path and the secondary-path model. If the secondary-path model is accurate, so that $\hat{S}(z) = S(z)$, Equation 19 can be written as

$$d(n) + (1-\beta)y'(n) + \beta y'(n) = d(n) + y'(n) = 0. \quad (20)$$

The error signal can now be expressed as

$$e(n) = d(n) + (1-\beta)y'(n) = d(n) - (1-\beta)d(n) = \beta d(n). \quad (21)$$

Thus, the error signal $e(n)$ contains a residual component of the narrowband noise whose amplitude is controlled by adjusting the gain value β. With $\beta = 0$, the adaptive noise equaliser is reduced to the adaptive notch filter [52].

The weights of the adaptive notch filter, or adaptive noise equaliser, can be adapted using the FXLMS algorithm. In the following, adaptive notch filter for controlling a single frequency or multiple frequencies are described. The multiple-channel case with several output and error signals is also discussed.

3.1.1 Single-frequency system

A single frequency adaptive noise canceller/equaliser has two adaptive weights and two reference inputs, the sine and cosine wave. The output of the system is

$$y(n) = w_1(n)x_1(n) + w_2(n)x_2(n), \quad (22)$$

where w_1 and w_2 are the adaptive weights and x_1 and x_2 are the sine and cosine wave. The weights are adapted using the FXLMS algorithm,

$$w_i(n+1) = w_i(n) - \mu x'_i(n)e(n),\ i = 1,2, \quad (23)$$

where μ is the step size and x'_i is the reference signal filtered by the secondary-path model [3].

3.1.2 Multiple-frequency system

In practical ANC systems, periodic noise usually contains tones at the fundamental frequency and at several harmonic frequencies. This kind of noise can be attenuated by a filter with multiple notches. The realisation of multiple notches requires higher-order filters which can be realised by parallel or cascade connection of multiple second-order sections.

In *direct form*, the reference signal is a sum of J sinusoids and the adaptive filter has a length of L_w so that $L_w \geq 2J$. When a sum of sinusoids is applied to an adaptive filter, a notch will be formed at each reference frequency. Therefore, a narrowband ANC system will provide effective cancellation of every sinusoidal component of the disturbance. If the frequencies of the reference sinusoids are close together, a long filter ($L_w >> 2J$) is required to give good resolution between adjacent frequencies. This is an undesired solution since a higher-order adaptive filter results in slower convergence and higher excess error. The block diagram of

the direct-form multiple-frequency ANF is shown in Figure 14, where $W(z)$ is the adaptive filter and $x(n)$ is the reference signal consisting of several sinusoids [3].

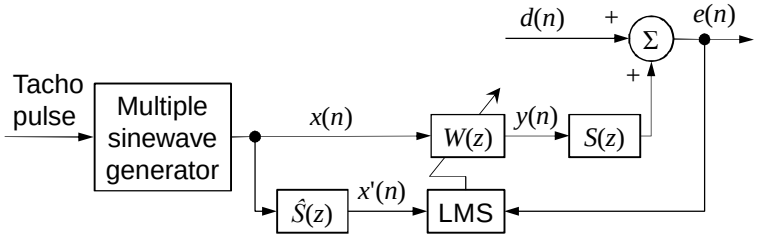

Figure 14. Block diagram of the direct-form multiple-frequency adaptive notch filter.

In *parallel form*, J two-weight adaptive filters are connected in parallel to attenuate J sinusoidal components of the primary noise. The signal for cancelling jth sinusoid is

$$y_j(n) = w_{j,1}(n)x_{j,1}(n) + w_{j,2}(n)x_{j,2}(n), \tag{24}$$

which corresponds to the single-frequency case when $J = 1$. The output of the parallel-form adaptive notch filter is

$$y(n) = \sum_{j=1}^{J} y_j(n). \tag{25}$$

Each reference input is filtered by the secondary-path model $\hat{S}(z)$ which has a length of L_s. Reference signal filtering requires intensive computation when both J and L_s are large. Similar to the single-channel case, the update equations for the adaptive weights are

$$w_{j,1}(n+1) = w_{j,1}(n) - \mu x'_{j,1}(n)e(n) \tag{26}$$

$$w_{j,2}(n+1) = w_{j,2}(n) - \mu x'_{j,2}(n)e(n), \tag{27}$$

where $j = 1,2,...,J$ is the channel index and $x'_{j,1}(n)$ and $x'_{j,2}(n)$ are the secondary-path filtered sine and cosine waves at jth reference frequency [3].

The block diagram of the parallel-form multiple-frequency adaptive notch filter is shown in Figure 15. The system consists of J two-tap adaptive filters, $W_j(z)$, having the reference signal $x_j(n)$ which consists of the sine and cosine wave at jth frequency component.

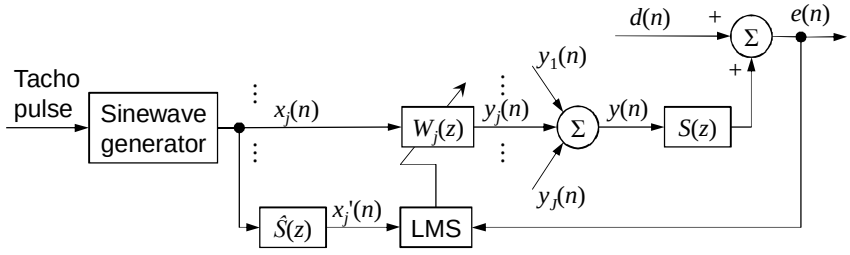

Figure 15. Block diagram of the parallel-form multiple-frequency adaptive notch filter.

3.2 Command-FXLMS algorithm

The objective of the FXLMS algorithm is to force the error signal to zero. However, in active sound profiling, the target is to drive the error signal to a desired value. This target can be achieved using the command-FXLMS (C-FXLMS) algorithm, which requires the error signal to tend towards a given command signal having a predetermined amplitude, instead of zero [24]. This is done by subtracting the command signal from the error signal and creating a new pseudo-error signal. The pseudo-error is then used in the calculation of the gradient term, so that the FXLMS algorithm minimises the pseudo-error.

The block diagram of the command-FXLMS algorithm with a single-frequency adaptive notch filter is shown in Figure 16. The command signal is denoted as *c*(*n*) and the pseudo-error is *e*'(*n*). The weights of the adaptive notch filter are updated as

$$w_i(n+1) = w_i(n) - \mu x'_i(n)e'(n),\ i = 1,2. \tag{28}$$

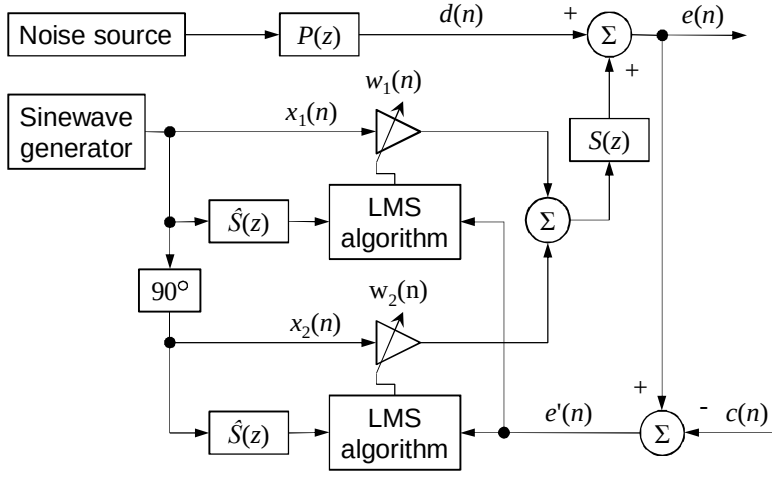

Figure 16. Block diagram of the single-frequency command-based FXLMS algorithm.

In active sound profiling, the command signal values are determined using a psychoacoustic profile. In the profile, the desired sound pressure levels for each controlled engine order are specified at each frequency. The profile can be implemented as a lookup table where the desired amplitude values for $c(n)$ are stored as a function of frequency. The command signal is then generated by taking the reference signal from the sinewave generator and multiplying it by the desired amplitude at that specific frequency.

The command-FXLMS algorithm provides fast convergence and is stable against errors in the secondary-path model. For C-FXLMS algorithm, the same stability conditions and limits for the step size as with the FXLMS algorithm hold [53]. A drawback of the algorithm is that the control effort becomes excessive if the command signal is out of phase with the disturbance. The control effort is equal to the mean-square value of the output signal and is proportional to the loudspeaker power required to drive the pseudo-error to zero [53]. More sophisticated algorithms have also been developed for active sound profiling. They include Internal Model FXLMS, Phase Scheduled Command-FXLMS and Automatic Phase Command-FXLMS [24], [53]. They are extensions to the command-FXLMS algorithm and provide a smaller control effort but, on the other hand, they are not as stable as the command-FXLMS. The extended algorithms are also more complicated and thus require more computation.

The adaptive noise equaliser shown in Figure 13 is more sensitive to errors in the secondary-path model. It is also unable to produce a non-zero output if the disturbance signal is zero [24]. In [54], ANE is combined with filtered-error LMS (FELMS) algorithm and normalised reference signal generator to obtain a more stable system with faster convergence.

In [55] and [56], a NEX-LMS algorithm is described for the equalisation of harmonic noise components. It is based on internal model control and reference signal normalisation and provides an improved convergence rate with the cost of increased complexity. Filter adaptation can also be done in frequency domain [57].

3.3 Multiple-channel active sound profiling

Combining the multiple-channel FXLMS algorithm described in Chapter 2.2 with the command-FXLMS, an algorithm for controlling multiple narrowband components with several secondary sources and error sensors is obtained. The multiple-channel narrowband ASP system consisting of J references, K secondary sources and M error sensors is illustrated in Figure 17.

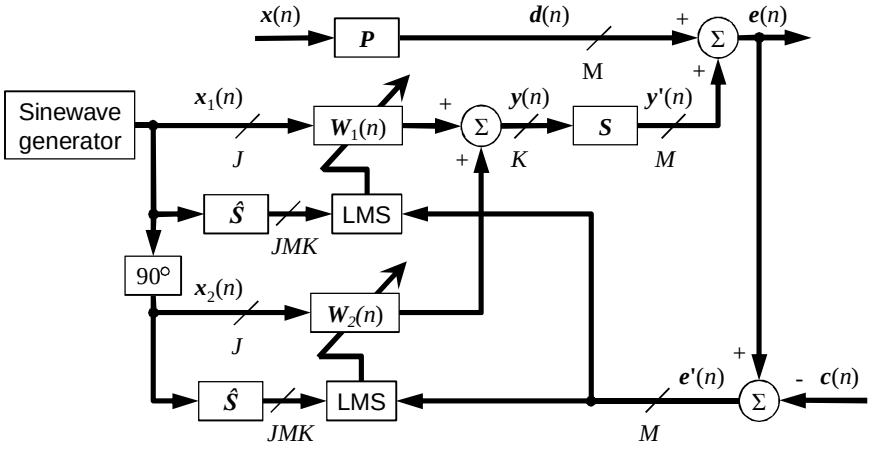

Figure 17. Multiple-channel active sound profiling system using C-FXLMS algorithm.

Matrices $\boldsymbol{W}_1(n)$ and $\boldsymbol{W}_2(n)$ contain the weights of the adaptive notch filters for the reference sines and cosines, respectively. There are two reference signal vectors,

$$\boldsymbol{x}_1(n) = [x_{1,1}(n) \quad \dots \quad x_{J,1}(n)] \tag{29}$$

$$\boldsymbol{x}_2(n) = [x_{1,2}(n) \quad \dots \quad x_{J,2}(n)], \tag{30}$$

where $\boldsymbol{x}_1(n)$ contains the sine waves and $\boldsymbol{x}_2(n)$ the cosine waves. The adaptive weight matrices $\boldsymbol{W}_1$ and $\boldsymbol{W}_2$ represent the response from the J sine and cosine waves to the K outputs. They can be written as

$$\boldsymbol{W}_1(n) = \begin{bmatrix} w_{11,1}(n) & w_{12,1}(n) & \dots & w_{1J,1}(n) \\ w_{21,1}(n) & w_{22,1}(n) & \dots & w_{2J,1}(n) \\ \vdots & \vdots & \ddots & \vdots \\ w_{K1,1}(n) & w_{K2,1}(n) & \dots & w_{KJ,1}(n) \end{bmatrix} \tag{31}$$

$$\boldsymbol{W}_2(n) = \begin{bmatrix} w_{11,2}(n) & w_{12,2}(n) & \dots & w_{1J,2}(n) \\ w_{21,2}(n) & w_{22,2}(n) & \dots & w_{2J,2}(n) \\ \vdots & \vdots & \ddots & \vdots \\ w_{K1,2}(n) & w_{K2,2}(n) & \dots & w_{KJ,2}(n) \end{bmatrix}. \tag{32}$$

The output to the kth secondary source is

$$y_k(n) = \sum_{j=1}^{J} y_{kj}(n), \tag{33}$$

where

$$y_{kj}(n) = w_{kj,1}(n)x_{j,1}(n) + w_{kj,2}(n)x_{j,2}(n) \tag{34}$$

is the component of the kth output signal derived from the jth reference.

There are $M \times K$ secondary paths between the secondary sources and error sensors, which are modeled by FIR filters $\hat{S}_{mk}(z)$. They are used for generating the $J \times M \times K$ filtered versions of the sine and cosine waves. The weights of the adaptive notch filters $\boldsymbol{W}_1(n)$ and $\boldsymbol{W}_2(n)$ are adjusted by the FXLMS algorithm. The update equations for the adaptive weights from jth reference to kth output are

$$w_{kj,1}(n+1) = w_{kj,1}(n) - \mu \sum_{m=0}^{M-1} x'_{jkm,1}(n) e'_m(n) \tag{35}$$

$$w_{kj,2}(n+1) = w_{kj,2}(n) - \mu \sum_{m=0}^{M-1} x'_{jkm,2}(n) e'_m(n) \tag{36}$$

where $x'_{jkm,1}(n)$ and $x'_{jkm,2}(n)$ are the filtered sine and cosine waves, respectively.

The pseudo-error signals $e'_m(n)$ are computed as

$$e'_m(n) = e_m(n) - c_m(n), \tag{37}$$

where $e_m(n)$ is the error signal from mth error sensor and $c_m(n)$ is the corresponding command signal. There are J narrowband components to be controlled so $c_m(n)$ is a sum of J sinusoids having the desired amplitudes at error sensor m.

The multiple-channel C-FXLMS algorithm differs from the general multiple-channel FXLMS algorithm in a way that each adaptive filter has only two weights. Since each reference signal for an adaptive notch filter consists of a sine and cosine wave, there are twice as many reference signals as in the general multiple-channel FXLMS algorithm. The computational demand of the multiple-channel C-FXLMS algorithm using adaptive notch filters is summarised in Table 2.

Table 2. Computational demand of the multichannel narrowband C-FXLMS algorithm.

	Multiplications	**Additions**
Filter adaptation	$2JK(M + 1)$	$2JKM + M$
Output computation	$2JK$	$2K(J - 1)$
Reference signal filtering	$2JKML_s$	$2JKM(L_s - 1)$

3.4 Reference signal generation

In the narrowband active control systems, the reference signals are related to the frequency of the disturbance. Adaptive notch filters require the sine and cosine waves having the frequencies of the narrowband noise components that are to be controlled. In the case of engine noise, information about the engine rotation is typically obtained using a tachometer. Engine speed can then be estimated from the pulses produced by the tachometer.

The first step in the reference signal generation is to estimate the fundamental frequency of the engine rotation. Tachometer signal can be nearly rectangular or sinusoidal, and the fundamental frequency is estimated by counting the number of

samples belonging to the tachometer pulse. The fundamental engine rotation frequency can then be calculated as

$$f_0 = \frac{1}{N_p T_0}, \tag{38}$$

where N_p is the number of tachometer pulses per revolution and T_0 is the length of the pulse.

The accuracy of the estimation of the fundamental frequency depends highly on the sampling frequency of the tachometer signal [58]. Estimation of the fundamental frequency is crucial for the operation of the overall active system, and errors in the frequencies of the generated reference signals lead to decreased performance. The engine rotation is usually measured from a toothed wheel. In some cases, one tooth may be missing and the missing pulse has to be taken into consideration in frequency estimation.

Based on the fundamental frequency, the sine and cosine waves can be generated. The sine and cosine functions are usually avoided because they are computationally heavy. A simple and reliable way is to use a lookup table containing one cycle of a sine wave. The values of the lookup table are then repeatedly cycled with a step relative to the desired frequency. The lookup table has to be large enough so that a sufficiently accurate estimate of the sinusoidal waveforms is obtained. Another way to generate the sinusoidal waveforms is to use a recursive oscillator [3]. With a marginally stable two-pole resonator, the new waveform samples are computed recursively using the previous samples. The implementation of a two-output (sine and cosine) oscillator requires a little amount of memory and two multiplications per sample. In applications where the memory usage is crucial, a recursive oscillator is thus recommended. Both methods introduce quantisation errors that affect the quality of the generated waveforms.

4. Development of the active sound profiling algorithm

In this chapter, the multiple-channel narrowband active sound profiling algorithm introduced in the previous chapter is considered. The algorithm is enhanced to be more robust and computationally efficient, so that it operates in a more reliable way and requires less computation.

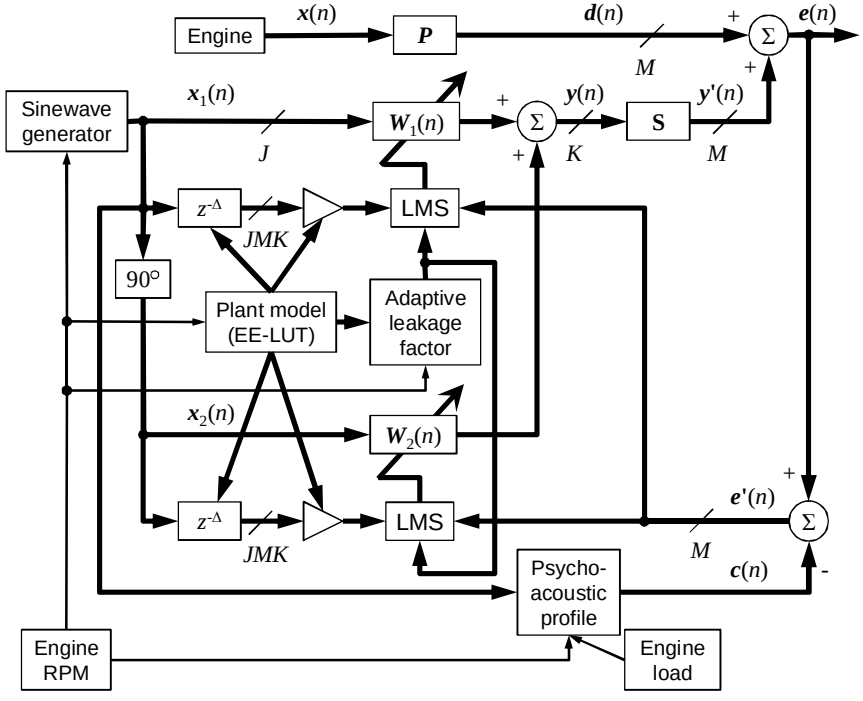

Figure 18. Block diagram of the developed ASP algorithm.

A block diagram of the developed ASP algorithm is shown in Figure 18. It combines the multiple-channel C-FXLMS algorithm with a new technique to obtain the

filtered reference signals. The technique is based on delaying of the sinusoidal reference signals and modifying their amplitude. The adaptive weights are updated using the leaky FXLMS algorithm in which the leakage factor is adaptive. Adaptation of the leakage factor is based on the phase difference in the eigenvalue-equalised plant model. The magnitude and phase of the plant model are stored in lookup tables (LUT).

4.1 Reference signal filtering using lookup tables

Computationally, the most demanding part of the multiple-channel filtered-reference algorithms is the filtering of the reference signals. The computational burden of the C-FXLMS algorithm is given in Table 2. In a typical multiple-channel system in a car cabin, the number of references, J, is 3–6, number of outputs, K, is 2–8 and number of errors, M, is 2–8. The length of the secondary-path model, L_s, is typically quite large so that a sufficient estimate of the secondary-path response is obtained. For $J = 3$, $K = 2$, $M = 2$ and $L_s = 100$, the weight adaptation and output computation require 48 multiplications whereas the reference signal filtering takes 2400 multiplications at each time step. With $J = 6$, $K = 8$, $M = 8$ and $L_s = 100$, the weight adaptation and output computation take 960 multiplications while the reference signal filtering require 76800 multiplications. These examples show that most of the computational power is needed by the reference signal filtering. In order to reduce the computational burden of the multiple-channel C-FXLMS algorithm, other techniques for obtaining the filtered reference signals have to be considered. In the following, simplified methods for computing the filtered reference signals in a narrowband ANC system are considered.

In a narrowband active system, the reference signals are sinusoidal and filtering such signals means a modification of the magnitude and phase of the sinusoid. This idea has been introduced in [28] , where passing the reference signal through the secondary-path models was done by modifying the magnitude and phase rather than filtering it with an FIR representation of the secondary path. In [59], the filtered reference signals are obtained by shifting the phase of each narrowband component. The idea of delaying the reference signals is utilised in the following.

4.1.1 Delay compensation

In the simplest case, the secondary-path model is replaced by $z^{-\Delta}$, where Δ is the secondary-path delay. The time delay can be estimated by an off-line system identification procedure. However, the delay is generally a function of frequency. The frequency-dependent delay can be determined by taking the discrete Fourier transform of the secondary-path impulse response and calculating the delay from the phase values by

$$\tau(\omega) = -\frac{\varphi(\omega)}{\omega}, \tag{39}$$

where $\tau(\omega)$ is the time delay in seconds at frequency ω and $\varphi(\omega)$ is the phase of the secondary-path model in radians. The value of Δ at angular frequency ω_0 is then calculated as

$$\Delta = \text{round}\left(\frac{\tau(\omega_0)}{T}\right), \tag{40}$$

where round is a function rounding the value to the nearest integer and T is the sampling period [3].

Since the delay is a function of frequency, a method for selecting the correct delay value is needed if the frequency changes. One solution is to use a lookup table containing the frequency-dependent delay values. In the lookup-table based delaying, a buffer is used to store the reference signal samples. The buffer can be denoted as

$$\boldsymbol{x} = [x(n) \quad x(n-1) \quad \cdots \quad x(n-\Delta) \quad \cdots], \tag{41}$$

where $x(n)$ is the reference signal sample at time n and Δ is the delay. The delayed reference signal is obtained by selecting the value $x(n\text{-}\Delta)$. The buffer is updated at each time step by shifting the samples rightwards and inserting the new sample in the leftmost position. If the frequency and hence the delay changes, the delayed reference signal sample can be read from the buffer by taking the value located in the position corresponding to the new delay.

In adaptive notch filters, two buffers are needed for each reference signal. The buffer for the sine wave is denoted as

$$\boldsymbol{x}_{j,1} = \left[x_{j,1}(n) \ \ldots \ x_{j,1}(n-\Delta_{km}) \ \ldots \ x_{j,1}\left(n-\Delta_{km,\max}\right)\right] \tag{42}$$

and the buffer for the cosine wave is

$$\boldsymbol{x}_{j,2} = \left[x_{j,2}(n) \ \ldots \ x_{j,2}(n-\Delta_{km}) \ \ldots \ x_{j,2}\left(n-\Delta_{km,\max}\right)\right] \tag{43}$$

where $x_{j,1}(n)$ and $x_{j,2}(n)$ are the current sine and cosine wave samples for jth reference, Δ_{km} is the delay of the secondary path from the kth secondary source to the mth error sensor and $\Delta_{km,\max}$ is the maximum delay of the secondary path. The jth filtered reference signal for the secondary path from the kth secondary source to the mth error sensor is

$$x'_{jkm,1} = \boldsymbol{x}_{j,1}[\Delta_{km} + 1] = x_{j,1}(n-\Delta_{km}) \tag{44}$$

$$x'_{jkm,2} = \boldsymbol{x}_{j,2}[\Delta_{km} + 1] = x_{j,2}(n-\Delta_{km}) \tag{45}$$

for the sine and cosine waves, respectively. In Equations 44 and 45, notation $\boldsymbol{x}[n]$ means that the nth element of buffer $\boldsymbol{x}$ is taken.

The buffer pickup method does not require any computational operations such as multiplications or additions, only shifting of the buffers. There are $M \times K$ lookup tables for the secondary-path delay and a total number of $2J$ buffers so a considerable amount of memory is needed, however. The memory usage depends on

the maximum delays of the secondary path and the size of the lookup tables. The size of the lookup tables can be reduced by increasing the frequency resolution which is used for calculating the delay values.

4.1.2 Reference signal filtering using magnitude and delay lookup tables

The delay compensation does not take the magnitude of the secondary paths into account. A way to compensate the magnitude is using a variable step size in the FXLMS algorithm. The lookup table method can also be extended to include the magnitude values.

In this case, two buffers are required for each reference signal and secondary path, so there are 2*JKM* buffers

$$\boldsymbol{x}_{jkm,1} = \left[x_{jkm,1}(n) \ \ldots \ x_{jkm,1}(n-\Delta_{km}) \ \ldots \ x_{jkm,1}\left(n-\Delta_{km,\max}\right)\right] \tag{46}$$

$$\boldsymbol{x}_{jkm,2} = \left[x_{jkm,2}(n) \ldots \ x_{jkm,2}(n-\Delta_{km}) \ \ldots \ x_{jkm,2}\left(n-\Delta_{km,\max}\right)\right] \tag{47}$$

where $\Delta_{km,\max}$ is the maximum delay of the secondary path from the *k*th secondary source to the *m*th error sensor and $x_{jkm,1}(n)$ and $x_{jkm,2}(n)$ are the magnitude-compensated sine and cosine wave samples at time *n*. The magnitude-compensated samples are obtained so that when a new sample is inserted to the buffer, it is multiplied by the magnitude at the current frequency. The *j*th filtered reference signal components for the secondary path from the *k*th secondary source to the *m*th error sensor are then

$$x'_{jkm,1} = \boldsymbol{x}_{jkm,1}[\Delta_{km} + 1] = x_{jkm,1}(n-\Delta_{km}) \tag{48}$$

$$x'_{jkm,2} = \boldsymbol{x}_{jkm,2}[\Delta_{km} + 1] = x_{jkm,2}(n-\Delta_{km}). \tag{49}$$

The method described above requires more memory and computational power than the delay compensation.

4.1.3 Lookup-table based filtering using normalised magnitudes

The lookup-table based reference signal filtering can be combined with the EE-FXLMS algorithm which uses magnitude-normalised versions of the secondary-path models. First, the magnitude-normalised secondary-path models are computed as described in Chapter 2.1.3. The lookup tables for the magnitude and delay values are then calculated from the magnitude-normalised filters. Since the magnitudes of the secondary-path models are flat, only one magnitude value is needed for each secondary path. Using the delay buffers introduced in Chapter 4.1.1, the filtered reference signal components for the *j*th reference signal and secondary path from *k*th output to *m*th error can be obtained as

$$x'_{jkm,1} = A_{km}\boldsymbol{x}_{j,1}[\Delta_{km} + 1] = A_{km}x_{j,1}(n - \Delta_{km}) \tag{50}$$

$$x'_{jkm,2} = A_{km}\boldsymbol{x}_{j,2}[\Delta_{km} + 1] = A_{km}x_{j,2}(n - \Delta_{km}) \tag{51}$$

where A_{km} is the magnitude of the secondary-path model.

Exploiting the EE-FXLMS algorithm, the size of the magnitude lookup tables can be remarkably reduced. Another benefit is that frequency-independent convergence is achieved.

4.1.4 Creating lookup tables from the secondary-path model

The lookup tables are created from the secondary-path model which is obtained via the system identification process described in Chapter 2.3. The secondary-path FIR model is then equalised using the process given in Chapter 2.1.3. Using Equation13, the magnitude-normalised frequency response of the secondary-path model is obtained. The delay values can be computed from the phase response as

$$\Delta = \text{round}\left(-\frac{\varphi(\omega)}{\omega}f_s\right), \tag{52}$$

where $\varphi(\omega)$ is the phase response at angular frequency ω and f_s is the sampling frequency. The magnitude and phase delay values can then be stored in lookup tables.

The lookup table for the magnitude values contains only one value for each secondary path. The size of the lookup table for the frequency-dependent delay values depends on the number of frequency points chosen for representing the phase response. The number of frequency points is defined by the frequency range and the frequency resolution, so that the number of frequency points becomes

$$N_f = \frac{(f_N - f_1)}{\delta f} + 1, \tag{53}$$

where f_1 and f_N are the first and last frequency in the lookup table and δf is the frequency resolution. The frequency resolution is expressed as

$$\delta f = \frac{f_s}{N_{FFT}}, \tag{54}$$

where N_{FFT} is the number of points in the FFT. If the sampling frequency is assumed to be constant, the frequency resolution can be enhanced by increasing the number of points in FFT.

4.2 Adaptive leakage factor

The performance of the FXLMS algorithm is highly affected by the phase response of the secondary path. The overall delay of the secondary path has an influence on the step size, and the phase error of the secondary-path model should be small

enough. Large phase shifts in the secondary path also affect the operation of the FXLMS algorithm, distracting the adaptation of the filter weights and deteriorating the performance. In particular, the large difference in the phase response of the secondary path becomes a problem when the frequency of the disturbance, and hence the reference signal, changes which is the case in acceleration or deceleration. In this case, leaky FXLMS algorithm introduced in Chapter 2.1.4 provides a more robust operation by restricting the adaptive weights. Usage of the leakage factor may decrease the operation of the algorithm in other situations, however, and an adaptive leakage factor can be used to avoid that problem. When the secondary-path response changes rapidly, the value of the leakage factor becomes smaller, leading to larger leak of adaptive weights. In other situations, the leakage factor can be equal to 1, so that no leakage is used.

Leaky FXLMS algorithm with an adaptive leakage factor can be expressed as

$$\boldsymbol{w}(n+1) = \lambda(n)\boldsymbol{w}(n) - \mu\boldsymbol{x}'(n)e(n), \tag{55}$$

where $\lambda(n)$ is the adaptive leakage factor updated by the following algorithm:

1. Calculate the difference in the phase response of the secondary-path estimate at the frequency of the sinusoidal reference. This can be expressed as

   $$\delta\varphi = |\varphi(f_{i+1}) - \varphi(f_i)|, \tag{56}$$

   where $\varphi(f_i)$ is the phase angle at the frequency of the sinusoidal reference and $\varphi(f_{i+1})$ is the phase angle at the adjacent frequency.

2. Check if $\delta\varphi$ exceeds a given limit, e.g. 90°.

3. If the limit is exceeded, the leakage factor becomes active and is adapted as

   $$\lambda(n+1) = \beta\lambda(n) + (1-\beta)\left(1 - \frac{\delta\varphi}{a}\right), \tag{57}$$

   where β ($0 << \beta < 1$) is the smoothing factor, a is a scaling constant and $\lambda(0) = 1$.

4. If the limit is not exceeded, the leakage factor is inactive and is updated as

   $$\lambda(n+1) = \beta\lambda(n) + (1-\beta). \tag{58}$$

In the active state, the leakage factor changes from 1 to $1\text{-}\delta\varphi/a$. When the leakage phenomenon needs to be set to inactive state, the leakage factor is set to 1 again.

For verifying the operation of the adaptive leakage factor, a simulation model was created in Matlab. The model consisted of a single-channel active noise control system with a simple secondary path. The secondary path was modelled as a second-order elliptic filter. The objective was to cancel a single sine wave having a constantly increasing frequency. The ANC system was based on the combination of the EE-FXLMS and leaky FXLMS algorithms. The benefit of the EE-FXLMS algorithm is that a frequency-independent step size can be used. With the simulation

model, the performance of active noise control was tested in three different cases: with a constant leakage factor, with an adaptive leakage factor and without leakage. The frequency of the sine wave changed from 18 Hz to 58 Hz during 40 s.

The frequency response of the secondary path is shown in Figure 19. Around 25 Hz, the magnitude response has a notch and the phase changes 180°. At frequencies close to the phase shift, the performance of the active noise control system is assumed to be decreased.

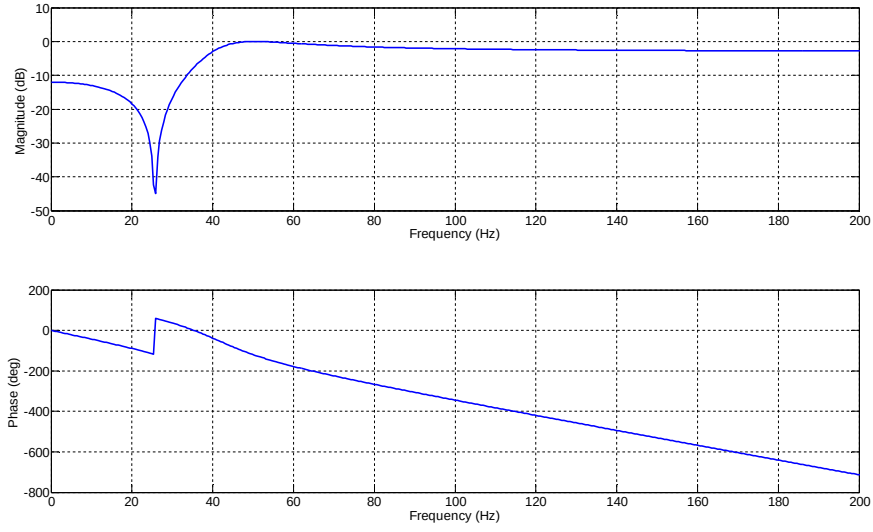

Figure 19. Frequency response of a simple secondary-path model.

In Figure 20, the simulation results are given. In the upper figure, amplitudes of the error signal in each case are shown. The objective is to minimise the amplitude. The phase shift of 180° occurs at 7 s and around that time the amplitude is remarkably increased in every case. Without the leakage factor, the amplitude is higher around 4–6 s than with a leakage factor. Using a leakage factor, the amplitude of the error signal is increased less around 4 s. After that, the error signal is minimised less effectively with a constant leakage factor than with an adaptive leakage factor. The conclusion is that, around the large phase shift, leakage of the filter weights is needed. When the phase shift is small, leakage degrades the operation of the system, so no leakage is preferred.

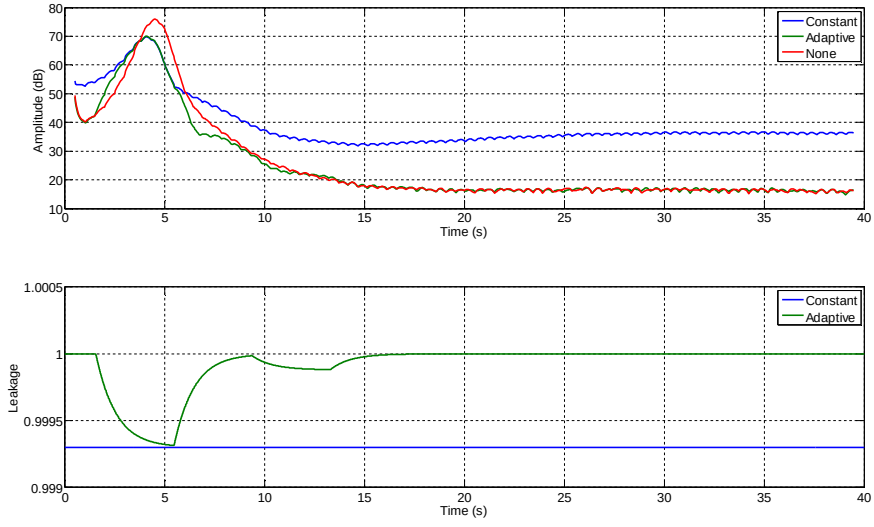

Figure 20. Error signal amplitude (upper) and value of the leakage factor (lower).

In multiple-channel case with several reference signals, output signals and error signals, the update equation of the FXLMS algorithm with adaptive leakage factor is

$$\boldsymbol{w}_{kj}(n+1) = \boldsymbol{\Lambda}_{jk}(n)\boldsymbol{w}_{kj}(n) - \mu\sum_{m=1}^{M}\boldsymbol{x}'_{jkm}(n)e_m(n), \tag{59}$$

where j, k and m are the indices of the reference, output and error signal, respectively. The adaptive leakage factors form a $J \times K$ matrix $\boldsymbol{\Lambda}$, whose elements are updated as follows:

1. For each reference signal (j = 1,…,J) and output (k = 1,…,K), calculate the difference in the phase response from output k to all error sensors m = 1,…,M:

   $$\delta\varphi_{km} = |\varphi_{km}(f_{i+1}) - \varphi_{km}(f_i)|, \tag{60}$$

   where φ_{km} is the phase angle of the secondary path from kth output to mth error and f_i is the frequency of the jth reference.

2. Check if $\delta\varphi_{km}$ exceeds a given limit at least in one secondary path from output k to all error signals.

3. If the limit is exceeded, the leakage factor becomes active for all secondary paths from output k. The leakage factor is then adapted as

   $$\boldsymbol{\Lambda}_{jk}(n+1) = \beta\boldsymbol{\Lambda}_{jk}(n) + (1-\beta)\left(1 - \frac{\delta\varphi_{mean}}{a}\right), \tag{61}$$

   where β is the smoothing factor, a is a scaling constant and $\delta\varphi_{mean}$ is the average difference in the phase angle calculated as

$$\delta\varphi_{mean} = \frac{1}{M}\sum_{m=1}^{M}|\varphi_{km}(f_{i+1}) - \varphi_{km}(f_i)|. \quad (62)$$

4. If the limit is not exceeded, the leakage factor is inactive and is updated as

$$\boldsymbol{\Lambda}_{jk}(n+1) = \beta\boldsymbol{\Lambda}_{jk}(n) + (1-\beta). \quad (63)$$

The leakage factor becomes active, if one of the secondary paths from a secondary source to all error sensors contains a large phase difference.

The reason for the degraded performance with the large phase difference of the secondary path is probably related to the estimation error of the secondary-path model. Sudden phase shifts are caused by resonances, for example. Such phase response is difficult to model using relatively short FIR filters and the phase error is largest around the resonances. Estimation errors cause also other kind of problems in narrowband systems, like out-of-band overshoot [60] and misequalisation [61].

5. Simulation of the developed algorithm

The operation of the multiple-channel active sound profiling algorithm is simulated in a car model. The algorithm is based on the block diagram shown in Figure 18 in Chapter 4. The simulation model is based on a real car in which an ASP system has been installed. With the model, performance of the ASP algorithm is evaluated. The algorithm is also tested as an ANC algorithm which minimises the error signals.

5.1 Simulation model

The ASP system has been modelled in Simulink. The simulation model is shown in Figure 21. It consists of two main blocks, the control system block and the plant and excitation block. The plant and excitation block contains an engine model for producing the primary noise signal. The engine model also provides the engine RPM and load information for the control system. The block also contains the secondary-path models and the summation of the primary and secondary noise signals at the error sensors.

In the control system block, the output signals are computed based on the error signals and RPM and load information. The RPM information is used for generating the reference (sine and cosine) signals that are then modified by the plant model to produce the filtered reference signals. The error signals are modified based on the target profile in order to obtain the pseudo-error signals. The values of the adaptive leakage factor are also calculated. The plant model is obtained via an offline identification process which is executed before the ASP algorithm is launched. The system identification is described in Chapter 5.3.

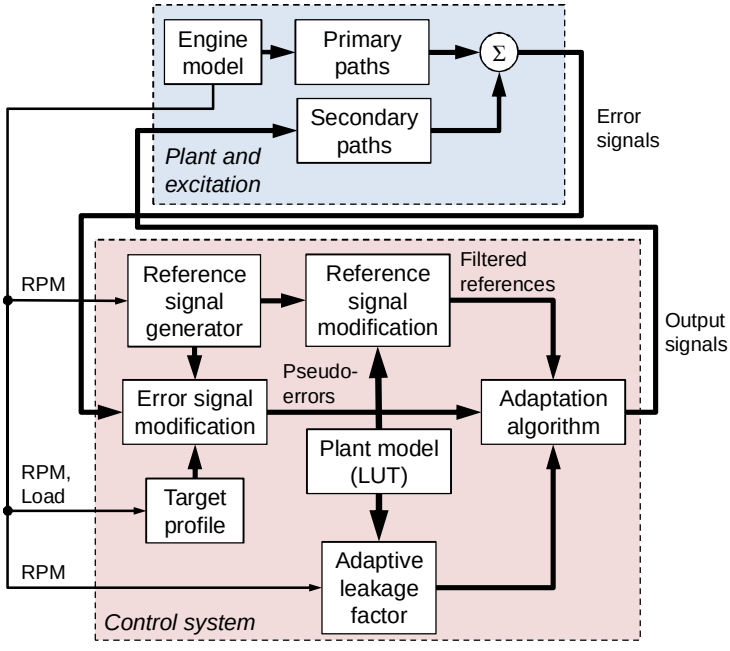

Figure 21. Simulation model.

5.2 Modelling of the plant and engine

The simulation model is based on an experimental ASP system installed in a car. In the passenger cabin of the car, four loudspeakers have been installed in the roof so that two loudspeakers are located above the driver and two above the co-driver. Four microphones have been mounted in the headrests of the driver and co-driver. Detailed locations of the loudspeakers and microphones are given in Figure 22.

The plant consists of the secondary paths from each loudspeaker to each error microphone. In the case of 4 loudspeakers and 4 error microphones, the plant contains 16 secondary paths. The plant is assumed to be an LTI (linear and time-invariant) system and has been modelled by measuring the frequency responses of the secondary paths and estimating them with long IIR filters. Each secondary path consists of the transfer function of the loudspeaker, the acoustic transfer path between the loudspeaker and microphone and the transfer function of the microphone. The acoustic transfer path consists of the delay between the loudspeaker and error microphone and the dynamics of the car cabin. In Figure 23, the frequency responses from loudspeaker 1 to all error microphones are shown. It can be seen that the dynamics of the secondary path is complex. The phase shift over the frequency range is large, mostly due to the distance between the loudspeaker and the microphones.

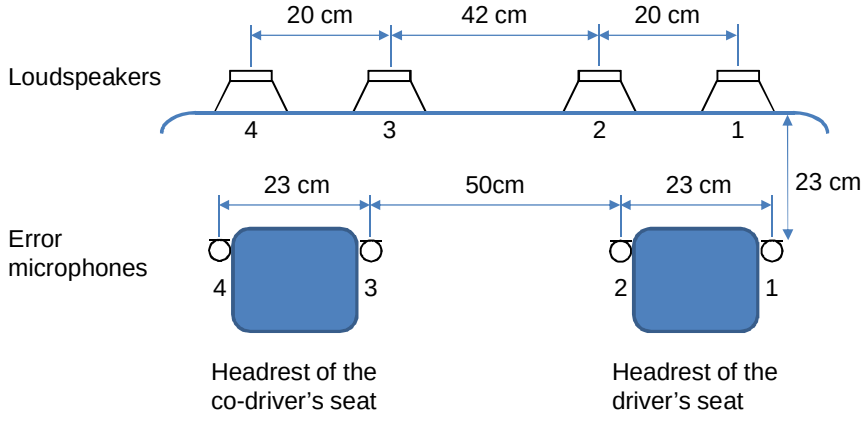

Figure 22. Locations of the loudspeakers and error microphones.

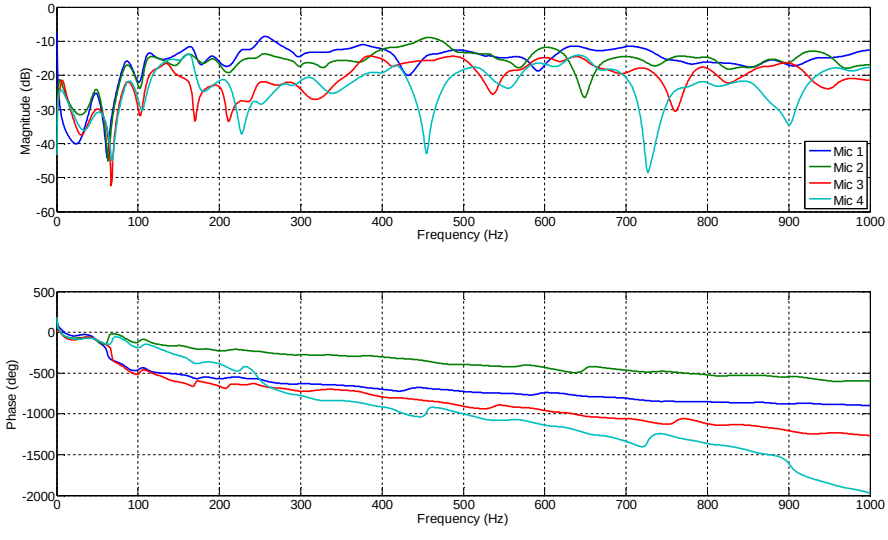

Figure 23. Frequency responses from loudspeaker 1 to all error microphones.

The engine noise of the car has been analysed and the dominant engine orders have been detected. The engine noise over the whole RPM range has been measured, and an order spectrogram of the engine noise is shown in Figure 24. In the middle, the levels of each engine order are given as a function of time, and the corresponding RPM is shown in the bottom. The most dominant engine order is the 2nd order, the firing frequency of the engine. Also the 3.5th, 4th, 5th, 5.5th and 6th orders are clearly detected.

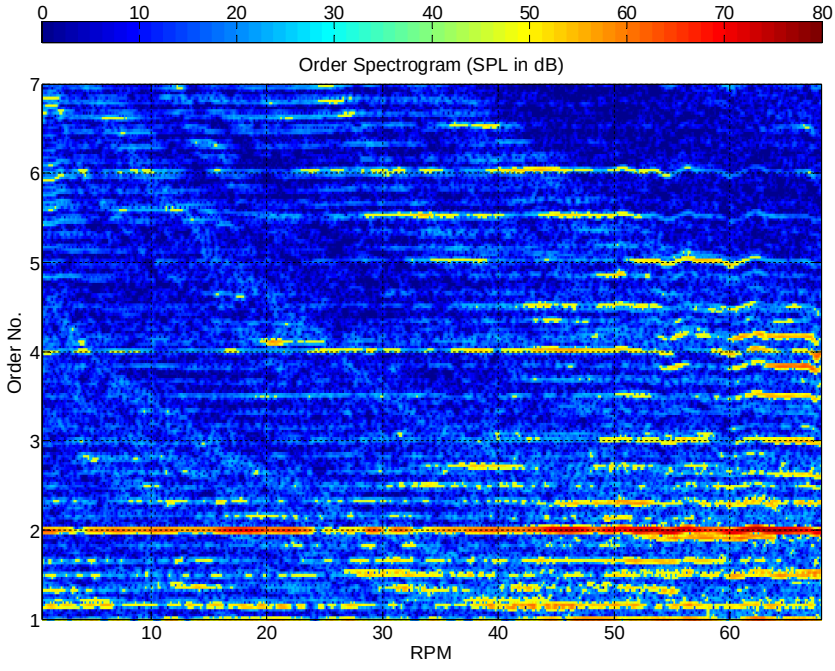

Figure 24. Spectrogram of engine noise measured in the car.

The primary paths from the noise source, i.e. engine, to each error microphone have been modelled as pure delays. The engine has been modelled as a source of multiple sinusoids and white noise. The frequencies of the sinusoids modelling the engine orders may be kept constant or changed with constant rate. This way different driving conditions like cruising or acceleration can be tested. In the simulations, only the controlled engine orders (2^{nd}, 3.5^{th}, 4^{th}, 5^{th}, 5.5^{th} and 6^{th}) have been generated and their amplitudes are constant at all RPM's. In a real engine noise, other engine orders are also present and the amplitudes of the orders vary as a function of RPM. Especially at high RPM's, the amplitudes are increased, as can be seen in Figure 24.

5.3 System identification

When the simulation is started, the system identification is executed to obtain the lookup tables of the secondary-path models. During the identification, white noise is fed to one loudspeaker at a time and the transfer functions from the loudspeaker to all error microphones are identified. The system identification works in three phases:

1. Identification of secondary paths using FIR filters and LMS algorithm.
2. Computing of the magnitude and phase of each FIR filter using FFT.
3. Storing the mean value of the magnitude and the frequency-dependent delay values for each secondary path to lookup tables.

In Figure 25, identification results of one secondary path are given. The results show the magnitude and phase responses of the original secondary path, the FIR model and the LUT model. The phase errors between the original secondary path and the FIR/LUT models are also given. The length of the FIR filter is 256 and, according to the results, the filter length is sufficient for modeling the secondary path. The magnitude response of the LUT model is flat, and the value of the magnitude is equal to the average of the magnitude response of the FIR model. The number of points for FFT in calculation of the lookup tables is 1024, which gives a frequency resolution of approximately 2 Hz, since the sampling frequency is 2034.5 Hz. The phase error of the lookup table is about ±10 degrees at low frequencies up to 150 Hz but after that the error increases to almost ±40 degrees at 500 Hz. The error is mainly caused by the rounding error in the calculation of the delay for the lookup table. According to Chapter 2.3, phase error of ±40 degrees does not affect the operation of the algorithm.

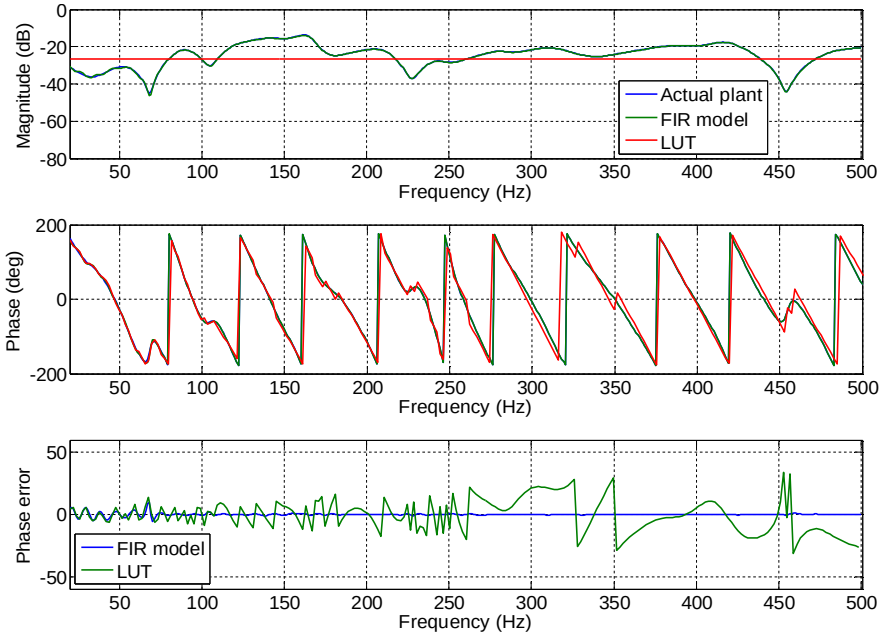

Figure 25. Identification results from loudspeaker 1 to error microphone 4.

5.4 Performance of ASP and ANC algorithms

The performance of the ASP algorithm has been tested with the simulation model. The algorithm has also been tested in active noise control, in which the target levels of the error signals are zeros. The system was tested in three conditions:

- Constant low RPM, which corresponds to low speed cruising.
- Constant high RPM, which corresponds to high speed cruising.
- Increasing RPM, which corresponds to acceleration.

The performance of the ASP and ANC algorithms are evaluated by calculating the amplitude of each engine order at all error sensors. The mean value of the amplitudes is taken and shown as a function of time. The ASP/ANC system is initially switched off and, at 2 s, the system is switched on.

5.4.1 Constant low RPM

With constant low RPM, the fundamental frequency of the engine is 35 Hz which is equal to 2100 RPM. This corresponds to cruising at low speed.

The spectrograms with ASP and ANC are given in Figure 26. The convergence at the 2^{nd} and 3.5^{th} engine orders are shown in Figures 27 and 28. The convergence curves for the rest of the engine orders are given in Figures 51–54 in Appendix A. The figures indicate that, at each engine order, the ASP algorithm converges within 1.5 seconds. After convergence, the error between the desired amplitude and the actual amplitudes is less than 1 dB at the 2^{nd}, 4^{th} and 6^{th} engine orders. At the 5^{th} and 5.5^{th} engine order, the steady-state error is less than 2 dB. The largest error, 2–3 dB, is at the 3.5^{th} engine order. With ANC, the convergence is also fast and the engine orders are totally cancelled, except the 2^{nd} order which has the largest magnitude. Still, the 2^{nd} order has been significantly attenuated, almost 20 dB.

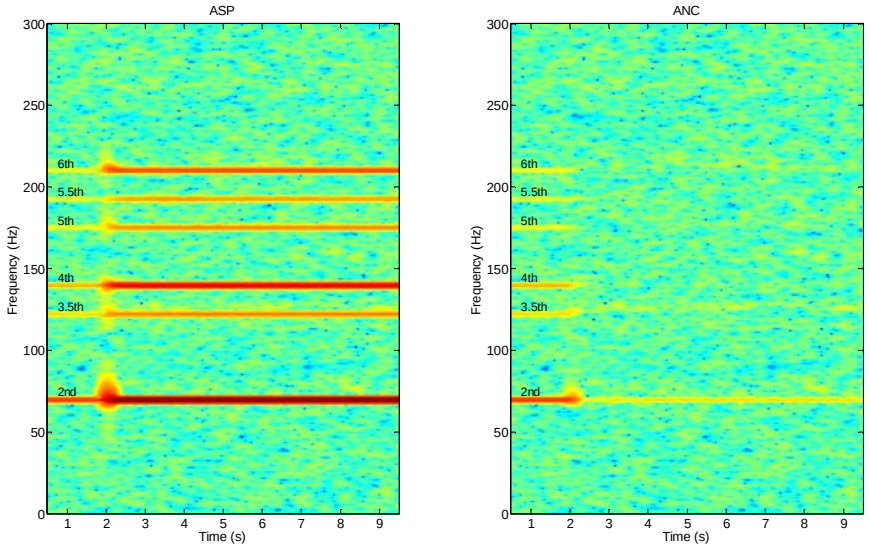

Figure 26. Spectrograms at constant RPM of 2100 with ASP and ANC.

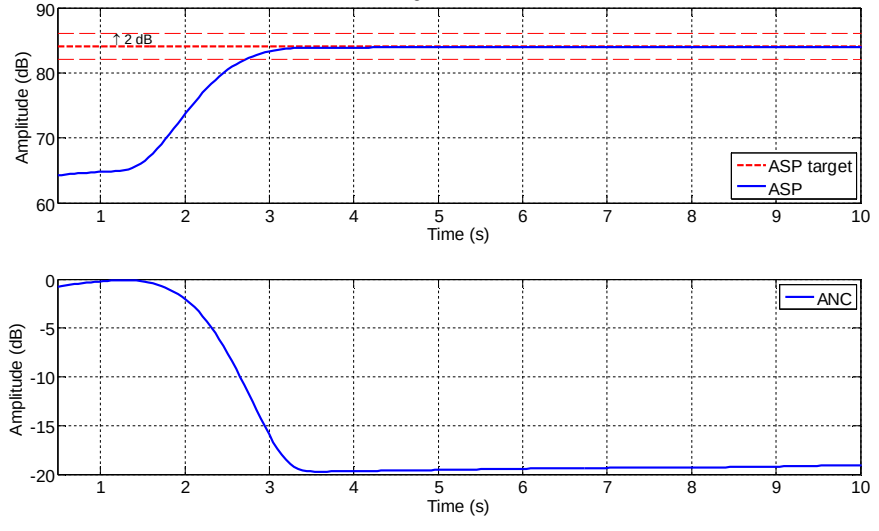

Figure 27. Convergence of the ASP (upper) and ANC (lower) algorithms at 2nd engine order.

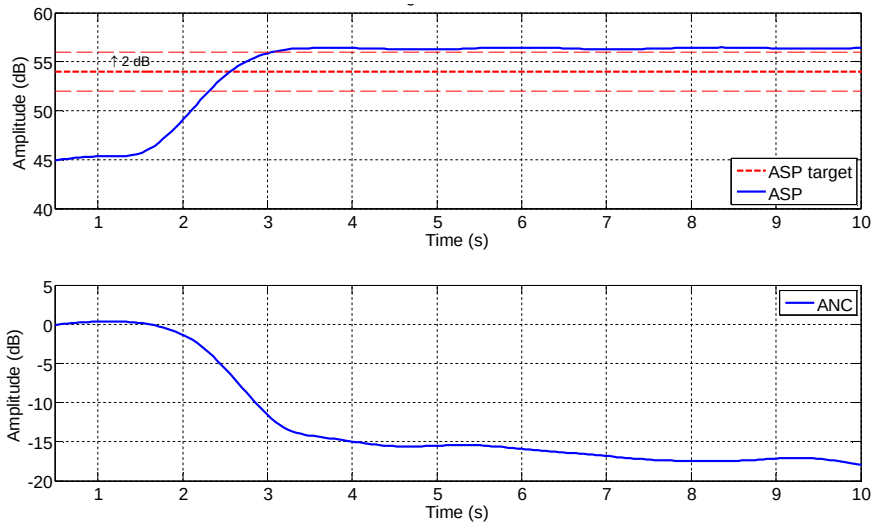

Figure 28. Convergence of the ASP (upper) and ANC (lower) algorithms at 3.5th engine order.

5.4.2 Constant high RPM

With constant high RPM, the fundamental frequency of the engine is 66 Hz which is equal to 3960 RPM. This corresponds to driving at high speed on a motorway.

The spectrograms with ASP and ANC are given in Figure 29. The convergence at the 2nd and 5.5th engine orders are shown in Figures 30 and 31. The convergence curves for the rest of the engine orders are given in Figures 56–60 in Appendix A. The results show that, at the 2nd, 3.5th and 4th engine orders, the convergence is fast and the error between the target level and the actual amplitude is less than 1 dB. At the 5th, 5.5th and 6th engine order, the convergence is slower, especially at the 5.5th engine order. At these engine orders, the steady-state error is less than 2 dB. With ANC, the 2nd, 3.5th, 4th and 6th engine orders are significantly attenuated. The attenuation at the 5th and 5.5th engine orders is relatively small but their initial levels are also low.

Due to stability problems at higher engine orders (5th, 5.5th and 6th), the step sizes of the FXLMS algorithm at these engine orders had to be decreased. This is against the idea of the eigenvalue-equalisation of the plant model which should make the step sizes independent of the frequency, so that a constant step size can be used at all RPM's. The problem is probably caused by the phase errors in the plant model.

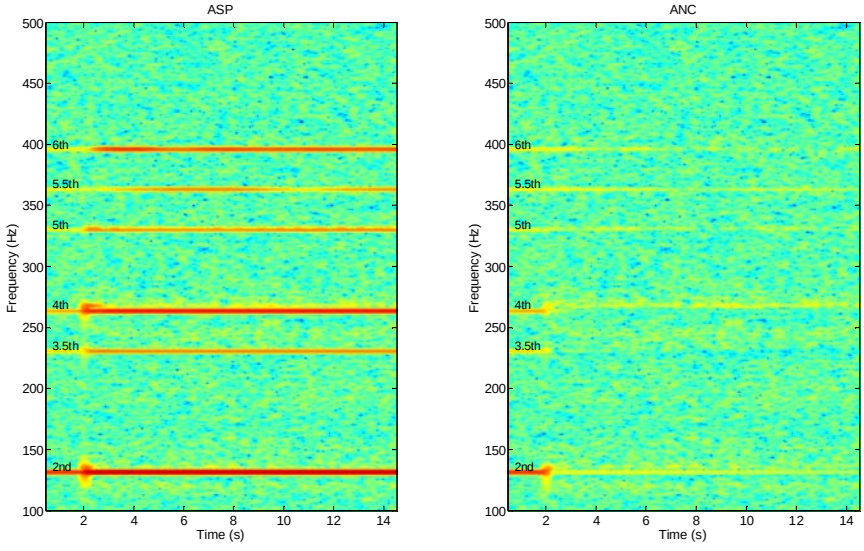

Figure 29. Spectrogram with active sound profiling at constant fundamental frequency of 66 Hz.

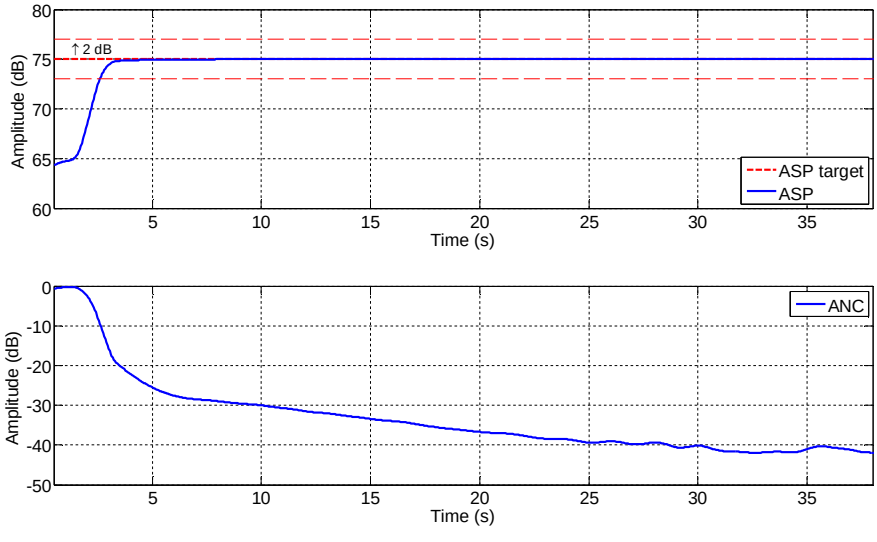

Figure 30. Convergence of the ASP (upper) and ANC (lower) algorithms at 2nd engine order.

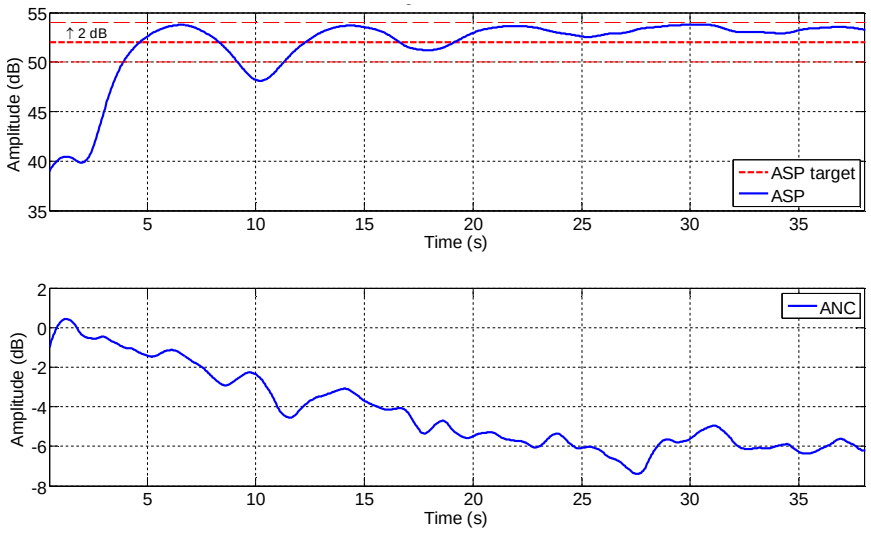

Figure 31. Convergence of the ASP (upper) and ANC (lower) algorithms at 5.5th engine order.

5.4.3 Increasing RPM

With increasing RPM, the fundamental frequency of the engine changes from 17 Hz to 67 Hz in 12.5 seconds, which is equal to 1020–4000 RPM. This corresponds to acceleration of the car. After 12.5 seconds, the RPM is kept constant at 4000 RPM. The RPM is given in Figure 32.

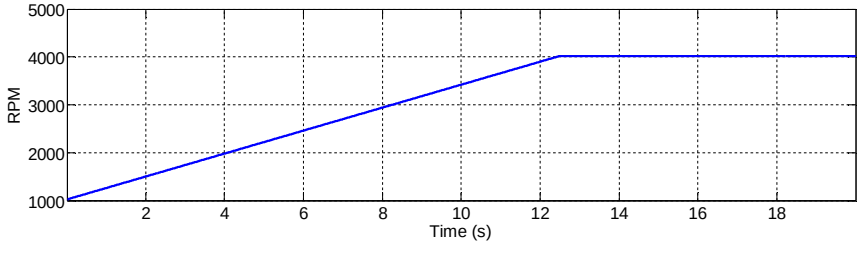

Figure 32. RPM during the acceleration.

The spectrograms with ASP and ANC are shown in Figure 33. The convergence at the 4nd and 5.5th engine orders are shown in Figures 34 and 35. The convergence curves for the rest of the engine orders are given in Figures 61–66 in Appendix A. The results indicate that, at 2nd, 3.5th, 4th and 5th engine orders, the algorithm quickly adapts to the target level. The error between the target level and the actual amplitude is less than 2 dB at the 4th engine order and 3–4 dB at maximum

at the 2nd, 3.5th and 5th engine orders. At the 5.5th and 6th engine orders, the ASP algorithm is able to track the target level with an error of 6 dB at maximum. With ANC, all engine orders have been attenuated so that the attenuation is 10–30 dB at the 2nd, 3.5th and 4th engine orders. At the higher engine orders, the attenuation is less than 10 dB.

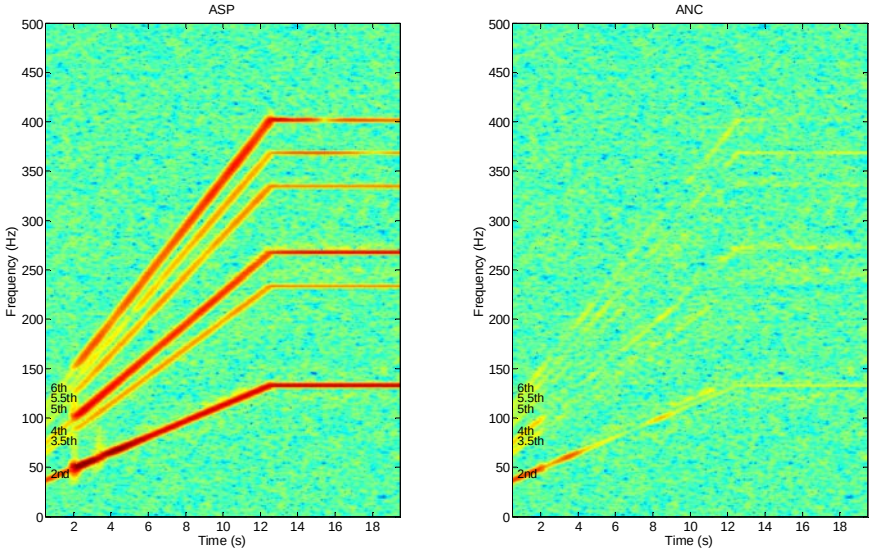

Figure 33. Spectrogram with active sound profiling at increasing fundamental frequency.

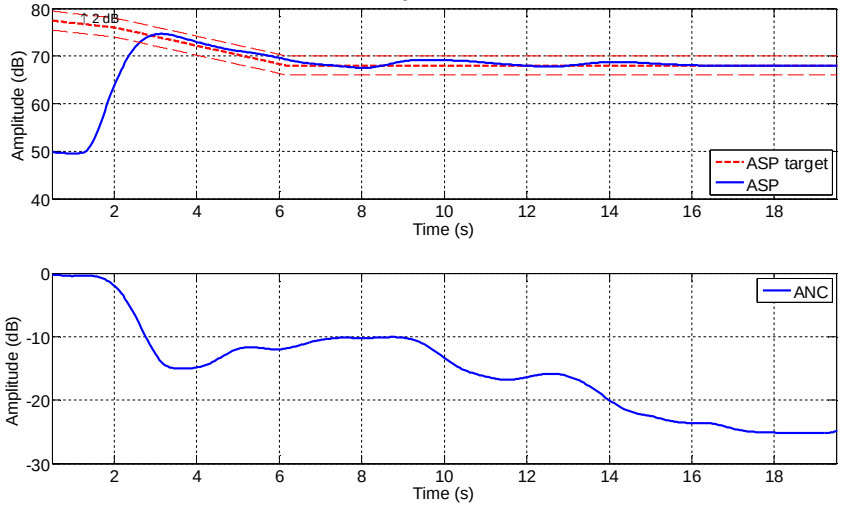

Figure 34. Convergence of the ASP (upper) and ANC (lower) algorithms at 4th engine order.

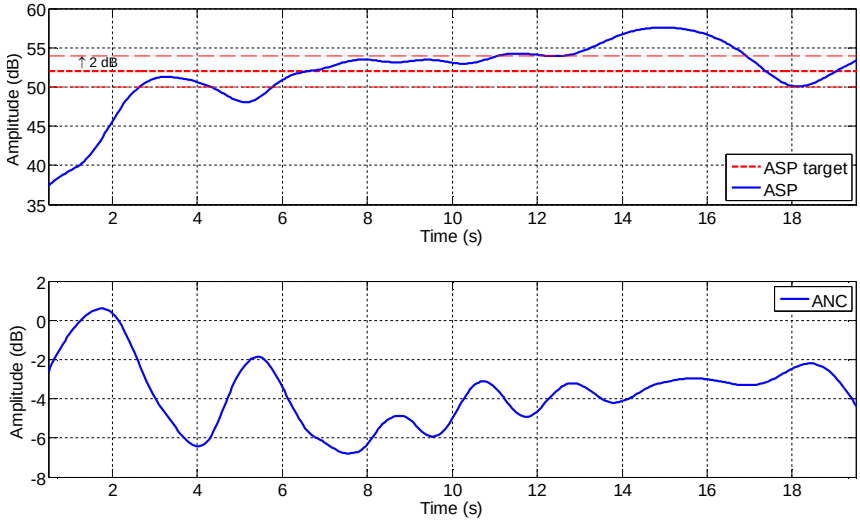

Figure 35. Convergence of the ASP (upper) and ANC (lower) algorithms at 5.5th engine order.

5.5 Effect of reference signal filtering method

The performance of the ASP system using LUT-based reference signal filtering has been compared with a conventional system using eigenvalue-equalised FIR filters for reference signal filtering. The objective is to analyse the effect of the larger phase errors introduced by the LUT-based filtering.

The ASP system was first simulated at a constant RPM of 3960 which corresponds to a fundamental frequency of 66 Hz. The convergence curves at the 5.5th engine order with both filtering methods are shown in Figure 36. It can be seen that, at the 5.5th engine order, the FIR-based filtering gives a better and faster performance than the LUT-based filtering. At the 6th engine order, the FIR-based system performed slightly better than the LUT-based system, but at the lower engine orders (2nd, 3.5th, 4th and 5th), the results were almost equal.

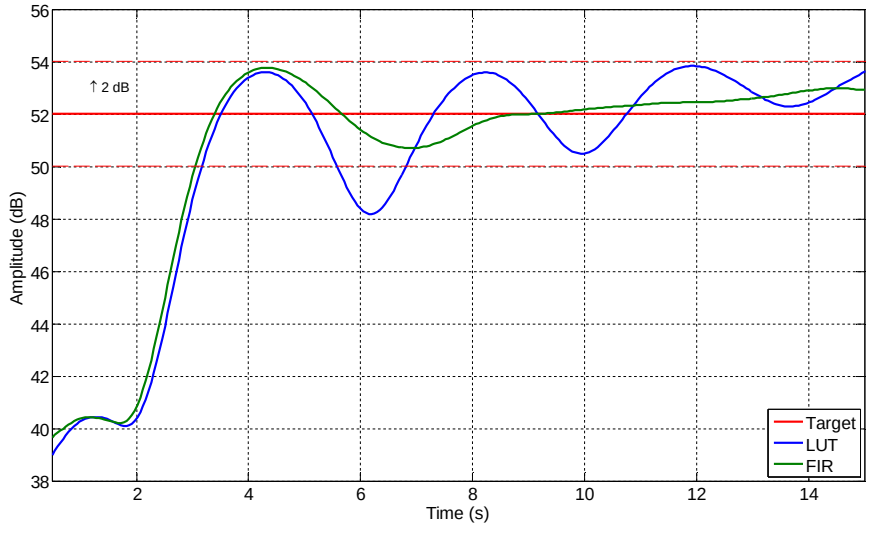

Figure 36. Convergence at 5.5th engine order in constant speed.

The ASP system was then simulated with increasing RPM. The fundamental frequency of the engine changed from 17 Hz to 67 Hz in 12.5 seconds, which corresponds to 1020–4000 RPM. In this case, the results were almost identical with both filtering methods at all engine orders. The results at the 5.5th engine order are given in Figure 37.

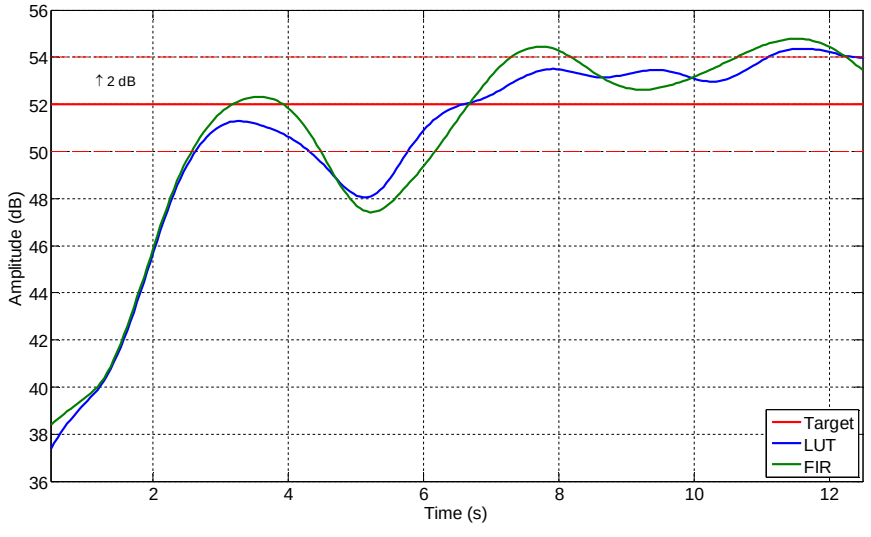

Figure 37. Convergence at 5.5th engine order during acceleration.

6. Experimental ASP system in a car

The operation of the multiple-channel active sound profiling algorithm has been tested with an experimental ASP system installed in a car. The car has been driven on public roads and the performance of the ASP algorithm has been evaluated at the error microphones and also at microphones installed in an artificial head which is located at the co-driver's seat.

6.1 Active sound profiling system in a car

The active sound profiling system has been constructed inside a Ford C-Max passenger car. The system is illustrated in Figure 38. There are four loudspeakers installed in the roof of the car and four error microphones located in the headrests of the front seats, as shown in Figure 22 in Chapter 5.1.

Figure 38. Ford C-Max car in which the ASP system has been installed.

The ASP system is illustrated in Figure 39. Based on the error microphone signals and the reference information obtained from the engine, the control system drives the loudspeakers so that the desired sound profile is achieved on the front seats of the car. A subwoofer located in the trunk is used for producing low frequency sound. The information obtained from the engine includes the tachometer signal proportional to the rotation speed of the engine and the load of the engine.

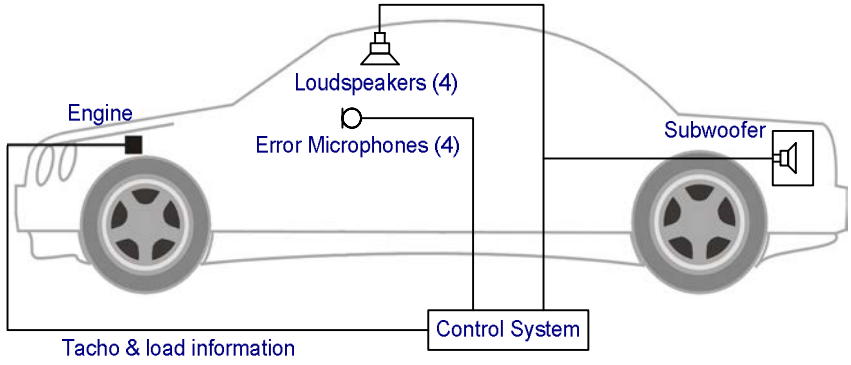

Figure 39. Active sound profiling system in a car [64].

The control system is based on Texas Instruments TMS320C6713 floating-point digital signal processor. The process flow from the simulation model to the DSP program has been described in [62] and [63]. The idea is that the Simulink algorithm can be easily converted to C code which is transferred to the DSP.

6.2 Test results

The practical performance of the ASP system was tested in road conditions. The car was driven on public roads and the noise inside the car cabin was recorded at several positions. During the experiments, the noise was recorded using binaural microphones installed in an artificial head and torso simulator located at the co-driver seat. Also the error microphone signals were recorded. The performance of the system has already been evaluated in [64] and [62].

For the evaluation of the performance, two different cases were chosen. In the first case, the car was driven at a constant speed of 80 km/h on a motorway. In the second case, the car is accelerated at the 3rd gear. Engine orders that are controlled with the ASP system are the 2nd, 3.5th, 4th, and 5th order.

6.2.1 Driving at constant speed

The measurement results at the constant speed are shown in Figures 40–43. The results are calculated by averaging the amplitudes measured at the artificial head

and at the error microphones of the driver's and co-driver's headrests. The ASP system is initially switched off. At 10 s, the system is switched on and, after 30 s, it is switched off.

At the 2nd engine order, the effect of the ASP system is unclear because the target level is close to the original sound pressure level of that order. At the higher engine orders, however, the effect can be clearly seen and the levels of the orders quickly reach the target level. Considering the results at the error microphones, the maximum error between the target level and the actual amplitude is 5 dB at the 3.5th engine order and 3 dB at the 4th and 5th engine orders. At the artificial head, the error is a few decibels larger, which can be expected since the maximal operation of the ASP algorithm is obtained at the error microphones.

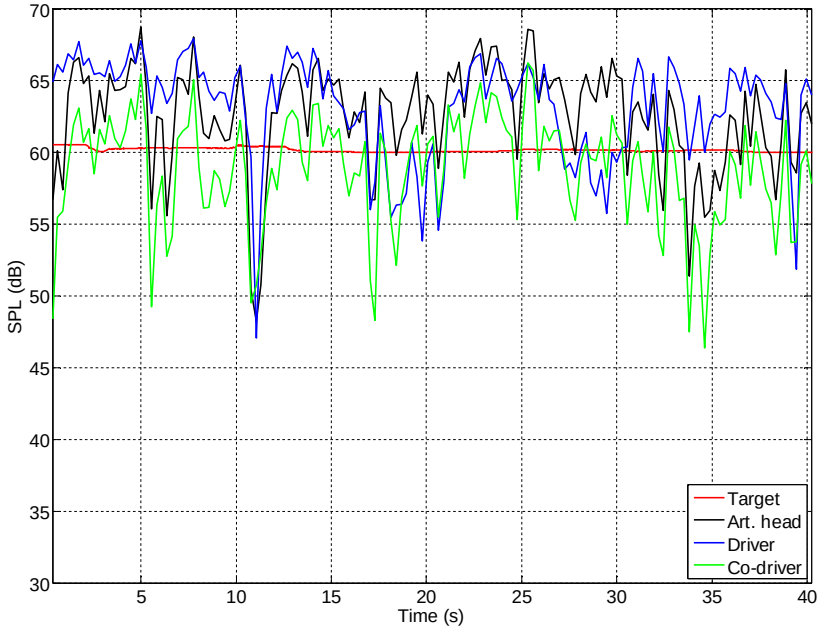

Figure 40. Results at the 2nd engine order with constant speed.

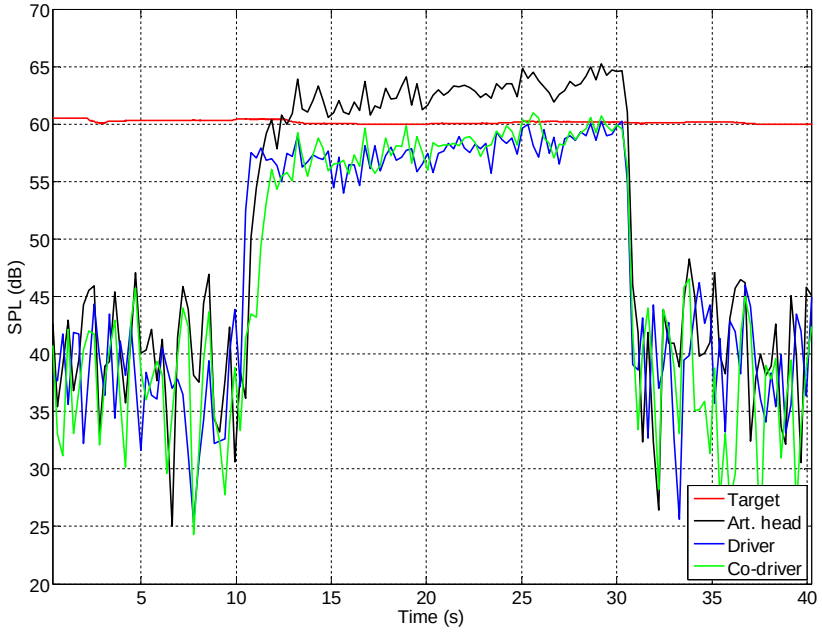

Figure 41. Results at the 3.5th engine order with constant speed.

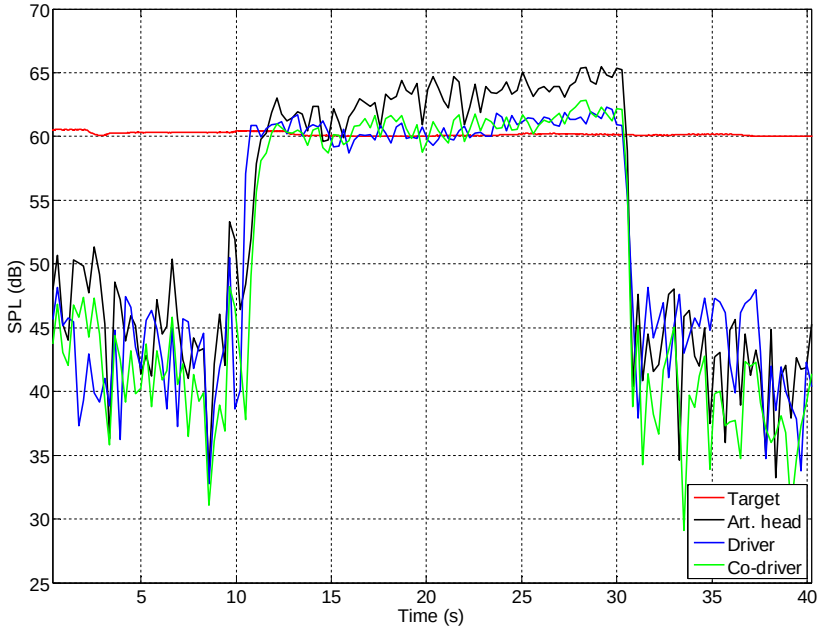

Figure 42. Results at the 4th engine order with constant speed.

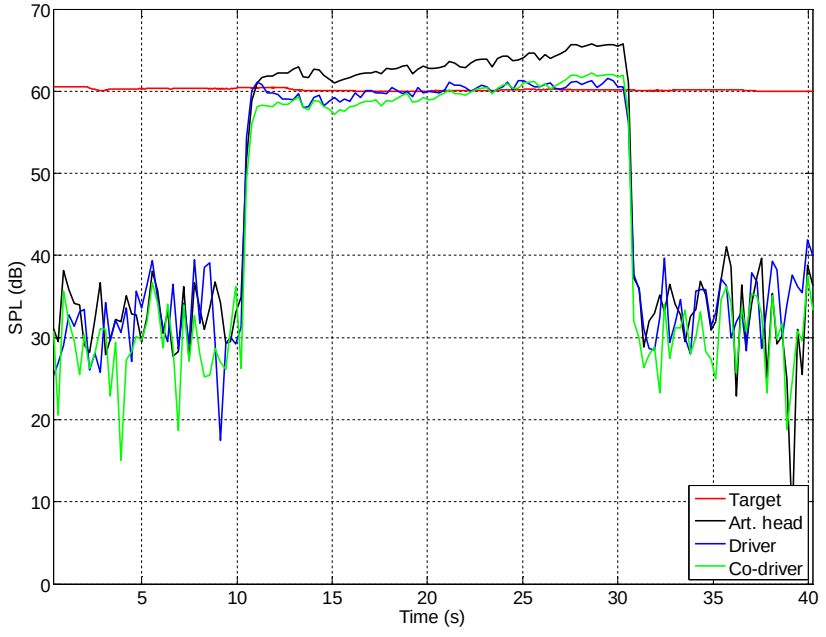

Figure 43. Results at the 5th engine order with constant speed.

6.2.2 Acceleration

During the acceleration, the engine rotation speed changes from 1500 RPM to 4500 RPM. The variation of the RPM is shown in Figure 44.

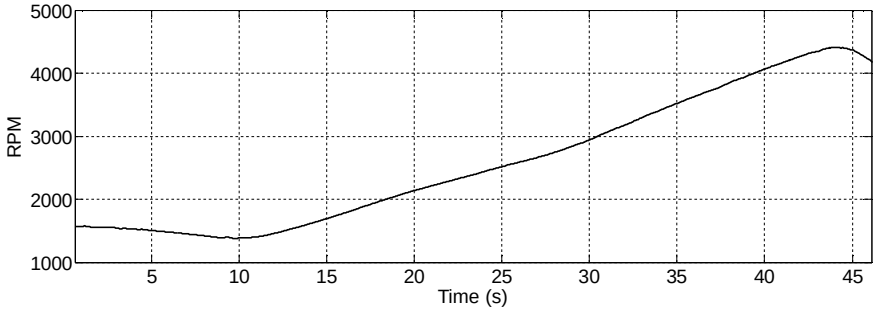

Figure 44. RPM during the acceleration.

The results with acceleration are given in Figures 45–48. Again, the ASP system is initially switched off. At 10 s, the system is switched on and, at 45 s, it is switched off. Like in the previous case, the effect of the ASP system is unclear at the 2nd engine order. At the higher engine orders, the levels of the orders follow the target level with adequate accuracy. The best results have been obtained at the 3.5th and 4th engine orders. Looking at the results at the error microphones, the maximum error between the target level and the actual amplitude is 5 dB at the 3.5th engine order, 4 dB at the 4th engine order and 10 dB at the 5th engine order. At the artificial head, the maximum error is 10 dB.

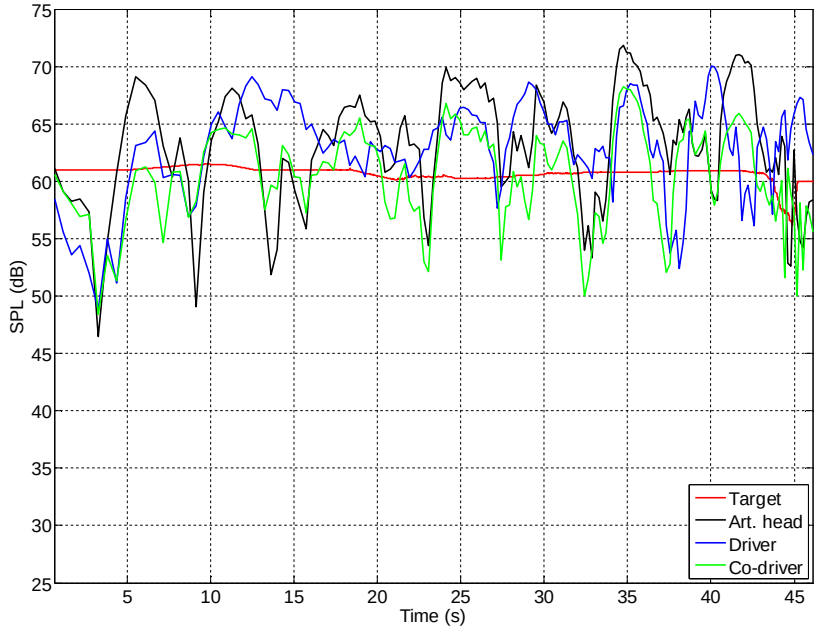

Figure 45. Results at the 2nd engine order with acceleration.

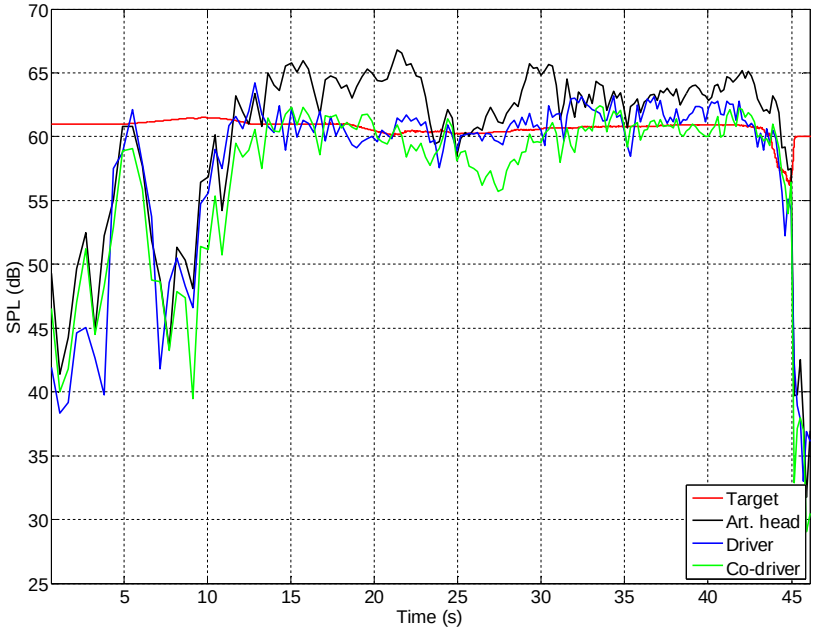

Figure 46. Results at the 3.5th engine order with acceleration.

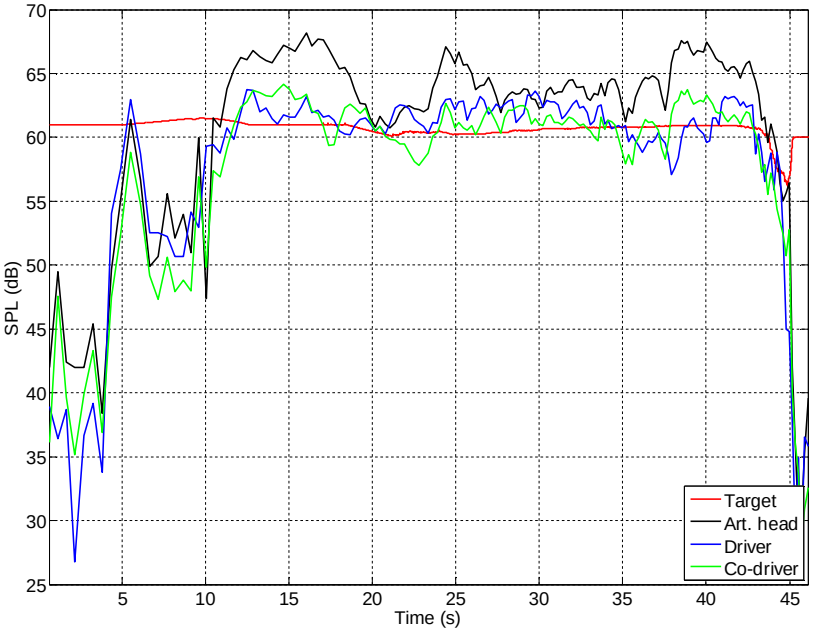

Figure 47. Results at the 4th engine order with acceleration.

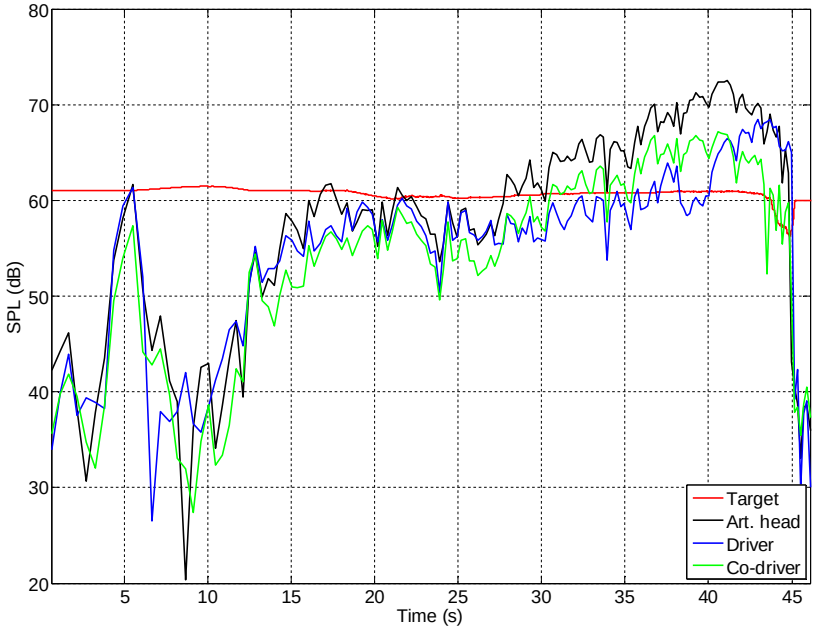

Figure 48. Results at the 5th engine order with acceleration.

7. Summary of contributions and conclusions

In this thesis, active sound profiling was applied to a passenger car. The objective was to develop a robust and computationally-efficient ASP algorithm which works in a reliable way and requires a minimal amount of computational power. The performance of the developed algorithm was tested in a simulation model and in an experimental ASP system installed in a car.

Active sound profiling is related to active noise control in which noise is cancelled using adjustable secondary sound. Both ASP and ANC are based on superposition of the noise field and the secondary sound field. In active sound profiling, the objective is to obtain a desired sound field, instead of cancelling the noise. In passenger cars, active sound profiling is used for modifying the engine noise inside the cabin. The objective is to increase the sound quality and modify the acoustic impression of the vehicle.

ANC systems have been installed in several car models since late 1980's while ASP systems are mainly on a prototype level. In hybrid cars, the engine noise is related to the source (combustion or electric engine) and changing the power source may be distracting to the driver. This is also the case in cars with variable-cylinder engines where part of the cylinders can be deactivated during light-load operation. In an electric vehicle, the noise level of the engine is low and other noise sources inside the vehicle become dominant. Active sound profiling can be utilised to produce a source-independent sound field inside a car or to generate the engine noise inside an electric vehicle.

The command-FXLMS algorithm is one of the simplest ASP algorithms. It also provides fast convergence and stability against errors in the plant model. It was used as a basis for developing the new algorithm. Advanced ASP algorithms exist but they are more complex and computationally heavier. C-FXLMS algorithm is an extension to the famous FXLMS algorithm which is widely used in active noise control. In the FXLMS algorithm and its variants, most of the computational burden is caused by the reference signal filtering. The amount of required computational power depends on the number of controlled engine orders, secondary sources and error sensors. Increasing the number of channels in the system dramatically increases the number of filtering operations.

The C-FXLMS algorithm requires a model of the plant which consists of the transfer paths from the secondary sources to the error sensors. The accuracy of

the plant model has a clear influence on the performance of the algorithm. Using FIR filters, the plant can be modelled with sufficient accuracy, except at frequencies where large phase shifts occur, i.e. at resonances. If the phase error between the actual plant and the plant model becomes too large, the C-FXLMS algorithm is no longer able to track the desired noise level or may even become unstable. It was found out in this work that introducing a leakage factor in the update equation of the algorithm improves the performance at large phase shifts of the plant model. At other frequencies, however, the performance is degraded by the leakage factor. Therefore, an adaptive leakage factor has been created. The value of the leakage factor depends on the phase shift of the plant model so that leakage becomes smaller at large phase shifts, causing a larger leak and helping the algorithm to maintain the desired noise level. If the phase shift is small, the leakage factor becomes inactive and no leakage is used.

The developed ASP algorithm combines the multiple-channel C-FXLMS algorithm with a new technique to obtain the filtered reference signals. The technique is based on delaying the sinusoidal reference signals and modifying their amplitude. The adaptive weights are updated using the leaky FXLMS algorithm with the adaptive leakage factor. Adaptation of the leakage factor is based on the phase difference in the eigenvalue-equalised plant model. Using the eigenvalue-equalised plant model, the step sizes of the multiple-channel FXLMS algorithm are constant at all frequencies since the magnitude of the plant model is constant for each secondary path. The benefits of the eigenvalue-equalisation are increased robustness and faster tuning of the step sizes. Before running the ASP algorithm, a system identification process is carried out to obtain the plant model required by the ASP algorithm. The plant model is then processed so that the magnitude of each secondary path becomes flat. The mean values of the magnitudes and frequency-dependent delay values are stored in lookup tables that are used for reference signal filtering.

The developed ASP algorithm was tested in a simulation model. The simulation model was based on an ASP system installed in a car. The system has four loudspeakers and four error microphones. The secondary paths from the loudspeakers to the error microphones were measured and a model of the plant was created. The engine was modelled as a source of sine waves and random noise. The simulation model consisted of the measured plant model, the engine model and the control system which was based on the developed algorithm. In the simulations, the performance of the ASP algorithm was tested with constant RPM and increasing RPM. These test cases correspond to driving a car at a constant speed or accelerating the car. The simulation results show that the algorithm quickly adapts to the desired target levels and is able to track the target levels with reasonable accuracy. At constant RPM, a higher accuracy is reached than with increasing RPM. Higher performance is obtained at lower engine orders, whereas at the highest engine orders, the performance is decreased as the frequency increases. One reason for the degraded performance is that the phase error between the plant and the identified plant model increases as a function of frequency. Another reason for the decreased performance at the highest engine orders with increas-

ing RPM is that the frequency difference becomes larger at higher engine orders if the RPM changes. At the higher engine orders, the algorithm has to adapt to a larger frequency change and tracking of the target level becomes more difficult.

The developed algorithm was also implemented in an ASP system installed in a car. The performance of the system was tested by driving the car on public roads. The experimental results show that the system is able to operate at constant speed and during acceleration. Although the highest engine orders used in the simulations were not controlled in the experiments, the experimental results match with the simulation results.

There are several sources causing errors and non-ideal operation of the ASP algorithm. They include the identification of the plant model, the estimation of the fundamental frequency of the engine, the sinewave generator and the lookup-table based reference signal filtering. In the future, the system can be improved by minimising the effect of the errors. The estimation of the fundamental frequency may not be an issue, since the RPM of the engine can be obtained via the CAN bus in some cars. The sinewave generator produces a quantisation error if implemented using a lookup table or a recursive oscillator. The error can be minimised by increasing the size of the lookup table. More sophisticated and memory-saving methods can also be studied for creating sine waves. The accuracy of the delay lookup table is an important issue, and the error in the delay estimate tends to increase as a function of frequency. The error is mostly caused by the rounding error in calculation of the delay. Errors occurring in the plant modelling have also an effect since the FIR estimate of the plant is not perfect, although it is usually sufficiently accurate. A way to decrease the errors in the delay lookup table is to find a more straightforward method to obtain the lookup table. In that method, an estimate of the frequency response of the plant is utilised without the need to identify the FIR filters. Resonances and other phenomena causing sudden phase shifts should be accurately modelled since they degrade the performance of the ASP algorithm.

Acknowledgements

I thank the examiners of my thesis, Professor Ioan Tabus from Tampere University of Technology, and Professor Vesa Välimäki from Aalto University. I also thank Ioan Tabus for acting as my supervisor over the last 12 years.

I also thank my Team Leader Kari Tammi, my former Team Leader Hannu Nykänen and my former Technology Manager Pekka Koskinen for their support. I'd like to thank my colleagues Marko Antila and Guangrong (Aron) Zou for the fruitful co-operation during InMAR, ANRAC and other related projects. I'd also like to thank my colleagues Antti Lankila and Denis Siponen for their help in the projects.

I'm grateful to my loved ones, my caring wife Ritva and my two wonderful children, Lasse and Elli. I'm also grateful to my parents, brothers and friends for their care and support, especially during the hardest times.

References

[1] Nelson, P. A. and Elliott, S. J. Active control of sound. Academic Press, 1993.

[2] Elliott, S. Signal processing for active control. Academic Press, 2001.

[3] Kuo, S. and Morgan, D. Active noise control: Algorithms and DSP implementations. Wiley-Interscience, 1996.

[4] Lueg, P. Process of silencing sound oscillations, US Patent 2043416, 1936.

[5] Elliott, S. J. and Nelson, P. A. Active noise control. IEEE Signal Processing Magazine, Oct. 1993, pp. 12–35.

[6] Conover, W. B. Fighting noise with noise, Noise Control, Vol. 2, 1956, pp. 78–82.

[7] Kataja, J. Applications of adaptive algorithms for active noise control, Master's thesis, Tampere University of Technology, Finland, 1999.

[8] Kataja, J. and Tabus, I. Application of the LS-LMS algorithm in active noise control in ducts. Proc. Signal and Image Processing (SIP 2000), Las Vegas, USA, Nov. 20–23, 2000.

[9] Burgess, J. C. Active adaptive sound control in a duct: A computer simulation. Journal of the Acoustical Society of America, Vol. 70, No. 3, Sept. 1981, pp. 715–726.

[10] Zander, A. C. and Hansen, C. H. Active control of higher-order acoustic modes in ducts. Journal of the Acoustical Society of America, Vol. 92, No. 1, July 1992, pp. 244–257.

[11] Sano, H., Yamashita, T. and Nakamura, M. Recent application of active noise and vibration control to automobiles. Proc. Active 2002, Southampton, UK, July 15–17, 2002, pp. 29–42.

[12] Elliott, S. J. A review of active noise and vibration control in road vehicles. ISVR Technical Memorandum No. 981, Dec. 2008.

[13] Elliott, S. J., Nelson, P. A., Stothers, I. M. and Boucher, C. C. In-flight experiments on the active control of propeller-induced cabin noise. Journal of Sound and Vibration, Vol. 140, No. 2, 1990, pp. 219–238.

[14] Kochan, K., Sachau, D. and Breitbach, H. Robust controller design of an active noise control system for a propeller aircraft. Proc. Internoise 2009, Ottawa Canada, Aug. 23–26, 2009.

[15] Maier, R. Challenges and applications for active noise and vibration control in aerospace. Proc. Active 2009, Ottawa, Canada, Aug. 20–22, 2009.

[16] Sachau, D. Adaptive control of broadband noise in a light jet. Proc. Internoise 2009. Ottawa Canada, Aug. 23–26, 2009.

[17] Thomas J. K., Lovstedt, S., Blotter, J. D., Sommerfeldt, S. D. and Faber, B. Eigenvalue equalization filtered-x (EE-FXLMS) algorithm applied to the active minimization of tractor noise in a mock cabin. Noise Control Engineering Journal, Vol. 56, No. 1, Jan–Feb 2008, pp. 25–34.

[18] Antila, M. and Kataja, J. Active noise control experiments in a moving machinery cabin. Proc. Internoise 2004, Prague, Czech Republic, Aug. 22–25, 2004.

[19] Hong, J. and Bernstein, D. Bode integral constraints, colocation, and spillover in active noise and vibration control. IEEE Transactions on Control Systems Technology, Vol. 6, No. 1, Jan. 1998, pp. 111–120.

[20] Olson, H. F. and May, E. G. Electronic sound absorber, Journal of the Acoustical Society of America, Vol. 25, No. 6, Nov. 1953, pp. 1130–1136.

[21] Carme, C. A new filtering method by feedback for A.N.C. at the ear. Proc. Internoise 88, Avignon, France, Aug. 30 – Sept. 1, 1988. Pp. 1083–1086.

[22] Rafaely, B. Active noise reducing headset – an overview. Proc. Internoise 2001, The Hague, The Netherlands, Aug. 27–30, 2001.

[23] Schirmacher, R. Active noise control and active sound design – Enabling factors for new powertrain technologies. Proc. 6th International Styrian Noise, Vibration & Harshness Congress, June 2010, Graz, Austria.

[24] Reese, L. Active sound-profiling for automobiles. Doctoral thesis, ISVR, Southampton, UK, 2004.

[25] http://paultan.org/2008/07/24/toyota-crown-hybrid-features-active-noise-control/. Checked 27th May 2011.

[26] Nikkei Electronics Asia, http://techon.nikkeibp.co.jp/article/HONSHI/20080428/151147/?P=2. Checked 27th May 2011.

[27] Tamamura, M. and Shibata, E. Application of active noise control for engine related cabin noise. JSAE Review 17, 1996, pp. 37–43.

[28] Winkler, J., Lippold, R. and Scheuren, J. Implementation of an active noise control system in a van. Proc. Active 97, Budapest, Hungary, Aug. 21–23, 1997.

[29] Zou, G., Antila, M., Lankila, A. and Kataja, J. Algorithm development and optimization for active noise control in a truck cabin. Proc. Active 2009, Ottawa, Canada, Aug. 20–22, 2009.

[30] Mclean, I. R. Active control of automotive air induction noise via source coupling. Proc. SAE 2001 Noise & Vibration Conference & Exposition, Grand Traverse, MI, USA, April 2001.

[31] Jeong, W., Kim, K., Lee, S. and Kim, J. Application of active noise control to car intake system. Proc. Inter-Noise 2002, Dearborn, MI, USA, Aug. 19–21, 2002.

[32] Lee, C.-H., Oh, J.-E., Joe, Y.-G. and Lee, Y. Y. The performance improvement for an active noise control of an automotive intake system under rapidly accelerated conditions. JSME International Journal Series C, Vol. 47, No. 1, 2004, pp. 314–320.

[33] Kim, H.-S., Hong, J.-S., Sohn, D.-G. and Oh, J.-E. Development of an active muffler system for reducing exhaust noise and flow restriction in a heavy vehicle. Noise Control Engineering Journal, Vol. 47, No. 2, Mar–Apr 1999, pp. 57–63.

[34] Krueger, J., Pommerer, M. and Jebanski, R. Lightweight active exhaust silencers for passenger vehicles. Proc. 6th International Styrian Noise, Vibration & Harshness Congress, Graz, Austria, June 2010.

[35] Boonen, R. and Sas, P. Design of an active exhaust attenuating valve for internal combustion engines. Proc. ISMA 2002, Leuven, Belgium, 2002.

[36] Jha, S. K. Characteristics and sources of noise and vibration and their control in motor cars. Journal of Sound and Vibration, Vol. 47, No. 4, 1976, pp. 543–558.

[37] Sutton, T. J., Elliott, S. J. and Nelson, P. A. The active control of road noise inside vehicles. Proc. Inter-Noise 90, Gothenburg, Sweden, Aug. 13–15, 1990. Pp. 1247–1250.

[38] Sutton, T. J., Elliott, S. J., McDonald, A. M. and Saunders, T. J. Active control of road noise inside vehicles. Noise Control Engineering Journal, Vol. 42, No. 4, Jul–Aug 1994, pp. 137–147.

[39] Oh, S.-H, Kim, H.-S. and Park, Y. Active control of road booming noise in automotive interiors. Journal of the Acoustical Society of America, Vol. 111, No. 1, Pt. 1, Jan. 2002, pp. 180–188.

[40] Sano, H., Inoue, T., Takahashi, A., Terai, K. and Nakamura, Y. Active control system for low-frequency road noise combined with an audio system. IEEE Transactions on Speech and Audio Processing, Vol. 9, No. 7, 2001, pp. 755–763.

[41] Zeller, P. Engine sound – a contribution to sharpening the character of a vehicle. Proc. 2nd Styrian Noise, Vibration and Harshness Congress, Graz, Austria, May 22–23, 2003.

[42] Kronast, M., Mellin, V. and Carme, C. A sound quality active noise profiling system for a passenger test vehicle. Proc. Euronoise 2006, Tampere, Finland, May 30 – June 1, 2006.

[43] Eisele, G., Wolff, K., Wittler, M., Abtahi, R. and Pischinger, S. Acoustics of hybrid vehicles. Proc. 6th International Styrian Noise, Vibration & Harshness Congress, Graz, Austria, June 2010.

[44] Breitz, T., Wagner, V. and Enigk, H. Importance of operational sounds for vehicle quality. Proc. Aachen Acoustics Colloqium, 2010. Pp. 33–36.

[45] Eisele, G., Genender, P., Wolff, K. and Schürmann, G. Electric vehicle sound design – Just wishful thinking? Proc. Aachen Acoustics Colloqium, 2010. Pp. 47–59.

[46] http://www.gizmag.com/lotus-active-noise-control/11486. Checked 27th May 2011.

[47] Haykin, S. Adaptive Filter Theory, 3rd Edition, Prentice Hall, 1996.

[48] Kuo, S. M., Kong, X., Chen, S. and Hao, W. Analysis and design of narrow-band active noise control systems. IEEE Transactions on Acoustics, Speech and Signal Processing, Vol. 6, 1998, pp. 3557–3560.

[49] Thomas, J., Lovstedt. S. P., Blotter, J. D. and Sommerfeldt, S. D. Eigenvalue equalization filtered-x algorithm for the multichannel active noise control of stationary and nonstationary signals. Journal of the Acoustical Society of America, Vol. 123, No. 6, 2008, pp. 4238–4249.

[50] Lovstedt, S. P. Improving performance of the filtered-x least mean square algorithm for active control of noise containing multiple quasi-stationary tones. Master's Thesis, Brigham Young University, USA, 2008.

[51] Elliott, S. J., Stothers, I. M. and Nelson, P. A. A multiple error LMS algorithm and its application to the active control of sound and vibration. IEEE Transactions on Acoustics, Speech, and Signal Processing, Vol. ASSP-35, No. 10, Oct. 1987, pp. 1423–1434.

[52] Kuo, S. M. and Ji, M. J. Development and analysis of an adaptive noise equalizer. IEEE Transactions on Speech and Audio Processing, Vol. 3, No. 3, May 1995.

[53] Reese, L. and Elliott, S. Adaptive algorithms for active sound-profiling. IEEE Transactions on Audio, Speech, and Language Processing, Vol. 14, No. 2, March 2006, pp. 711–719.

[54] Kuo, S. M., Gupta, A. and Mallua, S. Development of adaptive algorithm for active sound quality control. Journal of Sound and Vibration, Vol. 299, 2007, pp. 12–21.

[55] Gallo, M., Anthonis, J., Van der Auweraer, H., Janssens, K. and de Oliveira, P. R. Evaluation of an active sound quality control system in a virtual car driving simulator. Proc. Inter-noise 2010, Lisbon, Portugal, June 13–16, 2010.

[56] de Oliveira, L. P. R., Stallaert, B., Janssens, K., Van der Auweraer, H., Sas, P. and Desmet, W. NEX-LMS: A novel adaptive control scheme for harmonic sound quality control. Mechanical Systems and Signal Processing, Vol. 24, 2010, pp. 1727–1738.

[57] Kuo, M., Yenduria, R. K. and Gupta, A. Frequency-domain delayless active sound quality control algorithm. Journal of Sound and Vibration, Vol. 318, 2008, pp. 715–724.

[58] Antila, M. Engine speed tracking and reference generation for active noise profiling. Proc. Active 2009, Ottawa, Canada, Aug. 20–22, 2009.

[59] Lee, S. M., Lee, H. J., Yoo, C. H., Youn, D. H. and Cha, I. W. An active noise control algorithm for controlling multiple sinusoids. Journal of the Acoustical Society of America, Vol. 104, No. 1, July 1998, pp. 248–254.

[60] Kong, X. and Kuo, S. M. Analysis of asymmetric out-of-band overshoot in narrowband active noise control systems. IEEE Transactions on Speech and Audio Processing, Vol. 7, No. 5, Sept. 1999, pp. 587–591.

[61] Wang, L. and Gan, W. S. Analysis of misequalization in a narrowband active noise equalizer system. Journal of Sound and Vibration, Vol. 311, 2008, pp. 1438–1446.

[62] Lankila, A. Simulation model for an active noise control system – Development and validation, Master's Thesis, Helsinki University of Technology, Finland, 2008.

[63] Antila, M. and Lankila, A. Application-oriented development of an active noise profiling control system. Proc. Inter-Noise 2008, Shanghai, China, Oct. 26–29, 2008.

[64] Zou, G., Antila, M. and Kataja, J. Active noise profiling system development and algorithm implementation in a passenger car. Proc. Inter-noise 2010, Lisbon, Portugal, June 13–16, 2010.

[65] Zou, G., Antila, M. and Kataja, J. Practical active noise profiling in a passenger car. Proc. Akustiikkapäivät 2011, Tampere, Finland, May 11–12, 2011.

Appendix A: Simulation results

Simulation results with constant low RPM (2100 RPM) are shown in Figures A1–A6.

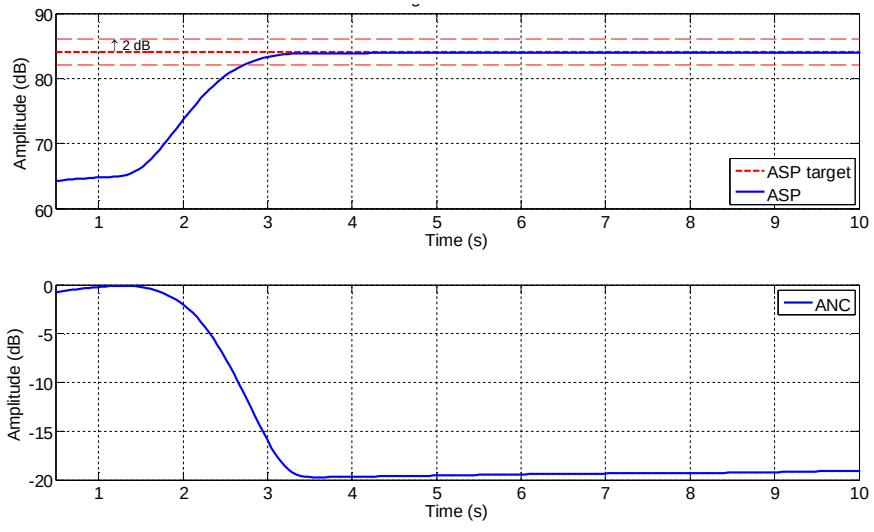

Figure A1. Convergence of the ASP (upper) and ANC (lower) algorithms at 2nd engine order.

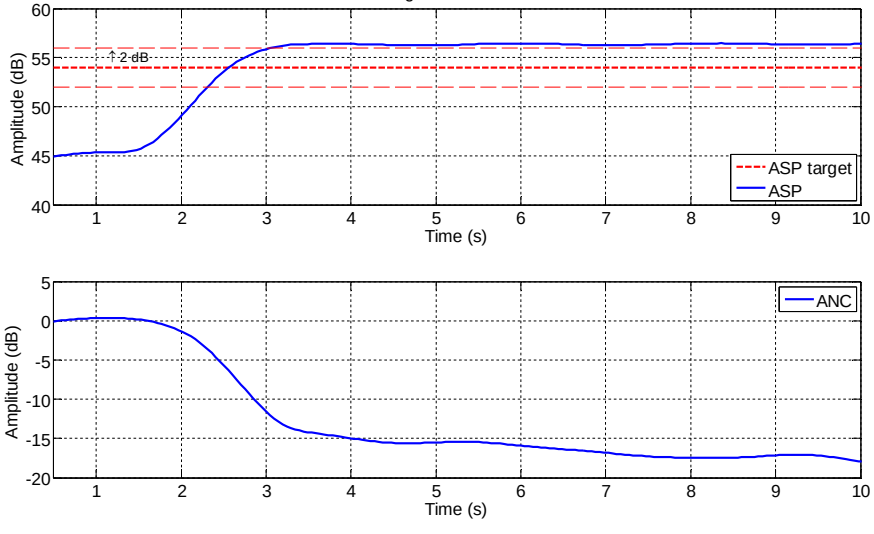

Figure A2. Convergence of the ASP (upper) and ANC (lower) algorithms at 3.5th engine order.

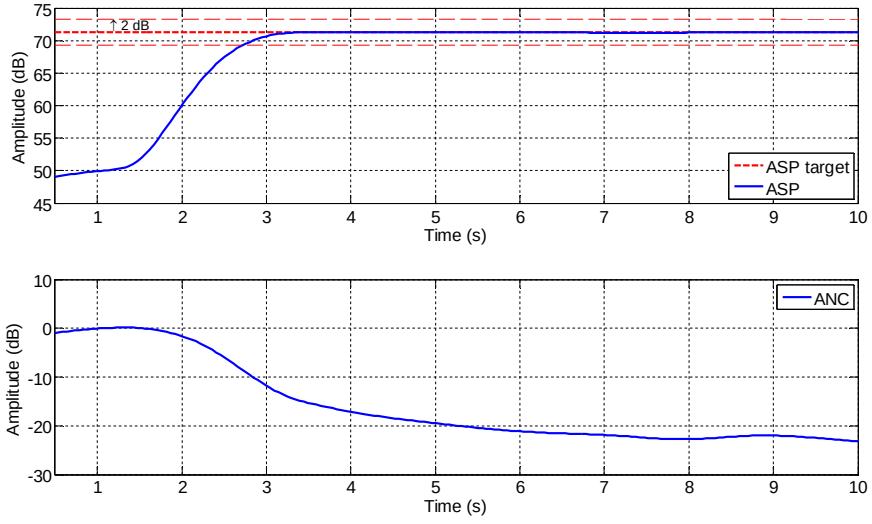

Figure A3. Convergence of the ASP (upper) and ANC (lower) algorithms at 4th engine order.

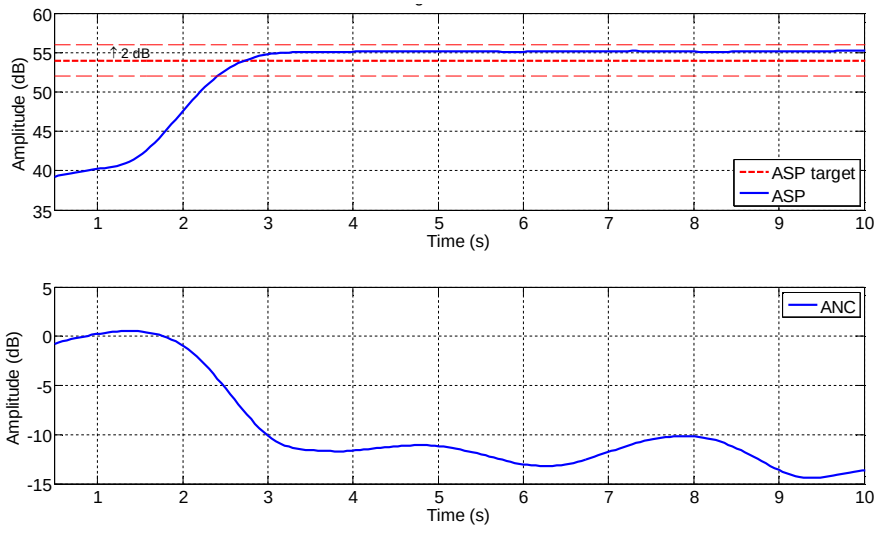

Figure A4. Convergence of the ASP (upper) and ANC (lower) algorithms at 5th engine order.

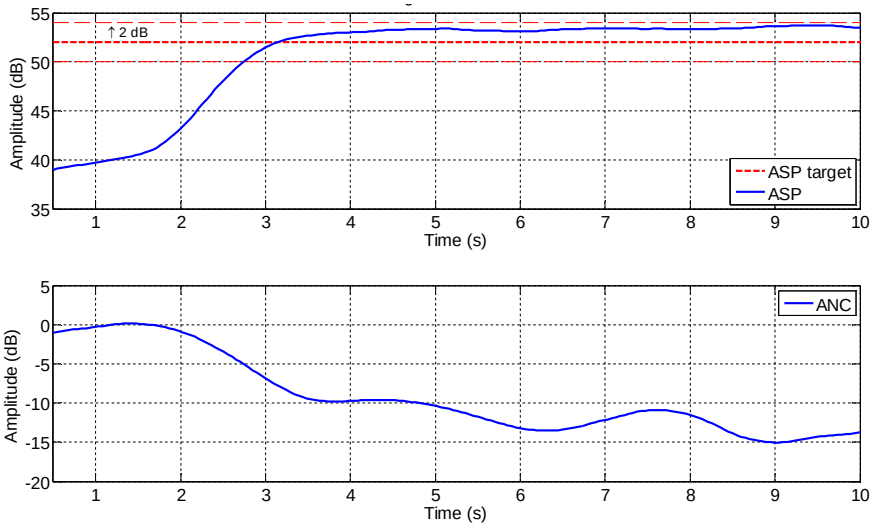

Figure A5. Convergence of the ASP (upper) and ANC (lower) algorithms at 5.5th engine order.

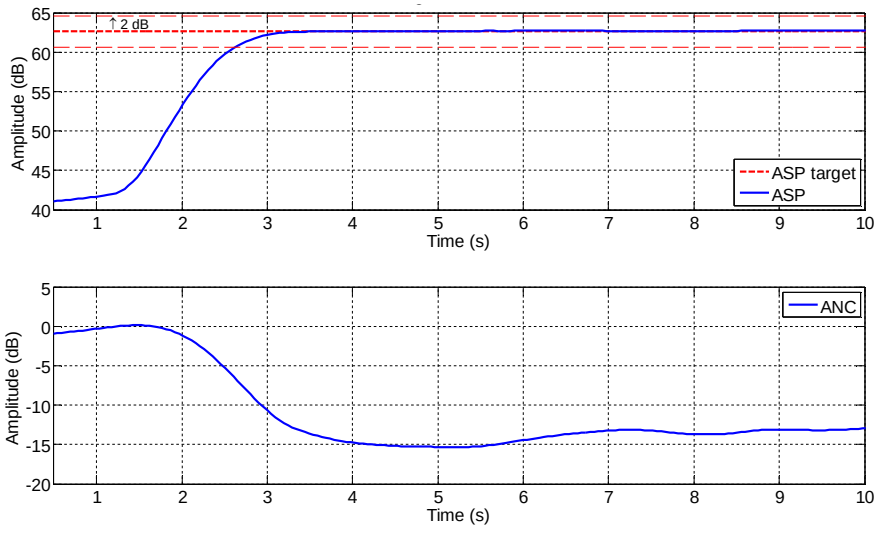

Figure A6. Convergence of the ASP (upper) and ANC (lower) algorithms at 6th engine order.

Simulation results with constant high RPM (3960 RPM) are shown in Figures A7–A12.

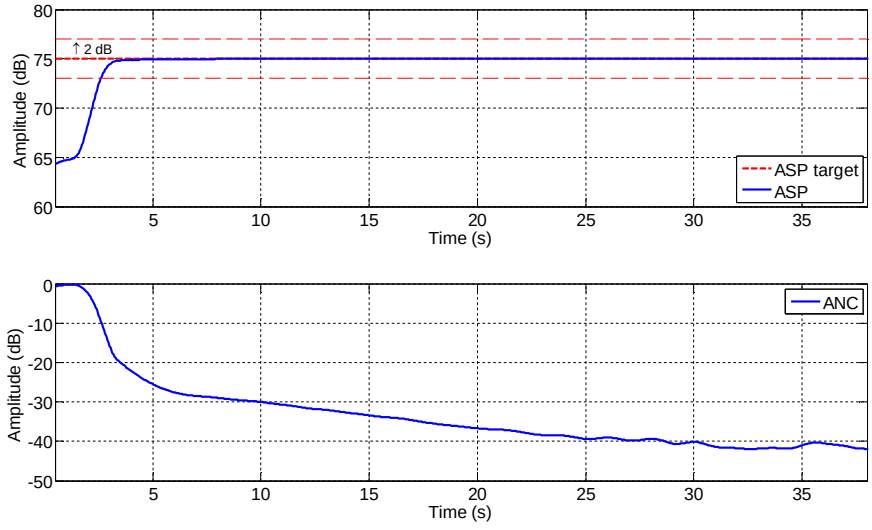

Figure A7. Convergence of the ASP (upper) and ANC (lower) algorithms at 2nd engine order.

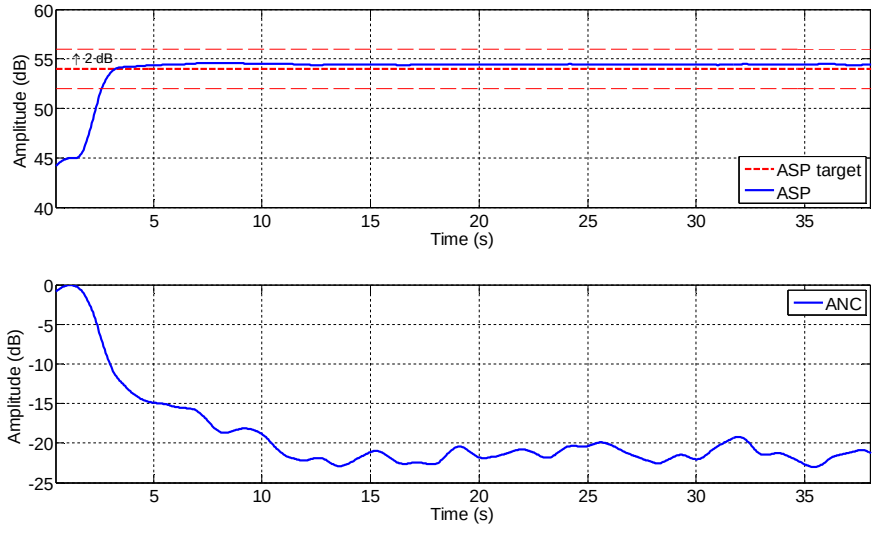

Figure A8. Convergence of the ASP (upper) and ANC (lower) algorithms at 3.5th engine order.

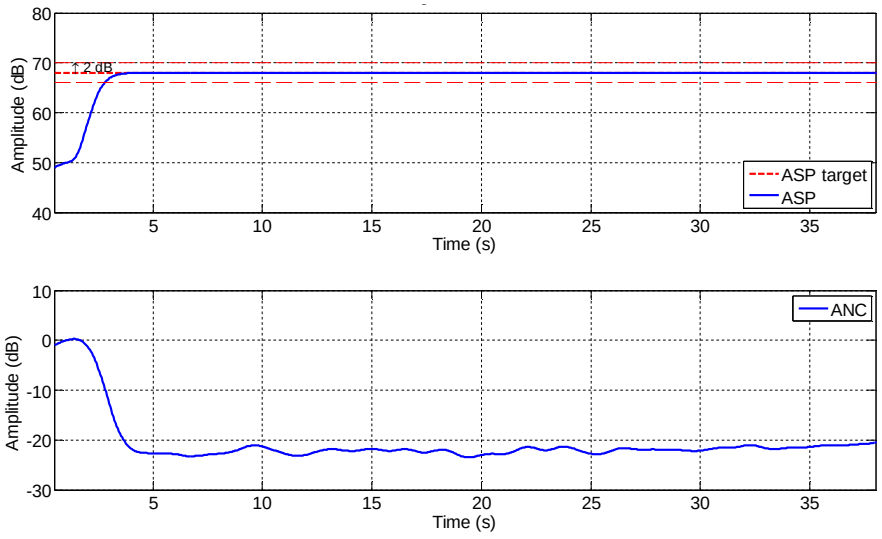

Figure A9. Convergence of the ASP (upper) and ANC (lower) algorithms at 4th engine order.

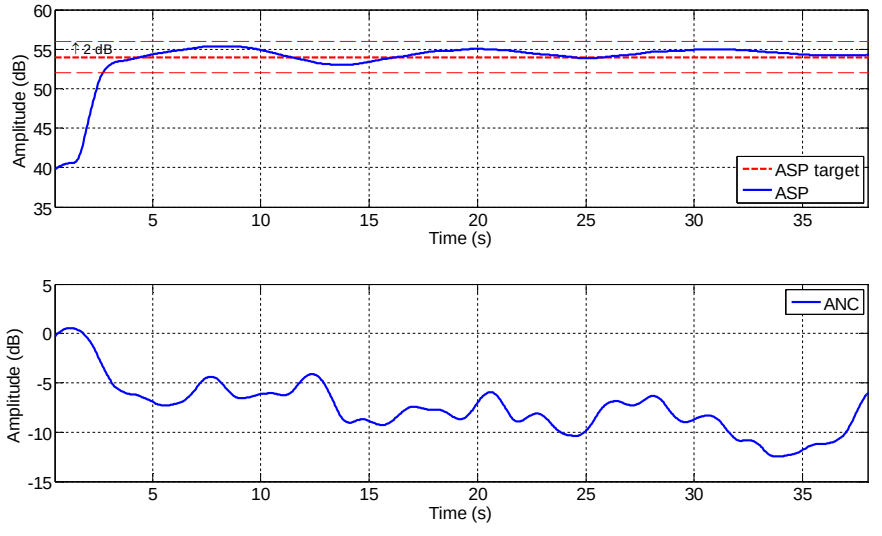

Figure A10. Convergence of the ASP (upper) and ANC (lower) algorithms at 5th engine order.

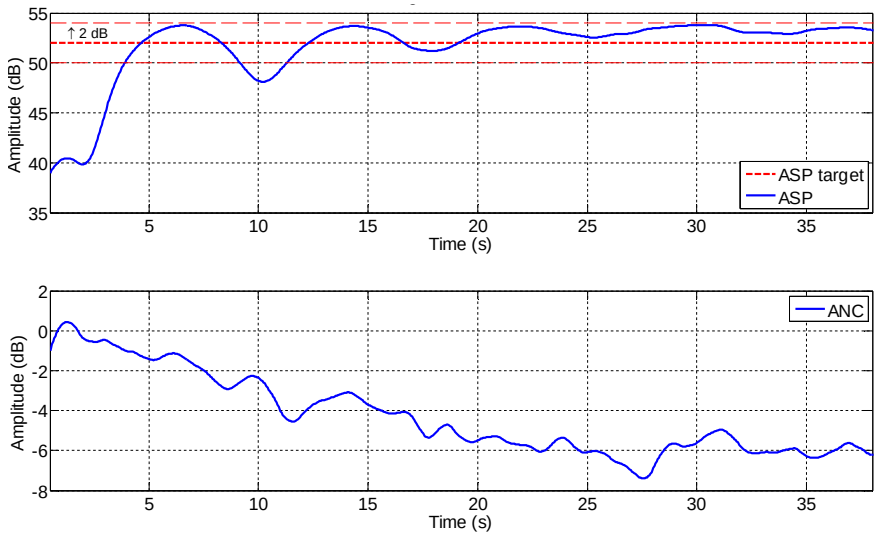

Figure A11. Convergence of the ASP (upper) and ANC (lower) algorithms at 5.5th engine order.

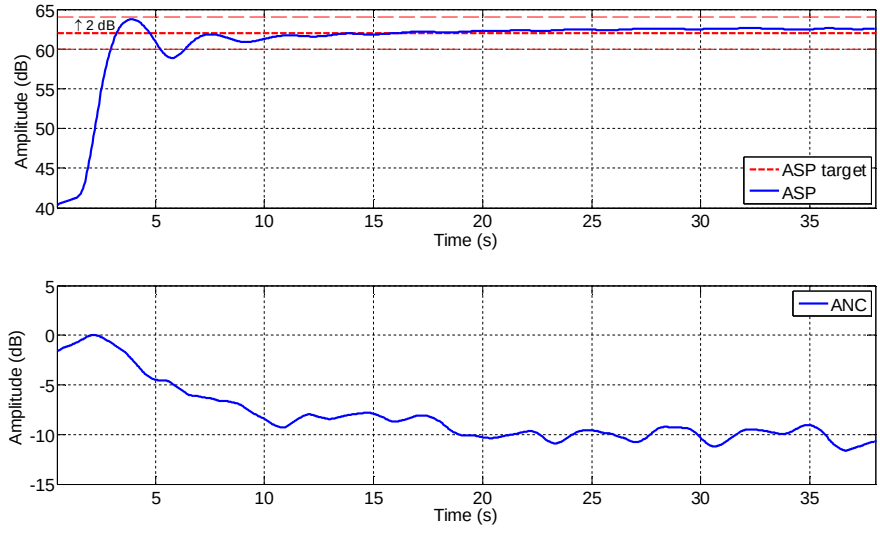

Figure A12. Convergence of the ASP (upper) and ANC (lower) algorithms at 6th engine order.

Simulation results with increasing RPM (1020–4000 RPM) are shown in Figures A13–A18.

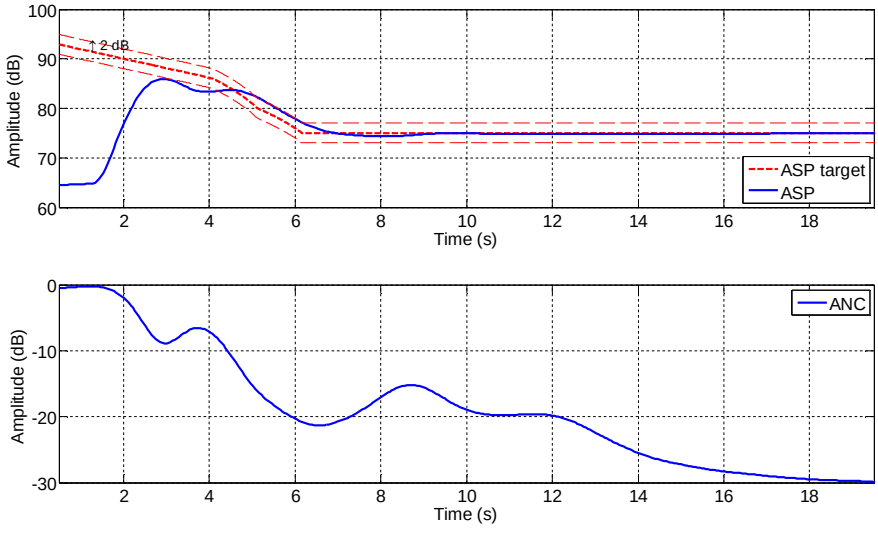

Figure A13. Convergence of the ASP (upper) and ANC (lower) algorithms at 2nd engine order.

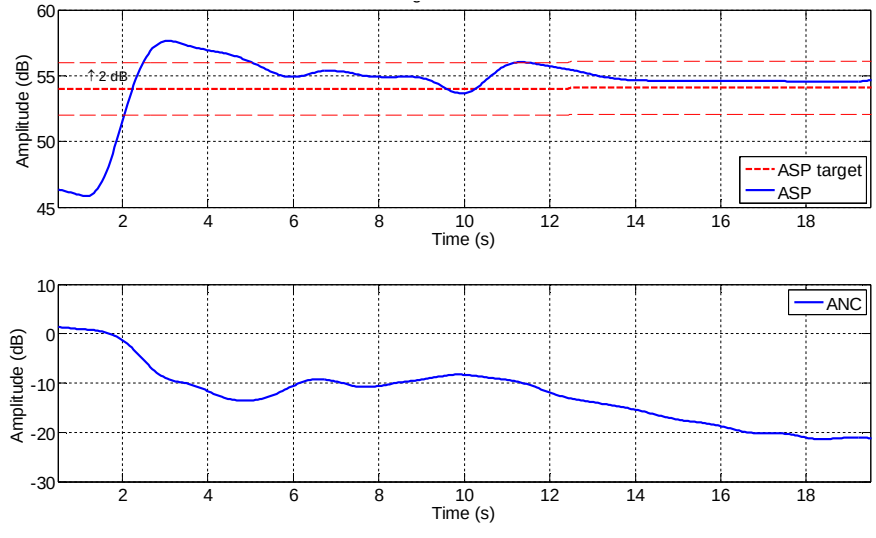

Figure A14. Convergence of the ASP (upper) and ANC (lower) algorithms at 3.5th engine order.

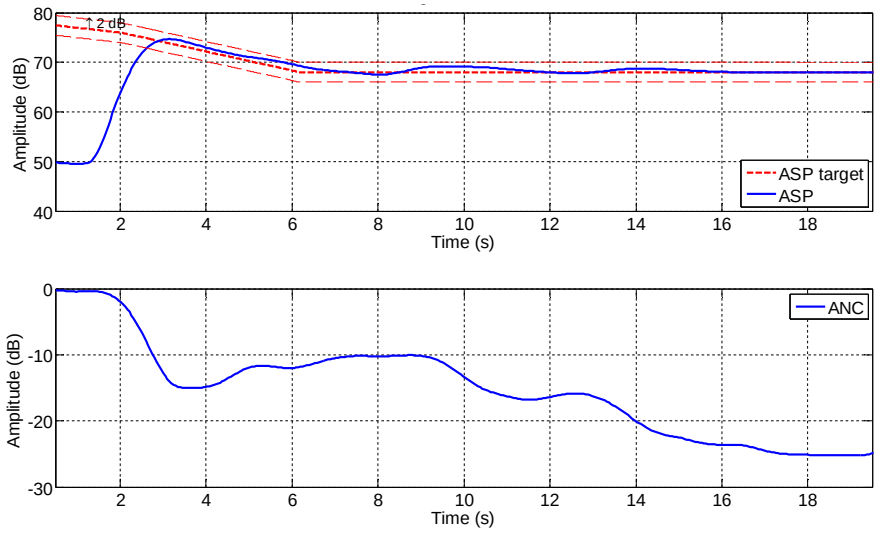

Figure A15. Convergence of the ASP (upper) and ANC (lower) algorithms at 4th engine order.

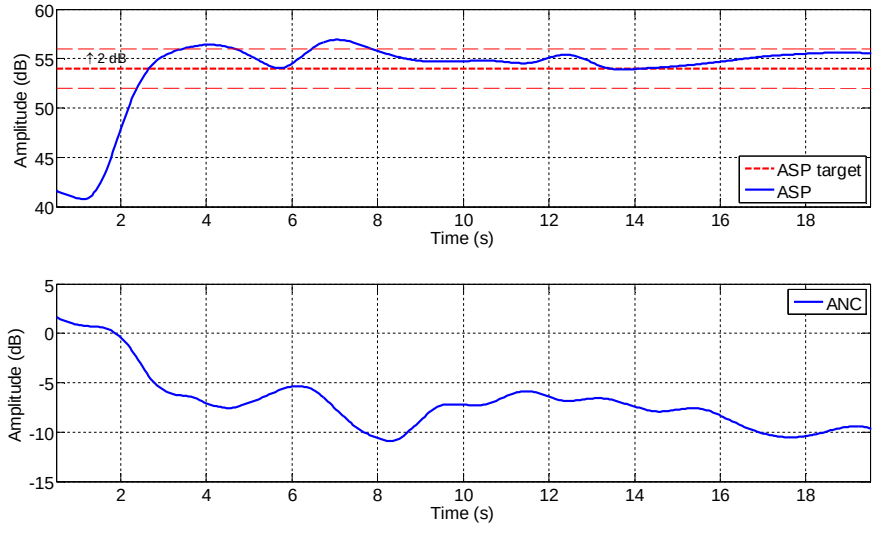

Figure A16. Convergence of the ASP (upper) and ANC (lower) algorithms at 5th engine order.

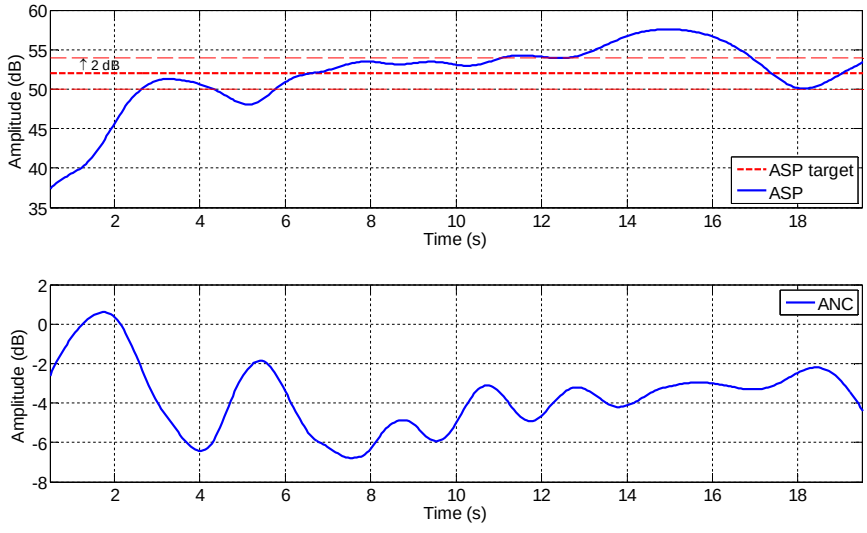

Figure A17. Convergence of the ASP (upper) and ANC (lower) algorithms at 5.5th engine order.

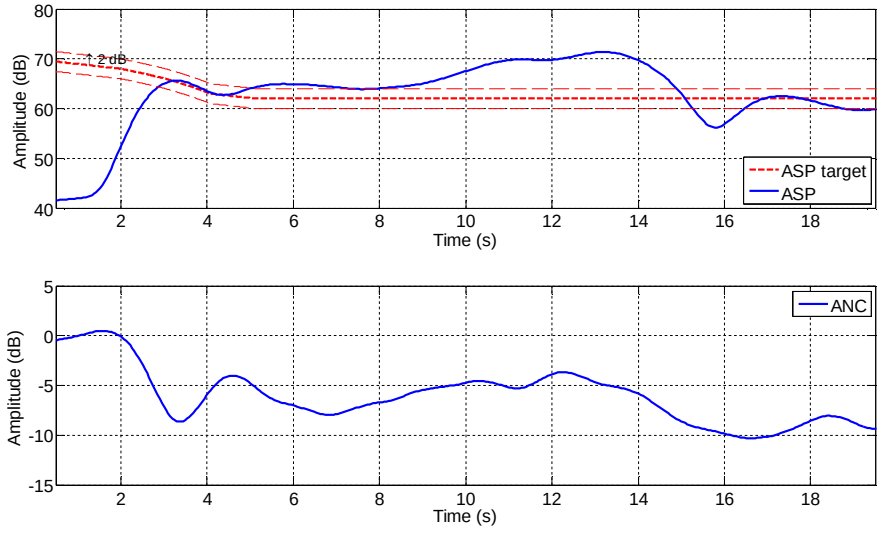

Figure A18. Convergence of the ASP (upper) and ANC (lower) algorithms at 6th engine order.

Simulation results with the LUT-based and FIR-filtering based ASP algorithms are shown in Figures A19–A30.

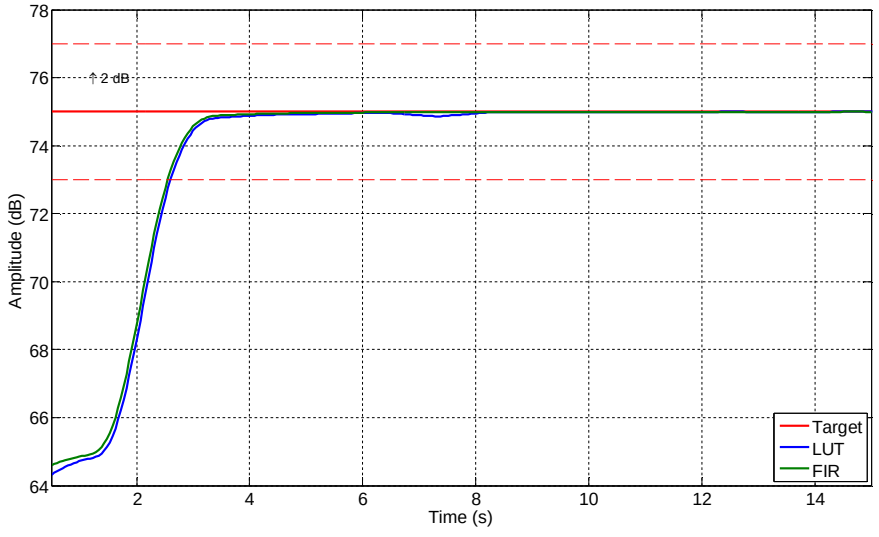

Figure A19. Convergence at 2nd engine order at constant speed.

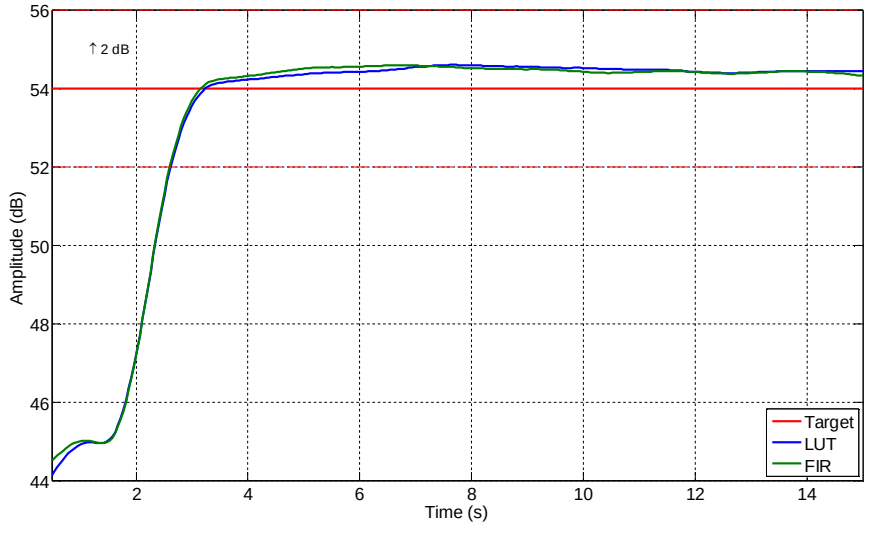

Figure A20. Convergence at 3.5th engine order at constant speed.

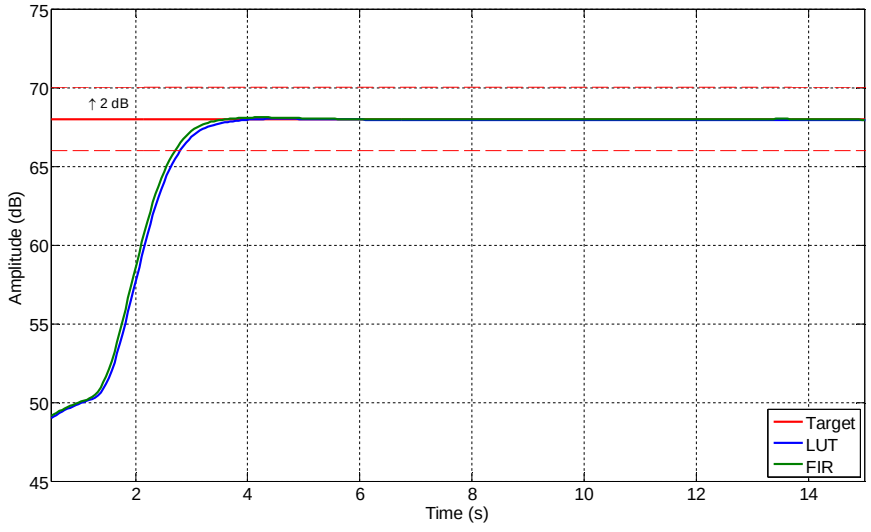

Figure A21. Convergence at 4th engine order at constant speed.

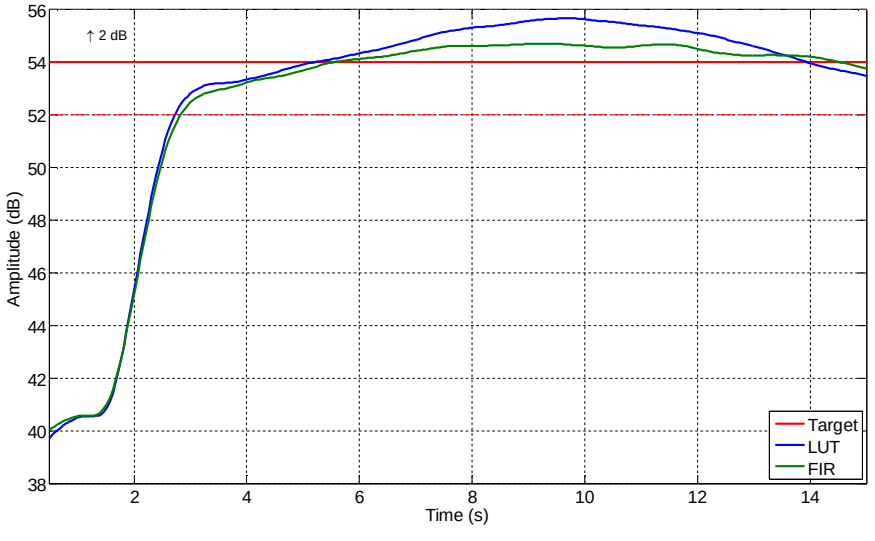

Figure A22. Convergence at 5th engine order at constant speed.

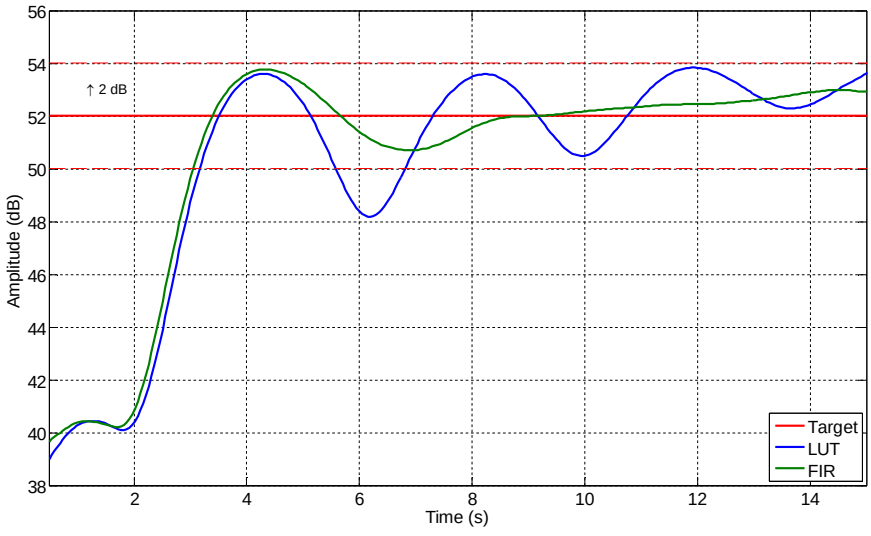

Figure A23. Convergence at 5.5th engine order at constant speed.

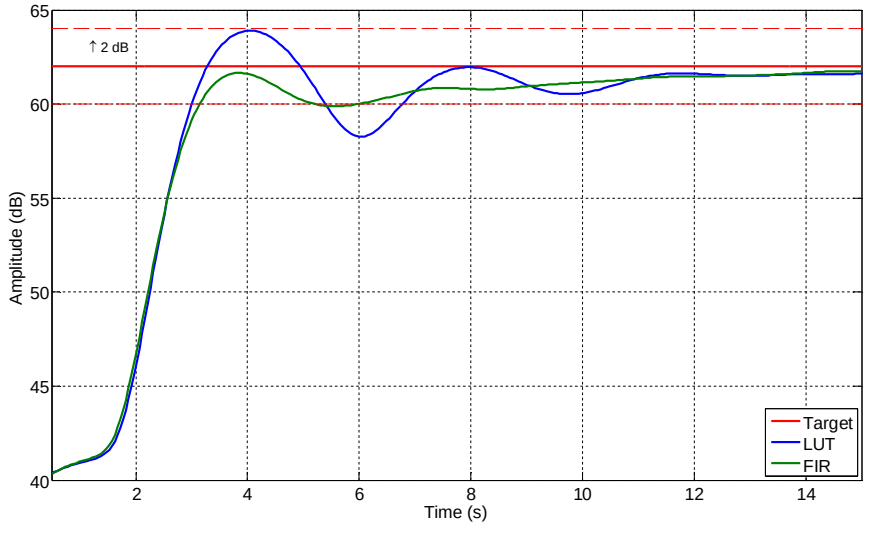

Figure A24. Convergence at 6th engine order at constant speed.

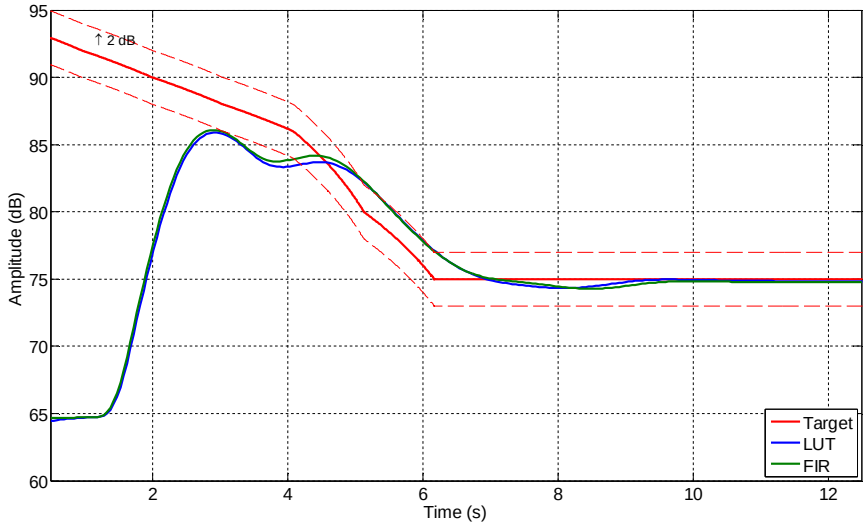

Figure A25. Convergence at 2nd engine order during acceleration.

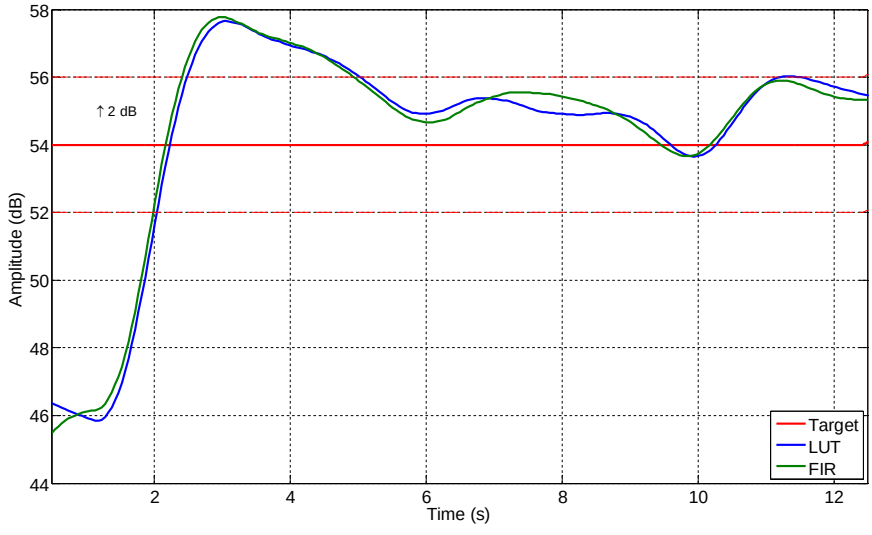

Figure A26. Convergence at 3.5th engine order during acceleration.

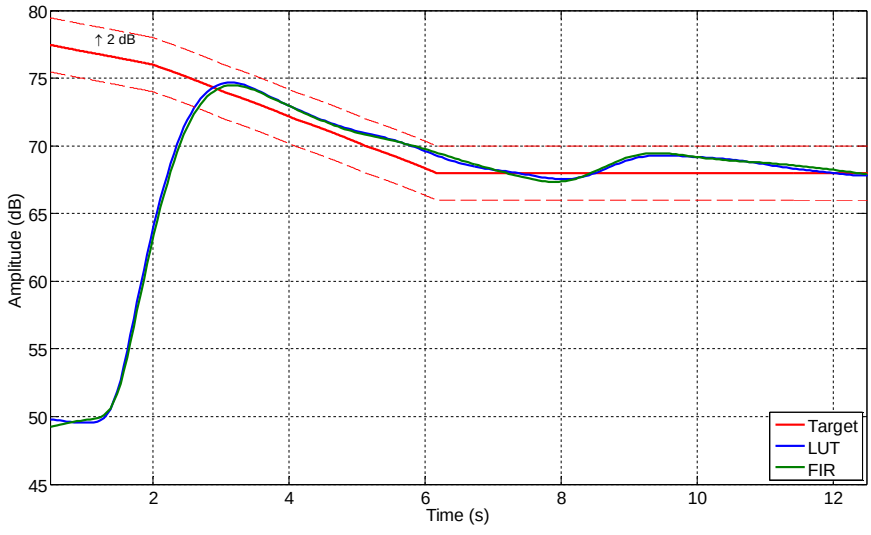

Figure A27. Convergence at 4th engine order during acceleration.

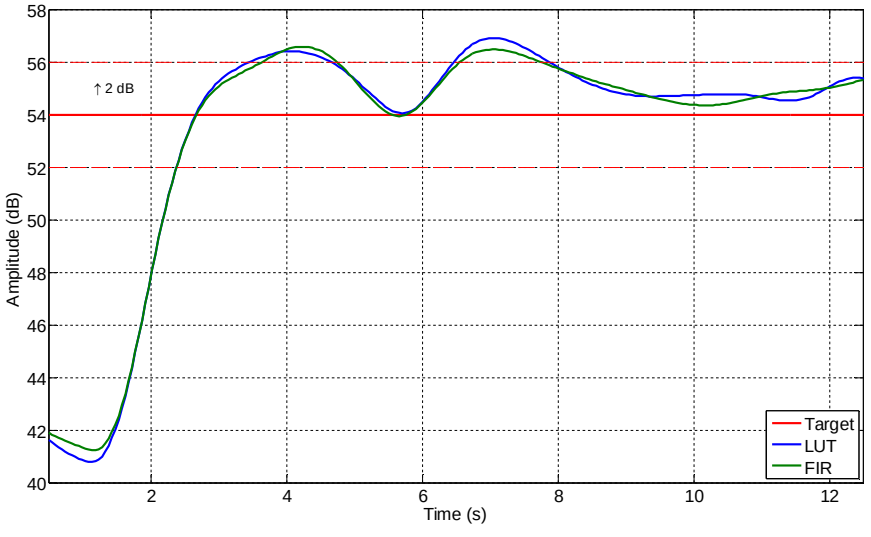

Figure A28. Convergence at 5th engine order during acceleration.

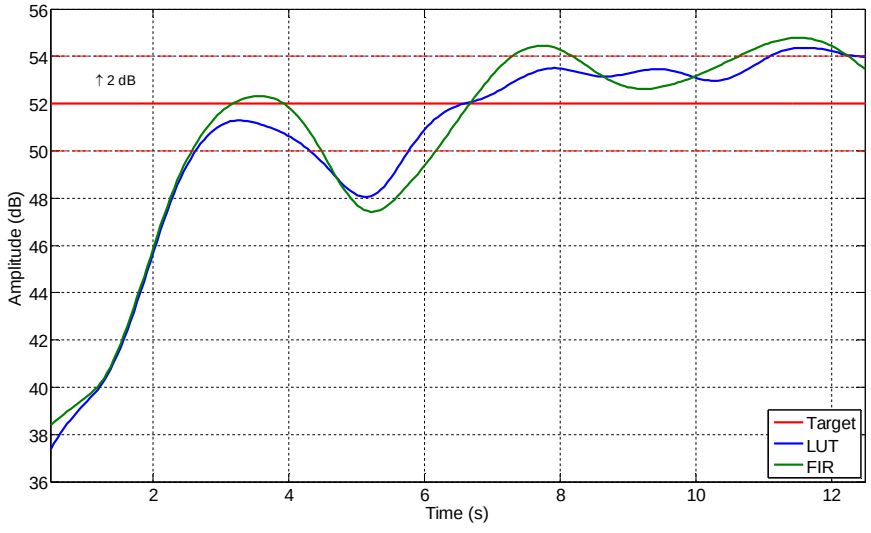

Figure A29. Convergence at 5.5th engine order during acceleration.

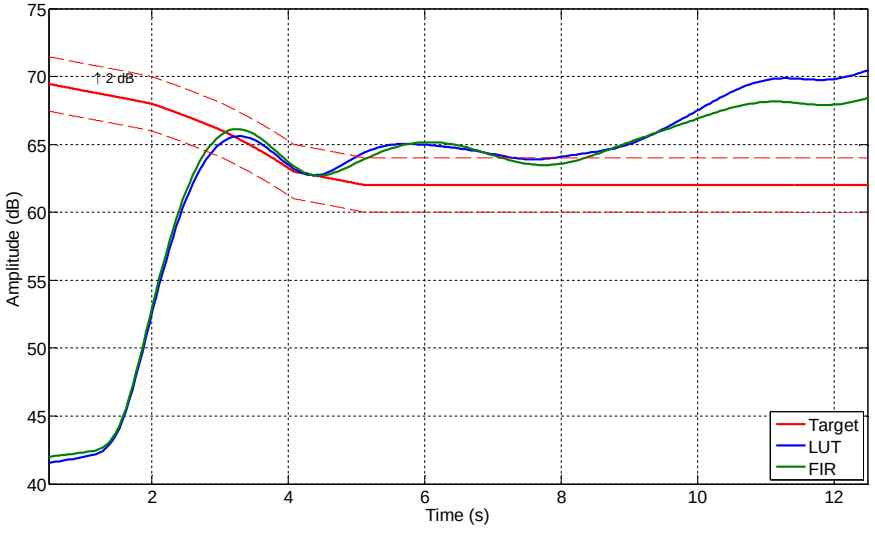

Figure A30. Convergence at 6th engine order during acceleration.

Series title and number
VTT Science 5

Title	**Development of a robust and computationally-efficient active sound profiling algorithm in a passenger car**
Author(s)	Jari Kataja
Abstract	Active noise control is a technique to cancel unwanted sound using adjustable secondary sound. In active sound profiling, the target is to obtain a certain sound field or profile and the power over specific frequencies can be altered in a desired way, even by amplifying it. Active sound profiling can be used for increasing the sound quality in a passenger car, for example, by modifying the engine noise inside the car cabin. A fundamental algorithm in active sound profiling is the command-FXLMS (C-FXLMS) algorithm, which is an extension of the famous FXLMS algorithm widely used in active noise control. The computational demand of the C-FXLMS algorithm becomes excessive in multiple-channel systems with engine noise components to be controlled using several loudspeakers and microphones. The most time-consuming part of the C-FXLMS algorithm is the filtering of the reference signals. In order to reduce the computational burden, a new way to modify the reference signals in narrowband systems has been developed in this work. Instead of conventional filtering operations, the new method is based on delaying the sinusoidal reference signals and modifying their amplitude. The algorithm should work reliably and maintain stability in all operating points. In this work, an adaptive leakage has been developed for the C-FXLMS algorithm to increase its robustness. The objective is to limit the adaptive filter coefficients at frequencies where the phase shift of the plant is large. Such phase shifts occur at resonances, for example, and the performance of the algorithm is drastically degraded. In this work, the C-FXLMS algorithm has also been combined with the EE-FXLMS algorithm so that frequency-independent step sizes can be used. This increases robustness and enables faster tuning of the algorithm. The developed algorithm has been tested in a simulation model and in an experimental active sound profiling system installed in a car. The results prove that the algorithm works with sufficient accuracy. The convergence is fast and stability is maintained in all operating points.
ISBN, ISSN	ISBN 978-951-38-7457-5 (soft back ed.) ISSN 2242-119X (soft back ed.) ISBN 978-951-38-7458-2 (URL: http://www.vtt.fi/publications/index.jsp) ISSN 2242-1203 (URL: http://www.vtt.fi/publications/index.jsp)
Date	April 2012
Language	English, Finnish abstract
Pages	77 p. + app. 15 p.
Name of the project	InMAR, ANRAC
Commissioned by	EU, VTT
Keywords	Active noise control, active sound profiling, command-FXLMS algorithm, sinusoidal signal filtering , adaptive leakage factor
Publisher	VTT Technical Research Centre of Finland P.O. Box 1000, FI-02044 VTT, Finland, Tel. 020 722 111

Julkaisun sarja ja numero
VTT Science 5

Nimeke	**Robustin ja laskennallisesti tehokkaan aktiivisen äänenprofilointialgoritmin kehittäminen henkilöautoon**
Tekijä(t)	Jari Kataja
Tiivistelmä	Aktiivinen melunvaimennus on menetelmä, jossa melua vaimennetaan säädettävällä vastaäänellä. Aktiivisessa äänenprofiloinnissa puolestaan on tavoitteena halutun ääniprofiilin saavuttaminen, jolloin tiettyjä taajuuksia voidaan jopa korostaa vaimentamisen sijaan. Aktiivista äänenprofilointia voidaan käyttää esimerkiksi äänenlaadun parantamiseen henkilöauton sisällä moottoriääntä muokkaamalla. Aktiivisen äänenprofiloinnin perusalgoritmi on command-FXLMS (C-FXLMS) -algoritmi, joka on kehitetty aktiivisessa melunvaimennuksessa paljon käytetystä FXLMS-algoritmista. C-FXLMS -algoritmi tarvitsee huomattavasti laskentatehoa monikanavaisessa muodossaan, jolloin useita moottoriäänen kerrannaisia muokataan usealla vastaäänilähteellä ja virhesensorilla. Suurimman osan laskentatehosta vie referenssisignaalien suodatus ja tehontarpeen vähentämiseksi on kehitetty uusi menetelmä sinimuotoisten referenssisignaalien suodatukseen. Uusi menetelmä perustuu signaalien viivästämiseen ja amplitudin muokkaamiseen. Algoritmin luotettavuus on myös tärkeä tekijä. Algoritmin pitää säilyttää suorituskykynsä kaikissa toimintapisteissä ja toimia stabiilisti. Robustisuuden parantamiseksi on C-FXLMS -algoritmiin kehitetty adaptiivinen vuotokerroin. Sen tarkoituksena on rajoittaa adaptiivisia suodinkertoimia toimintapisteissä, joissa järjestelmän vaihevaste muuttuu äkisti. Sellaisia muutoksia tapahtuu esimerkiksi resonanssitaajuuksilla, jotka aiheuttavat algoritmin suorituskyvyn heikkenemistä. Vuotokertoimen lisäksi C-FXLMS -algoritmi on yhdistetty EE-FXLMS -algoritmin kanssa, jolloin samaa askelpituutta voidaan käyttää kaikilla taajuuksilla. Se lisää robustisuutta ja nopeuttaa algoritmin virittämistä. Kehitettyä algoritmia on testattu simulointimallissa ja henkilöautoon asennetussa aktiivisessa äänenprofilointijärjestelmässä. Tulokset osoittavat, että algoritmi pystyy seuraamaan haluttua ääniprofiilia riittävällä tarkkuudella. Algoritmi myös suppenee nopeasti ja toimii stabiilisti kaikissa toimintatiloissaan.
ISBN, ISSN	ISBN 978-951-38-7457-5 (nid.) ISSN 2242-119X (nid.) ISBN 978-951-38-7458-2 (URL: http://www.vtt.fi/publications/index.jsp) ISSN 2242-1203 (URL: http://www.vtt.fi/publications/index.jsp)
Julkaisuaika	Huhtikuu 2012
Kieli	Englanti, suomenkielinen tiivistelmä
Sivumäärä	77 s. + liitt. 15 s.
Projektin nimi	InMAR, ANRAC
Toimeksiantajat	EU, VTT
Avainsanat	Active noise control, active sound profiling, command-FXLMS algorithm, sinusoidal signal filtering , adaptive leakage factor
Julkaisija	VTT PL 1000, 02044 VTT, Puh. 020 722 111

Development of a robust and computationally-efficient active sound profiling algorithm in a passenger car

Active noise control is a technique to cancel unwanted sound using adjustable secondary sound. In active sound profiling, the target is to obtain a certain sound field or profile. A promising application for active sound profiling is the modification of the engine noise inside a passenger car cabin. Using this technique, the acoustic impression of a car can be altered and the sound quality can be enhanced.

The control algorithms used in active sound profiling are presented. A new algorithm has been developed by improving robustness and computational efficiency of the basic sound profiling algorithm. The improved algorithm has been tested with a simulation model and in a prototype system installed in a car. Results prove that the algorithm works reliably and the computational burden is significantly lower.

ISBN 978-951-38-7457-5 (soft back ed.)
ISBN 978-951-38-7458-2 (URL: http://www.vtt.fi/publications/index.jsp)
ISSN 2242-119X (soft back ed.)
ISSN 2242-1203 (URL: http://www.vtt.fi/publications/index.jsp)